WSRC-STI-2007-00315
Rev. 0

Modeling of Ion-Exchange for Cesium Removal from Dissolved Saltcake in SRS Tanks 1-3, 37 and 41

Washington Savannah River Company
Savannah River Site
Aiken, SC 29808

Prepared for the U.S. Department of Energy under Contract No. DE-AC09-96SR18500

WSRC-STI-2007-00315
Rev. 0

KEYWORDS:
Ion Exchange
Resorcinol-Formaldehyde Resin
Crystalline Silicotitanate
Cesium
VERSE-LC Code
Column Modeling
RETENTION – Permanent

Modeling of Ion-Exchange for Cesium Removal from Dissolved Saltcake in SRS Tanks 1-3, 37 and 41

Frank G. Smith

Savannah River National Laboratory

Publication Date: August 2007

Washington Savannah River Company
Savannah River Site
Aiken, SC 29808

Prepared for the U.S. Department of Energy under Contract No. DE-AC09-96SR18500

DOCUMENT: **WSRC-STI-2007-00315, Rev. 0**
TITLE: **Modeling of Ion-Exchange for Cesium Removal from Dissolved Saltcake in SRS Tanks 1-3, 37 and 41**

APPROVALS

_____ Date: _____
Frank G. Smith, Author,
Advanced Process Development, SRNL

_____ Date: _____
William D. King, Technical Reviewer,
Advanced Characterization and Process Research, SRNL

_____ Date: _____
William R. Wilmarth, Level 4 Manager,
Advanced Characterization and Process Research, SRNL

_____ Date: _____
Timothy Punch,
Technology Development and Tank Closure, SRS

_____ Date: _____
Renee Spires, Manager, Technology Development and Tank Closure
Modular Salt Processing Project Owner

TABLE OF CONTENTS

LIST OF TABLES

LIST OF FIGURES

1.0 Executive Summary

This report presents an evaluation of the expected performance of engineered Crystalline Silicotitinate (CST) and spherical Resorcinol-Formaldehyde (RF) ion exchange resin for the removal of cesium from dissolved saltcake in SRS Tanks 1-3, 37 and 41. The application presented in this report reflects the expected behavior of engineered CST IE-911 and spherical RF resin manufactured at the intermediate-scale (approximately 100 gallon batch size; batch 5E-370/641). It is generally believed that scale-up to production-scale in RF resin manufacturing will result in similarly behaving resin batches whose chemical selectivity is unaffected while total capacity per gram of resin may vary. As such, the predictions provided within this report should provide reasonable estimates of production-scale column performance. Two versions of the RF cesium isotherm were used. The older version provides a conservative estimate of the resin capacity while the newer version more accurately fits the most recent experimental data.

1.1 Objectives

The objectives of this work were, through modeling, to predict the performance of CST and spherical RF resins for the removal of cesium from dissolved saltcake from SRS Tanks 1-3, 37 and 41. The scope of this task was provided in Task Technical and QA Plan "Task Plan for Modeling of Cesium Removal from Dissolved Salt Solution in Tanks 1-3, 37 and 41 Using Ion Exchange with CST and Spherical RF Resins," WSRC-TR-2007-00106, Rev. 1, (Smith, 2007). The study investigated the sensitivity in column performance to:

1. Flow rates of 5, 10 and 20 gpm with 10 gpm as the nominal flow.

2. Temperatures of 25, 35 and 45 °C with 25 °C as the nominal temperature.

3. Column lengths of 10, 15 and 25 feet with 15 feet as the nominal size.

Only the ion-exchange performance of RF resin in the loading phase is addressed in this document. That is, the elution of cesium from the RF resin is not modeled. The column performance predictions presented in this report reflect expected performance behavior for engineered CST IE-911 and for RF resin manufactured at the intermediate-scale (100 gallon batch size) and in its spherical bead form.

1.2 Modeling Approach

- Detailed thermodynamic equilibrium models were used to calculate cesium adsorption isotherms for CST and RF. Two models of RF behavior were used to generate two different isotherms.

- Ion-exchange column performance was simulated using "effective" single-component (cesium specific) isotherms and column transport models. Previous work has shown that

for the cesium loading-phase, the "effective" single-component model is adequate for design purposes.

- Based on this methodology, "best estimate" column simulations were run for the five feed streams of interest assuming a two-column (lead-lag) configuration. A bucket average concentration limit (i.e., an integral sum of the effluent cesium content) was imposed at the exit of the lag column.

- After review of the initial results, selected column simulations for all five feed streams were rerun using a single configuration. The selected simulations tested CST and one RF isotherm at 25 °C with three different column lengths and three different flowrates.

1.3 Quality Assurance

CST isotherms were generated using the ZAM code developed at Texas A&M. The ZAM code has been used in previous studies modeling CST with good success. RF isotherms were generated using the TMIXP and CERMOD codes recently developed at Savannah River National Laboratory (SRNL) by Aleman and Hamm (2007). Parameters in the CERMOD RF isotherm model are based on fitting to the most recent set of batch contact data from experiments conducted at SRNL for the Hanford RPP-WTP project. The TMIXP RF isotherm model is based on previous data obtained at SRNL with spherical RF resin which provides a more conservative estimate of RF column performance. Calculations using both RF isotherms are presented in this report.

The Liquid Chromatography code VERSE-LC (Whitley and Wang, 1998) was used to perform the ion-exchange column calculations. Prior to applying VERSE-LC in ion exchange modeling tasks, a verification process was completed and the results of that effort are reported by Hamm et al. (2000). The verification process provided quality assurance that the installed Windows PC version of VERSE-LC (Version 7.80) was capable of adequately solving the model equations and also helped to understand how to accurately use the VERSE-LC code (e.g., mesh refinement requirements and input/output options). For all column results presented in this report, numerical errors associated with the results from VERSE-LC should be very small when compared to the uncertainties associated with various model input parameters (bed density, particle radius, pore diffusion, etc.).

1.4 Results Summary

Table 1-1 gives the decontamination factors (DFs) that are achieved for each tank. DF is defined as the ratio of cesium concentration in the feed to the cesium concentration in the bucket average effluent from the lag column:

$$DF \equiv [Cs]_{feed} / [Cs]_{eluant}$$

The average effluent concentration limit was 45 nCi/g which is the saltstone feed limit. Table 1-2 provides a summary of the time that would be required to process the waste volume in Tanks 1-3, 37 and 41 through the ion-exchange columns at the three flow rates tested. The

results in Tables 1-1 and 1-2 apply for both ion-exchange resins and all of the different cases run with the lead-lag column configuration.

In all cases, either CST or RF resin was able to process a significant volume of dissolved salt cake in each ion-exchange cycle. During the first cycle when there are two clean columns in the ion-exchange train more waste volume can be processed than in subsequent cycles where the partially loaded lag column has been placed into the lead position. After the first cycle, essentially the same volume of waste can be processed in each subsequent cycle. Table 1-3 compares the volume of waste processed during the second cycle for all of the cases evaluated. Comparing the results obtained using the old RF isotherm to CST we find that CST consistently has close to twice the capacity for cesium and is able to process twice the solution volume. The revised (new) RF isotherm gives less consistent results. This is because the revision improved adsorption capacity primarily at lower cesium concentrations to obtain better agreement with the most recent experimental data. Therefore, using the new RF isotherm indicates significantly better performance for Tank 2 and Tank 41 which had the lowest cesium concentrations. For Tank 2 using the revised RF isotherm in some cases predicted column performance exceeding that obtained with CST. Potassium is a strong competitor for cesium on the RF resin sites and the low potassium concentrations in the dissolved salt cake appear to have had a greater impact on cesium loading with the revised isotherm.

For 24 out of the 35 cases (excluding Case 8), CST was able to process the largest volume, for the remaining 11 cases RF resin performed better using the new isotherm. CST always performed better for Tanks 1 and 37 that have the highest cesium concentration. Table 1-4 shows the estimated number of ion-exchange cycles required to process the volume of dissolved salt (see Table 1-2) in each tank.

Other general trends in the results with the lead-lag column configuration are:

- Lower flow relative to the nominal 10 gpm sharpens the breakthrough front and allows more volume to be processed in each ion-exchange cycle. However, decreasing the flow from 10 gpm to 5 gpm roughly increased the volume of solution processed by only about 10% for CST and 1% for RF while doubling the time required to run the material through the column for both media.

- Higher flow spreads out the breakthrough front and decreases the amount of solution that can be processed in each ion-exchange cycle. However, doubling the flow from 10 gpm to 20 gpm roughly decreased the volume of solution processed by about 17% for CST and about 4% for RF while also decreasing the time required to run the material through the column by a factor of two. Processing at a higher flow would also decrease the exposure of the RF resin, increasing the volume of waste that each batch could process before it is radiolytically degraded.

- Operating the column at higher temperatures decreases the adsorption capacity of the resin and decreases the amount of solution that can be treated in each cycle.

Operating at 45 instead of 25 °C decreased the RF resin capacity by approximately 50% and CST capacity by roughly 30%.

- Depending on operating conditions, estimates of the amount of CST required to process the planned volume of dissolved saltcake in Tanks 1-3, 37 and 41 ranged from about 56 to 75 metric tons.

- For nominal operating conditions it will take on the order of 10 ion-exchange cycles per tank to process the dissolved salt cake in Tanks 1-3 with CST media or RF resin using the newest RF isotherm. To provide a conservative bracket on the expected operating conditions with SRS waste, modeling was also performed using an older version of the RF isotherm. The original RF isotherm indicates that approximately twice as many ion-exchange cycles will be required.

- The experimental RF data was fit to a "new" Freundlich/Langmuir isotherm equation that more accurately represents batch contact data at low cesium concentrations, but the earlier Langmuir RF isotherm seems to fit better at high cesium concentrations. Testing with SRS waste would be required to confirm the expected performance of RF resin.

Detailed tables reporting results for each case run are presented in Sections 9, 10 and 11 of this report. Results from the single column runs are presented in Appendix A for CST ion-exchange medium and in Appendix B for RF.

Table 1-1. Decontamination factors calculated for each tank.

Tank Number	DF
1	5914
2	810
3	2803
37	4005
41	281

Table 1-2. Time in days required to process salt solution through ion-exchange columns.

	Waste Volume at 6 M Na (millions of gallons)	**Flow Rate**		
		5 gpm	**10 gpm**	**20 gpm**
Tank 1	1.87	259.7	129.9	64.9
Tank 2	2.08	288.9	144.4	72.2
Tank 3	2.09	290.3	145.1	72.6
Tank 37	1.00[1]	138.9	69.4	34.7
Tank 41	0.19[1]	26.4	13.2	6.6
Tank 37	4.10[2]	569.4	284.7	142.4
Tank 41	3.48[2]	483.3	241.7	120.8
	Total Volume	Total Column Processing Time in Years		
Tanks 1 – 3	6.04	2.30	1.15	0.57
All 5 Tanks[3]	7.23	2.75	1.38	0.69

[1] Volume of dissolved saltcake in tanks it is planned to process.
[2] Maximum volume of dissolved saltcake in tanks.
[3] Using volume of dissolved saltcake in Tanks 37 and 41 it is planned to process.

Table 1-3. Waste volume in thousands of gallons processed during second ion-exchange cycle for all test cases run.

Tank	Resin	1	2	3	4	5	6	7	8[1]
		15 ft	15 ft	15 ft	10 ft	25 ft	15 ft	15 ft	15 ft
		10 gpm	5 gpm	20 gpm	10 gpm	10 gpm	10 gpm	10 gpm	10 gpm
		25 °C	25 °C	25 °C	25 °C	25 °C	35 °C	45 °C	25 °C
1	**CST**	212	229	180	130	377	199	187	NA
	RF New	169	170	168	112	283	132	102	135
	RF Old	117	118	113	77	196	96	80	93
2	**CST**	193	211	168	120	345	175	160	NA
	RF New	247	254	235	160	421	157	103	198
	RF Old	98	103	92	63	169	75	58	79
3	**CST**	197	215	170	122	352	166	144	NA
	RF New	204	206	201	135	343	137	92	164
	RF Old	93	97	86	60	160	70	54	74
37	**CST**	390	418	335	241	689	310	246	NA
	RF New	257	258	254	170	430	198	151	206
	RF Old	164	166	156	107	276	136	113	131
41	**CST**	449	486	396	280	797	348	271	NA
	RF New	432	444	412	281	737	290	199	346
	RF Old	224	233	210	144	385	146	119	179

[1]Case 8 used 80% of the nominal RF resin capacity to simulate resin degradation from chemical and radioactive exposure.

Table 1-4. Number of ion-exchange cycles required to process dissolved salt.

Tank	Resin	1	2	3	4	5	6	7	8[1]
		15 ft	15 ft	15 ft	10 ft	25 ft	15 ft	15 ft	15 ft
		10 gpm	5 gpm	20 gpm	10 gpm	10 gpm	10 gpm	10 gpm	10 gpm
		25 °C	25 °C	25 °C	25 °C	25 °C	35 °C	45 °C	25 °C
1	**CST**	10	9	11	15	6	10	11	NA
	RF New	11	10	11	16	6	14	18	13
	RF Old	15	15	16	23	9	19	22	19
2	**CST**	12	11	13	18	7	13	14	NA
	RF New	8	8	8	12	4	12	19	10
	RF Old	20	19	21	30	11	26	33	25
3	**CST**	11	10	13	18	7	13	15	NA
	RF New	10	10	10	15	6	15	22	12
	RF Old	21	20	22	32	12	28	36	26
37	**CST**	11	11	13	18	7	14	18	NA
	RF New	15	15	15	23	9	20	26	19
	RF Old	24	24	24	36	14	29	34	30
41	**CST**	8	8	10	13	5	11	14	NA
	RF New	8	8	9	13	5	12	18	10
	RF Old	16	16	17	24	9	24	30	20

[1]Case 8 used 80% of the nominal RF resin capacity to simulate resin degradation from chemical and radioactive exposure.

2.0 Introduction and Background

A process is being designed to remove cesium from dissolved saltcake in SRS tanks. The primary treatment for dissolved saltcake from most of the SRS waste tanks will be by solvent extraction to remove cesium in the Salt Waste Processing Facility (SWPF). In the short term, it may be necessary to treat several tanks using ion-exchange, and, using another process could augment the solvent extraction process. As envisioned, the Small Column Ion-Exchange (SCIX) process would treat the dissolved saltcake using ion-exchange columns suspended inside a waste tank. The columns will use a selective ion exchange media to remove cesium from the waste. The media removes all of the cesium, about 25% of which is the radioactive ^{137}Cs isotope.

Two ion-exchange resins are under consideration for use in this process:

- Non-elutable Crystalline Silicotitanate (CST) resin, and
- Elutable spherical Resorcinol-Formaldehyde (RF) resin.

After sorption of cesium, the non-elutable CST would be sluiced from the column and disposed of in the DWPF glass melter by vitrification. A fresh batch of CST would then be loaded into the column. For the RF resin, the loaded cesium is eluted, and the cesium-containing eluate would also be sent to the DWPF glass melter. The eluted RF resin can be reused in another ion-exchange cycle. Both of these media and approaches are mature technologies for cesium removal from radioactive waste. The purpose of this modeling effort is to facilitate selection of the ion exchange media and provide input to the design parameters.

2.1 Ion Exchange Columns

The ion-exchange column design was previously developed by Oak Ridge National Laboratory and Savannah River National Laboratory. The design overcame earlier issues related to column overheating and long contact time using an annular configuration with an outer diameter of 28" and a 6-inch diameter inner cooling tube. The outer tube has a wall thickness of 5/16" and the inner tube is 6" schedule 40 pipe. The cross-sectional area of the annular ion-exchange bed is 0.3575 m^2.

The proposed design consists of two columns used in series during loading (i.e., a lead column followed by a lag column). When the integral sum average concentration of cesium in the effluent from the second (lag) column reaches the saltstone feed limit of 45 nCi/g the ion-exchange cycle is stopped. The first (lead) column is then removed from service, the partially loaded second (lag) column is placed in the lead position, a fresh column is placed in the lag position and the next cycle is started. In the case of CST, the cesium-loaded material from the lead column must be removed and disposed of. With RF resin, cesium will be eluted from the loaded column and the column reused as the lag in the next cycle. The RF resin can be reused until degradation from the exposure to chemicals and radioactivity becomes too

great. The modeling presented in this report considers only the loading phase of each ion-exchange cycle.

2.2 Salt Solution Compositions and Properties

Dissolved salt solution compositions were taken from Table 4 in LWO-PIT-2007-00040 (Tran, 2007). For reference, the compositions are listed in Table 2-1. Concentrations reported as less than some value were set to that value. The small calcium concentrations in each tank were neglected. The small strontium concentration is included since strontium is a competitor for cesium on CST. Similarly, the small rubidium concentration is included since rubidium is a competitor with cesium on RF resin. Oxalate was neglected since it does not appear in the isotherm models used.

The density and viscosity of each solution were calculated from the composition and temperature using the Stream Analyzer™ software from OLI Systems, Inc. As shown in Section 6, the cesium diffusivity in the bulk feed solution (free diffusivity) was calculated using the Nernst-Haskell equation. Based on fitting SRNL experimental data, the pore diffusivity for CST media was estimated to be 20% of the free diffusivity while the pore diffusivity for RF resin was estimated as 33% of the free diffusivity.

2.2 Ion Exchange Resins

CST and RF cation-exchange materials have been developed for the selective removal of cesium (containing some isotopic fraction of ^{137}Cs) from highly alkaline solutions. Crystalline Silicotitanate (CST) would be used in the granular, engineered form. The isotherm used in this report applies for UOP IONSIV® IE-911. Researchers at Texas A&M University and Sandia National Laboratory developed the sorbent, and UOP personnel developed the binder technology for producing a granular form suitable for use in an ion exchange column.

RF resin is prepared by condensation polymerization of resorcinol ($C_6H_6O_2$) and formaldehyde (CH_2O). The high selectivity for cesium has been attributed to the two weakly acidic hydroxyl groups on resorcinol, which ionize and become functional at high pH. Due to its weak acid nature, the resin has a strong preference for H^+ and can be eluted using acid to remove Cs^+ and its competitors. Our current estimate for the relative affinities of RF resin for ion-exchange are $H^+ > Cs^+ > Rb^+ > K^+ > Na^+$. Resorcinol-formaldehyde has been manufactured in crushed or granular form and in spherical form. The most recent RF isotherm model was primarily based on experimental data collected to support the Hanford Waste Treatment Plant. In particular, much of the data used the Hanford AP-101 waste composition for batch contact, kinetics and small column experiments. These experiments were conducted using Batch Lot Number 5E-370/641 of spherical RF ion exchange resin purchased from Microbeads AS in Skedsmokorset, Norway (Nash, et al., 2006 and Fiskum et al., 2006).

2.3 Report Overview

This report focuses on the cesium-loading phase of the ion-exchange cycle. An analysis methodology is developed incorporating available experimental data. This document represents a report based on our current knowledge and capability to model the ion-exchange process for the two media considered. The methodology and its application to the proposed SCIX process are discussed in the following sections.

Section 3 briefly discusses the transport model used to describe ion-exchange column behavior. The VERSE-LC code (Berninger et al., 1991) was used for the column modeling presented in this report based on its availability and its earlier use in previous ion-exchange analysis efforts at SRNL. In the column model, local equilibrium between the pore fluid and neighboring surface sites is assumed where an equilibrium adsorption isotherm must be specified. The isotherm models used for this purpose are discussed in Section 4. Key column properties are addressed in Section 5 where the constraint imposed by bed porosity, particle porosity, and bed density is highlighted. Solution properties and diffusion in the porous ion-exchange particles are addressed in Section 6. In Section 7 the constitutive models for film diffusion and axial dispersion are presented. Section 8 lists the SCIX case studies run. Section 9 presents modeling results for the CST system. Section 10 presents modeling results for the RF system using a most recent Freundlich/Langmuir isotherm. Section 11 presents modeling results for the RF system using the "old" Langmuir isotherm applied in previous work.

Table 2-1. Dissolved saltcake compositions in molarity.

Species	Tank 1	Tank 2	Tank 3	Tank 37	Tank 41
Na^{+1}	6.0	6.0	6.0	6.0	6.0
NO_3^{-1}	3.07	4.19	4.595	2.26	2.42
NO_2^{-1}	0.30	0.149	0.285	0.74	0.69
OH^{-1}	1.41	0.76	0.545	1.97	1.81
AlO_2^{-1}	0.30	0.29	0.062	0.35	0.34
CO_3^{-2}	0.18	0.13	0.079	0.11	0.13
SO_4^{-2}	0.25	0.032	0.095	0.15	0.15
PO_4^{-3}	0.003	0.005	0.003	0.01	0.01
Cl^{-1}	0.03	0.003	0.01	0.03	0.03
F^{-1}	0.06	0.0029	0.025	0.03	0.03
K^{+1}	0.02	0.007	0.002	0.01	0.01
Cs^{+1}	1.81×10^{-4}	1.70×10^{-5}	6.35×10^{-5}	1.08×10^{-4}	7.53×10^{-6}
Sr^{+1}	3.08×10^{-4}	3.08×10^{-4}	1.64×10^{-4}	3.02×10^{-6}	3.02×10^{-6}
Rb^{+1}	2.19×10^{-5}	6.26×10^{-6}	2.19×10^{-5}	1.18×10^{-5}	2.58×10^{-6}

3.0 VERSE-LC Column Model

The modeling of ion exchange columns is typically broken into two parts:

1. An adsorption isotherm model that specifies the equilibrium relationship between the concentration of adsorbing ions in solution and the solid phase, and
2. A column model based on one-dimensional (axial) solute transport.

In order of their importance with respect to predicting exit breakthrough curves, the five basic aspects of the ion exchange column that need to be addressed are:

- **Adsorption Isotherm** (high impact) – resin affinities for the various competing ions of interest have a very direct impact on overall column performance. The isotherms shift the entire breakthrough curve with respect to number of column volumes required to reach a specified concentration level and, for non-linear isotherms, alter the breakthrough curve shape as well as its sensitivity to inlet feed conditions.

- **Bed Definition** (high impact) – column size, geometry and resin mass have a direct impact on overall column performance, shifting the entire breakthrough curve with respect to the number of column volumes required to reach a specified concentration level, with particle geometry having a slightly less important impact. Bed volume can vary over the course of an ion-exchange cycle for resins such as RF that swell and shrink as solution ionic strength and pH change. In this report bed volume (or column volume) refers to the conditions associated with the feed conditions during the loading cycle (6 M $[Na^+]$).
- **Pore Diffusion** (moderate impact) – intra-particle mass transport by pore diffusion to available surface sites has a moderate impact on overall column performance. Pore diffusion alters the shape of exit breakthrough curves about the 50% breakthrough concentration level with a slight shifting of the breakthrough curve. Increased pore diffusion enhances the rate of mass transfer between the liquid and solid which tends to sharpen the breakthrough curve.
- **Film Diffusion** (low impact) – liquid mass transport by film diffusion across the particle-to-bed boundary has a low impact on overall column performance. Film diffusion alters the shape of exit breakthrough curves about the 50% breakthrough concentration level with a slight shifting of the breakthrough curve.
- **Axial Dispersion** (low impact) – mass transport along the column length by axial dispersion has a relatively low impact on overall column performance. Axial dispersion alters the shape of exit breakthrough curves about the 50% breakthrough concentration level with a slight shifting of the breakthrough curve.

Mechanisms such as surface migration or adsorption kinetics are not included in our column model since their impacts were considered to be negligible or indirectly incorporated into the other features during our parameter estimation process.

3.1 Single-Component Model

The VERSE-LC code was used for the ion-exchange column modeling presented in this report (Berninger et al., 1991) based on its availability and previous experience with its use. VERSE-LC solves a set of equations describing one-dimensional transport along the axial dimension of the ion-exchange column coupled to one-dimensional diffusion within a porous particle representing the resin. In general, a multi-component ion exchange model can be used in VERSE-LC to describe adsorption of species from the liquid phase onto the resin. Under certain situations the multi-component transport equations can be decoupled into a series of single-component transport equations. The reduction to single-component equations is valid when the total ionic strength is the same in the column's local and feed solutions or is a reasonable approximation when one ion absorbs onto the resin significantly more than others. Cesium adsorption on both CST and RF can be adequately modeled using the single-component approach which achieves a significant savings in computational time. In the model, we assume that kinetics associated with local ion exchange at an active resin surface site are very fast compared to the various liquid mass transfer mechanisms that transport ions to the site.

For each species, the one-dimensional (ion) transport equation in the liquid phase solved by VERSE-LC is:

$$\varepsilon_b \frac{\partial c_b}{\partial t} + \varepsilon_b u \frac{\partial c_b}{\partial z} = \varepsilon_b E_b \frac{\partial^2 c_b}{\partial z^2} - \left(\frac{3}{< R_p >} \right) (1-\varepsilon_b) k_f \left(c_b - c_p\big|_{r=R_p} \right), \tag{3-1a}$$

storage **advection** **axial dispersion** **liquid film diffusion (mass transfer)**

with boundary and initial conditions

$$z = 0, \qquad E_b \frac{\partial c_b}{\partial z} = u\left[c_b - c_b^{\text{feed}}(t)\right], \tag{3-1b}$$

$$z = 1, \qquad \varepsilon_b E_b \frac{\partial c_b}{\partial z} = 0, \tag{3-1c}$$

$$t = 0, \qquad c_b = c_b(0, z). \tag{3-1d}$$

In Eqs. (3-1a) – (3.1d):

ε_b ..... Bed or column porosity

ε_p ..... Particle porosity

u ..... Interstitial fluid velocity, cm/min

c_b ..... Concentration in bed fluid, M

c_p ..... Concentration in pore fluid, M

E_b ..... Axial diffusion coefficient, cm^2/min

$< R_p >$ ..... Average particle radius, cm

k_f ..... Liquid film mass transfer coefficient, cm/min

r ..... Radial coordinate within average size particle, cm

z ..... Axial coordinate, cm

t..... Time, min

The one-dimensional species transport equation within a resin particle pore is:

$$\underset{\text{storage}}{\varepsilon_p \frac{\partial c_p}{\partial t}} + \underset{\text{surface adsorption}}{(1-\varepsilon_p)\overline{C}_T\left(\frac{\partial q}{\partial c_p}\right)\frac{\partial c_p}{\partial t}} = \underset{\text{Fickian pore diffusion}}{\varepsilon_p D_p \frac{1}{r^2}\frac{\partial}{\partial r}\left[r^2 \frac{\partial c_p}{\partial r}\right]}, \tag{3-2a}$$

with boundary and initial conditions

$$r = 0, \qquad \frac{\partial c_p}{\partial r} = 0 \ , \tag{3-2b}$$

$$r = <R_p>, \qquad \varepsilon_p D_p \frac{\partial c_p}{\partial r} = k_f\left(c_b - c_p\right) \ , \tag{3-2c}$$

$$t = 0, \qquad c_p = c_p(0, r) \ . \tag{3-2d}$$

In Eqs. (3-2a) – (3-2d):

$\overline{C}_T$ ..... Total ion-exchange capacity of resin, moles/liter bed volume

q ..... Species loading on resin

D_p ..... Pore diffusion coefficient, cm^2/min

Assuming local equilibrium between the pore fluid and its neighboring surface sites, a multicomponent equilibrium isotherm model for the ion exchange between the pore liquid and solid phases can be expressed as:

$$q = f\left(\overline{C}_T, c_{p1}, c_{p2}, \cdots, c_{pN_s}\right) \tag{3-3}$$

where it has been assumed that surface loading can be explicitly related to the local liquid concentrations. An example of a single-component equilibrium isotherm model for ion exchange between the pore fluid and solid phase is:

$$q = f(c) = \frac{C_T \, c_p}{\beta + c_p} \ , \tag{3-4}$$

where Eq. (3-4) is of the Langmuir form and β is a function of the feed conditions.

4.0 Equilibrium Cesium Isotherms

Detailed thermodynamic models were used to generate cesium isotherm data for each feed composition and each resin. These simulated isotherm data was then fit to an appropriate algebraic isotherm model that could be used in VERSE-LC. The ZAM (Zheng, Anthony, Miller) model developed at Texas A&M was used to generate isotherm data for CST. The TMIXP (Thermodynamic Model for Ion Exchange Processes) and CERMOD (Cation Exchange Resin Model) models developed by Hamm and Aleman at SRNL were used to generate isotherm data and algebraic fits for RF. TMIXP is described in Appendix A of the report by Hamm et al. (2003). A detailed discussion of the CERMOD code is given in the separate report being prepared by Aleman and Hamm (2007). The RF isotherms are for the loading phase of the RF ion-exchange cycle only and the elution phase of the RF ion-exchange cycle is not modeled.

The ZAM code is software developed at Texas A&M University by Rayford G. Anthony and Zhixin Zheng. The ZAM code is a product of several years development and research in Professor Anthony's Kinetics, Catalysis and Reaction Engineering Laboratory in the Department of Chemical Engineering at Texas A&M University. ZAM is written in FORTRAN 90 using the Microsoft Developer's Workbench. For applications run at SRNL, PC based versions running under MS-DOS are used. No extensive user guide exists for ZAM; however, a brief user guide is available from Professor Anthony. A description of the ZAM model is provided by Zheng et al. (1997).

In our column modeling, we assume that the rate of ion exchange at a surface site is very fast compared to the rates of diffusion within the pore fluid and mass transfer across the liquid film at the outer boundaries of the particles. In other words, we assume that local equilibrium exists between the pore fluid and its neighboring surface sites. With this assumption, an algebraic expression relating ionic or species concentrations between the pore fluid and the solid CST or RF resin surface sites (referred to as our "isotherm model") can be developed for use in VERSE-LC column simulations. No explicit attempt is made in this report to verify this assumption. In an indirect manner, this assumption is either incorporated into some of the model parameters or verified by the comparison of model results to data. In addition, we assume that for each unique feed stream the total cesium capacity of the ion-exchange resin (active sites for cesium per gram of resin) remains independent of ionic strength and solution composition throughout the ion-exchange process.

4.1 Isotherm Model for VERSE-LC Application

The most general form of isotherm model we have used in VERSE-LC calculations is the Freundlich/Langmuir Hybrid model which is expressed in general as:

$$\overline{C}_{pi} = \frac{a_i c_{pi}^{M_{ai}}}{\beta_i + b_1 c_{p1}^{M_{b1}} + b_2 c_{p2}^{M_{b2}} + b_3 c_{p3}^{M_{b3}} + b_4 c_{p4}^{M_{b4}} + b_5 c_{p5}^{M_{b5}}} \qquad \text{for} \quad i = 1...5, \qquad (4\text{-}1)$$

where

$\overline{C}_{pi}$ ..... species i solid surface concentration based on bed volume, gmole/L-BV

c_{pi} ..... species i concentration in pore fluid, M

β_i, a_i, b_i ..... Freundlich/Langmuir Hybrid model coefficients for species i

M_{ai}, M_{bi} .... Freundlich/Langmuir Hybrid model exponents for species i

The five species considered in the isotherm models are: Cs^+, Na^+, K^+ and H^+ along with Sr^+ for CST and Rb^+ for RF.

The Freundlich/Langmuir Hybrid model can also be used for an "effective" single-component (Cs^+) case. Here the hydrogen, potassium, sodium, and strontium or rubidium concentrations throughout the column are assumed to be at their feed concentration levels. For an "effective" single-component total cesium isotherm, Eq. (4-1) reduces to:

$$\overline{C}_{p1} = \frac{a_1 c_{p1}^{M_{a1}}}{\left[\beta_i + b_2 c_{p2}^{M_{b2}} + b_3 c_{p3}^{M_{b3}} + b_4 c_{p4}^{M_{b4}} + b_4 c_{p5}^{M_{b5}}\right] + b_1 c_{p1}^{M_{b1}}} \Rightarrow \frac{a_1 c_{p1}^{M_{a1}}}{\hat{\beta}_1 + b_1 c_{p1}^{M_{b1}}}, \tag{4-2}$$

where $\hat{\beta}_1$ is the Freundlich/Langmuir "effective" single-component isotherm constant for cesium. The beta parameter for cesium is dependent upon the potassium, sodium, rubidium, and hydrogen feed concentrations. Without loss of generality, we can divide the numerator and denominator of Eq. (4-2) by b_1 to obtain:

$$\overline{C}_{p1} = \frac{a_1' \, c_{p1}^{M_{a1}}}{\beta_1' + c_{p1}^{M_{b1}}}, \tag{4-3}$$

Equation (4-3) uses the resin capacity expressed in terms of mmol per liter of bed volume whereas the resin capacity Q_{Cs} is typically calculated as mmol per gram resin. The VERSE-LC isotherm coefficient a_1' in Eq. (4-3) is therefore computed as:

$$a_1' = \rho_b \, \eta_{df} \, \overline{C}_T, \tag{4-4}$$

where ρ_b is the bed density of the active column in sodium form, g/ml and η_{df} is a resin degradation factor that can be used to lower the total capacity to account for the effects of chemical or radioactive exposure. The final form of the isotherm model as used in VERSE-LC is then:

$$\overline{C}_{pCs} = \eta_{df} \left[\frac{\rho_b \, \overline{C}_T \, c_{pCs}^{M_{aCs}}}{\beta_{Cs} + c_{pCs}^{M_{bCs}}} \right], \tag{4-5}$$

where the prime on β has been dropped to simplify the notation. The composite impact on cesium loading from the other cation competitors is summed up in the beta parameter as

shown above in Eq. (4-2). The degradation factor, η_{df}, is set to unity for fresh resin and less than unity to account for resin aging effects induced by chemical or radioactive exposure.

4.2 The Cesium-CST System

The CST cesium adsorption isotherm used in this study is of the Langmuir form:

$$Q = \frac{a\,[Cs]}{b + [Cs]}$$

where Q is the cesium loading on the CST media in moles/liter bed volume, [Cs] is the total molar cesium concentration in solution, and the isotherm parameters a and b are calculated using the ZAM code. As described by Aleman (2003), the CST total capacity calculated by ZAM (parameter a) was multiplied by a factor of 0.68 to account for the difference between CST powder and the engineered form of the material.

4.3 The Cesium-RF System

Based on our current understanding of the cesium-RF resin system, the competition for cation exchange loading at the resin sites is primarily among cesium, rubidium, potassium, and sodium. From batch equilibrium studies, relative resin affinities are: $Cs^+ > Rb^+ > K^+ > Na^+$. Two cesium isotherm models were used in this study. The "new" Freundlich/Langmuir RF cesium adsorption isotherm is:

$$Q = \frac{a\,[Cs]^{M_a}}{b + [Cs]^{M_b}}$$

where Q is the cesium loading on the RF resin in moles/liter bed volume, [Cs] is the total molar cesium concentration in solution, and the isotherm parameters a, b, M_a and M_b are calculated using the CERMOD code developed at SRNL. The parameters in this isotherm model are based on the most recent experimental data collected by Nash et al. (2006). The second RF cesium adsorption isotherm is the "old" Langmuir form:

$$Q = \frac{a\,[Cs]}{b + [Cs]}$$

where Q is the cesium loading on the RF resin in moles/liter bed volume, [Cs] is the total molar cesium concentration in solution, and the isotherm parameters a and b are calculated using the TMIXP code. Parameterization of this model is based on data collected with RF resin in a previous experimental study conducted by King et al. (2003). Both isotherms are a valid application of the theoretical fits of the data. To distinguish which method better fits the column performance, testing with SRS type feeds is required. Results from both isotherms are shown here in an effort to bracket the expected performance.

5.0 Column Properties

Certain material properties such as resin density and total ionic capacity are unique to the ion-exchange material and vary only between batches. On the other hand, composite properties associated with an ion-exchange column such as bed density and porosity are inherently column specific. Even when different columns are made from the same batch of resin, column properties can vary. The discussion that follows focuses on the column properties required to perform column transport simulations during the loading phase of a cycle.

5.1 Basic Constraint Functions

Based on geometrical considerations, not all densities and porosities are independent. The following two expressions place constraints on the porosities and densities:

$$\varepsilon_t = \varepsilon_b + (1-\varepsilon_b)\varepsilon_p\,, \tag{5-1}$$

and

$$\rho_b = \rho_s(1-\varepsilon_t) = \rho_s(1-\varepsilon_b)(1-\varepsilon_p)\,, \tag{5-2}$$

where

ε_t .....total porosity of column,
ε_b .....bed porosity of column,
ε_p .....pore porosity of resin particles,
ρ_b .....bed density of active column, g/ml
ρ_s .....solid (particle) density of resin, g/ml

For the five variables listed above only three are independent. The various porosities used in Eq. (5-1) are defined as:

$$\varepsilon_b = \frac{V_{void} - V_{pore}}{V_{bed}}; \quad \varepsilon_p = \frac{V_{pore}}{V_{part}}; \quad \varepsilon_t = \frac{V_{void}}{V_{bed}} = \frac{V_{bed} - V_{sld}}{V_{bed}} \tag{5-3}$$

where

V_{bed} .....total volume of active (bed) column, ml
V_{void} .....total volume of voids within active column, ml
V_{pore} .....total volume of pores within particles, ml
V_{part} .....total volume of particles within active column, ml
V_{sld} .....total volume of solid resin within active column, ml

5.2 CST Media Properties

CST physical parameters are the same as those used in the previous SCIX study performed by Aleman (2003):

Particle radius – 172 μm

Particle void fraction – 0.24

Bed void fraction – 0.50

Bed density – 1.0 kg CST media/liter bed volume

The bed void listed above may be somewhat high or, equivalently, the bed density may be somewhat low. These values are conservative for estimating the number of columns required to process the salt solution but will be non-conservative for estimating the total cesium loading used in thermal analysis and dose rates of the column. Lower bed void would increase the bed density leaving the overall mass of CST required to process the dissolved salt cake unchanged. However, lower bed void and the corresponding higher bed density will increase the cesium loading capacity in a single column. We note that the void fractions and bed density give a CST solid density of 2.63 g/cc.

5.3 Spherical RF Resin Properties

Physical parameters for RF resin used in this study are the same as those parameters used by Aleman et al. (2007). The particle size distribution of spherical RF resin from batch 5E-370/641 was characterized in both hydrogen and sodium form using a Microtrac® S3000 at both Battelle-Pacific Northwest Division (PNWD) and Savannah River National Laboratory (SRNL). Results from the PNWD and SRNL measurements are summarized in Fiskum et al. (2006) and Adamson et al. (2006), respectively. For ion-exchange column modeling, the particle size in sodium form is required. Microtrac® particle size data for spherical RF in sodium form was measured by Adamson et al. (2006). The bulk of the particle size distribution fell in the 400 to 600 micron range. PNWD (Fiskum, 2006) reports an average particle diameter of 452 μm for spherical RF in sodium form while SRNL measured an average particle diameter of 461 μm in AP-101 simulant. The average of these two values, 457 μm, was used as the RF particle diameter in the VERSE-LC calculations. This value corresponds to an average particle radius of 228.5 μm which is approximately 30% larger than the CST particle radius.

The particle ("skeletal") density of the resin in sodium form was also measured during pilot scale hydraulic testing by Adamson et al. (2006). For the column modeling presented in this report an average particle density of 1.615 g/ml for Na^+-form RF was employed.

The actual amount of resin present within a column is a parameter of prime importance with respect to column performance. For the column studies in this report, an estimate of column bed density was derived from data reported in the study by Nash et al. (2006). In that study, the dry mass of RF resin in H^+-form (2.886 g) and the bed volume during loading (11.26 ml)

were measured. The column bed density (ion-exchange material bulk density) is then computed as:

$$\rho_b = \frac{m_{resin}}{V_{bed}} = \frac{2.886}{11.26} = 0.2563\,\text{g/ml} \tag{5-4}$$

The bed density calculated in Eq. (5-4) represents our nominal value for RF resin in H^+-form. A factor of 1.25 (Nash et al., 2006) can be applied to convert the resin mass from H^+-form to Na^+-form.

The bed void fraction for a nominal sample of RF resin was provided by M. Thorson of the RPP-WTP project (personal communication 2006):

$$\varepsilon_b = \frac{V_{void} - V_{pore}}{V_{bed}} = 0.42 \tag{5-5}$$

The RF bed porosity given in Eq. (5-5) represents our nominal value. The average measured porosity for dense packing of mono-sized hard spheres is 0.363 as reported by German (1989). Greater packing fractions (or smaller bed porosities) can be achieved when multi-sized spheres are employed. The particle size distribution for the spherical RF material was quite narrow with the bulk of the distribution in the range 400 to 600 microns so a void volume somewhat greater than that for uniform hard spheres is reasonable.

Based on Eq. (5-2) the particle void fraction of the resin particles is known once the particle density, bed density and bed porosity are specified. Using the values presented in the above subsections, the particle void fraction of the resin particles becomes:

$$\varepsilon_p = 1 - \rho_b / \rho_s (1 - \varepsilon_b) = 1 - 1.25 \text{x} 0.2563 / 1.615 (1 - 0.42) = 0.6579 \tag{5-6}$$

The particle void fraction computed by Eq. (5-6) represents our nominal value for RF resin.

6.0 Solution Properties and Pore Diffusion

6.1 Molecular Diffusion Coefficients

Molecular diffusion coefficients are important in determining key dimensionless numbers (e.g., Schmidt Number, Sc) used in various constitutive law correlations for column transport modeling. They also provide an upper bound for pore diffusion coefficients. Binary diffusion (sometimes referred to as free stream) coefficients of electrolytes originating from a single salt in solution under dilute conditions can be reasonably estimated using the Nernst-Haskell equation (Reid et al., 1977):

$$D_{\pm}^{\infty} = \left(\frac{RT}{\mathbb{F}^2}\right)\left[\frac{\frac{1}{z_+}+\frac{1}{z_-}}{\frac{1}{\lambda_+^o}+\frac{1}{\lambda_-^o}}\right], \tag{6-1}$$

where

$D_{\pm}^{\infty}$ ..... binary diffusion coefficient at infinite dilution, cm^2/s

λ_+^o, λ_-^o ..... limiting ionic conductivity for cation and anion, mhos/equivalent

z_+, z_- ..... valences of cation and anion, respectively

$\mathbb{F}$ ..... Faraday constant, 96,500 C/g-equivalent

R ..... gas constant, 8.314 J/gmole-K

T ..... absolute temperature, K

Limiting ionic conductivities at 25 °C and infinite dilution for the various ions of interest in this study are tabulated in Table 6-1. Most of the conductivities were calculated using the correlation shown in Eq. (6-2) which is from Anderko and Lencka (1997):

$$\ln\left[\lambda^0(T)\eta(T)\right] = A + B/T, \tag{6-2}$$

where

A, B ..... correlation coefficients

$\eta(T)$ ..... viscosity of pure water in Pa-s (cP/1000)

The correlation coefficients A and B are listed in Table 6-1. In a few instances where the anion was not included in the Anderko correlation, literature values of the ionic conductivity (Reid et al., 1977; Perry, 1973, Glasstone and Lewis, 1960) were used.

Using Eq. (6-1) and the limiting ionic conductivities provided in Table 6-2, the binary molecular diffusion coefficient for certain single salts within an aqueous phase can be computed. To account for fluid property differences between a salt solution and pure water, a correction factor is applied. Based on hydrodynamic theory, the following expression,

typically referred to as the Stokes-Einstein equation, is obtained (Bird et al., 1960, page 514):

$$\frac{D_{AB}\,\mu_B}{\kappa T} = \frac{1}{6\pi R_A}, \tag{6-3}$$

where

D_{AB} ..... binary diffusion coefficient for A diffusing through solvent B
μ_B ..... dynamic viscosity of solvent mixture
R_A ..... radius of diffusing particle
κ ..... Boltzmann's constant

Based on Eq. (6-3), the ratio of the dynamic viscosity of pure water (representing conditions at infinite dilution) to that of the salt solution is a correction factor that can be applied to the molecular diffusion coefficients computed from Eq. (6-1) to estimate binary diffusion coefficients in the salt solution.

Binary pairs for the dominant cation-anion pairs (i.e., cesium paired with an individual anion) where the anions considered are based on the composition of the various salts and their computed binary molecular diffusion coefficients are listed in Table 6-2 at 25 °C. An overall diffusion coefficient for cesium was estimated as the average of the individual cesium pair diffusion coefficients weighted by the mole fraction of each pair in solution. Diffusion coefficients calculated using this method for the feed solutions used in this study are listed in Table 6-3.

6.2 Waste Solution Density and Viscosity

Two other physical properties needed for VERSE-LC simulations are the density and viscosity of the bulk liquid phase. Dissolved salt solution density and viscosity vary depending on temperature and composition. The density and viscosity of the dissolved saltcake feeds used in the VERSE-LC calculations were computed using OLI Systems, Inc. Stream Analyzer™ Version 2.0. The solution density and viscosity calculated for the five feed solutions at the three temperatures of interest are listed in Table 6-3.

6.3 Particle Kinetics Parameters

The rate of cesium uptake controls the transient behavior of the column. As the rate of cesium uptake by the resin is increased, the breakthrough curve becomes sharper (steeper) and utilization of the resin is increased. Thus, accurate evaluation of the parameters that control the rate of cesium uptake is essential for modeling column performance. We assume that the rate of chemical adsorption (i.e. exchange of ions at a surface site) is very fast when compared to the rates of diffusion within the pore fluid and mass transfer across the liquid film at the outer boundary of the particles. Hence, within the resin particles, the rate of cesium uptake is dominated by intra-particle diffusion. Diffusion within the particles is governed by the pore diffusivity, particle porosity, and size of the particles. Externally, the

rate of cesium transport from the inter-particle fluid to the particle surface depends upon the film mass transfer coefficient. Due to their influence on the rate of cesium uptake and, thus, the transient behavior of the column, the particle porosity, pore diffusivity, particle radius and the film mass transfer coefficient are referred to as *kinetics parameters*.

As shown in Section 7, in VERSE-LC the film mass transfer coefficient is calculated from a correlation developed by Wilson and Geankoplis (1966). Particle porosity is available from the data presented in Section 5. Therefore, of the kinetics parameters, the pore diffusivity and diffusion length remain to be determined. In the VERSE-LC code, the model for intra-particle diffusion assumes that the particles are spheres of uniform radius. To apply the VERSE-LC model it is therefore necessary to determine an average radius from the particle size distribution (discussed in Section 5) and an effective pore diffusivity.

We assume that the pore sizes are large relative to the size of the migrating ions of interest and that pore diffusion coefficients should not be significantly lower than their bulk or free stream values. However, some level of reduced diffusion in the pores is expected resulting from bends along the pore paths that are generally accounted for by a particle tortuosity factor τ defined as:

$$D_p = \frac{D_\infty}{\tau} \tag{6-4}$$

where

D_p ..... pore diffusivity of Cs^+ in the particle pore, cm^2/min

D_∞ ..... bulk diffusivity of Cs^+ in the free stream, cm^2/min

τ ..... particle tortuosity factor

Tortuosity factors for CST and RF resin have been determined by analyzing experimental data obtained at SRNL (Hamm et al., 2002 for CST, Aleman et al., 2007 for RF). In these studies, it was found that using $\tau = 5$ for CST and $\tau = 3$ for RF gave reasonable results.

Table 6-1. Limiting ionic conductivity fitting coefficients and calculated conductivities in water at 25 °C.

Ion		Ionic valance	A	B	Limiting ionic conductivity MHOS/equivalent
Cations	H^+	1	-3.9726	837.79	351.05
	Na^+	1	-3.3594	75.492	50.27
	K^+	1	-3.5730	254.36	73.97
	Rb^+	1	-3.6517	294.79	78.34
	Cs^+	1	-3.6512	291.42	77.46
Anions	OH^-	-1	-3.3346	468.13	192.30
	NO_3^-	-1	-3.6743	277.43	72.22
	NO_2^-	-1			72.00[b]
	F^-	-1			55.40[b]
	Cl^-	-1	-3.4051	216.03	76.94
	I^-	-1	-3.5660	265.28	77.27
	CO_3^{-2}	-2			69.30[b]
	SO_4^{-2}	-2	-2.9457	90.983	80.08
	PO_4^{-2}	-2			75.00[a]
	$Al(OH)_4^-$	-1			70.00[a]

[a] Estimated value, [b] Literature value

Table 6-2. Best estimate binary molecular diffusion coefficients at 25 °C for a solution containing essentially only cesium cations and anion of one particular species.

Cesium Ion Pairs	Molecular diffusion coef. in water (cm^2/min)	Molecular diffusion coef. in 5 M Na AP-101 waste (cm^2/min)
$Cs^+ - OH^-$	1.764E-03	5.006E-04
$Cs^+ - NO_3^-$	1.194E-03	3.388E-04
$Cs^+ - NO_2^-$	1.192E-03	3.383E-04
$Cs^+ - Al(OH)_4^-$	1.175E-03	3.333E-04
$Cs^+ - CO_3^{-2}$	8.763E-04	2.487E-04
$Cs^+ - SO_4^{-2}$	9.433E-04	2.677E-04
$Cs^+ - PO_4^{-2}$	9.129E-04	2.591E-04
$Cs^+ - Cl^-$	1.233E-03	3.499E-04
$Cs^+ - F^-$	1.032E-03	2.928E-04
$Cs^+ - I^-$	1.236E-03	3.507E-04

Table 6-3. Feed solution physical properties.

Tank	Temperature, C	Density, g/ml	Viscosity, Poise	Cs D_∞,[1] cm^2/min
1	**25**	1.240	0.0239	4.89E-04
	35	1.235	0.0191	5.13E-04
	45	1.229	0.0157	5.33E-04
2	**25**	1.246	0.0214	5.23E-04
	35	1.238	0.0172	5.43E-04
	45	1.230	0.0142	5.64E-04
3	**25**	1.245	0.0183	6.01E-04
	35	1.237	0.0148	6.20E-04
	45	1.229	0.0123	6.40E-04
37	**25**	1.232	0.0259	4.74E-04
	35	1.226	0.0204	5.02E-04
	45	1.220	0.0166	5.26E-04
41	**25**	1.234	0.0254	4.77E-04
	35	1.228	0.0201	5.04E-04
	45	1.222	0.0164	5.28E-04

[1] for CST $D_p = D_\infty/5$; for RF $D_p = D_\infty/3$

7.0 Film Diffusion and Axial Dispersion

In this section we present the correlations used to define: (1) mass transfer across the liquid film separating the bed fluid from its neighboring particle pore fluid and (2) axial dispersion along the bed length.

7.1 Film Diffusion

For laboratory-scale column tests and the proposed full-scale facility the Reynolds number range is approximately 0.1 to 1.0. With respect to published literature this is a very low Reynolds number range. Numerous mass transfer correlations exist as discussed by Foo and Rice (1975). One of the correlations compared in Foo and Rice (1975) is one developed by Wilson and Geankoplis (1966) based on low Reynolds number data. Large variations between correlations exist; however, the sensitivity of VERSE-LC results to the film coefficient has typically been low. VERSE-LC has the Wilson and Geankoplis (1966) correlation as an option and this correlation falls somewhat within the spread of available low Reynolds number data. Therefore, we have chosen it for all the column simulations in this report. For each ion species considered, the Wilson and Geankoplis (1966) correlation is expressed as:

$$J \equiv \left[\frac{k_{fi}}{u\varepsilon_b}\right] Sc_i^{2/3} = \frac{1.09}{\varepsilon_b} Re^{-2/3}. \qquad (7\text{-}1)$$

In Eq. (7-1), the Reynolds number is defined as:

$$Re \equiv \frac{2R_p \rho_w u \varepsilon_b}{\mu_w},$$

and the Schmidt number for each species is defined as:

$$Sc_i \equiv \frac{\mu_w}{\rho_w D_i^{\infty}}.$$

A standard deviation of approximately 25% is reported for Eq. (7-1) by Wilson and Geankoplis (1966), while from comparison to the various correlations presented by Foo and Rice (1975) a standard deviation of 100% to 200% is observed.

7.2 Axial Dispersion

Axial dispersion in packed columns is the result of mechanical dispersion added onto molecular diffusion. At practical flow rates mechanical dispersion dominates. For well-packed columns of sufficient diameter such that wall effects (channeling) are minimal a variety of correlations exist for long column performance. A brief discussion of minimum column sizing is presented in Brooks (1994).

In the low Reynolds number range of interest, the Chung and Wen (1968) correlation is applicable for sufficiently large columns (large diameter and length). The axial dispersion coefficient E_b (cm^2/min) is expressed as:

$$E_b = \frac{2R_p u \varepsilon_b}{0.2 + 0.011\,Re^{0.48}}, \tag{7-2}$$

The standard deviation of this correlation based on all available data points was reported to be 46%. Equation (7-2) applies for sufficiently large columns and correction factors must be considered for columns with small diameters and/or short active bed lengths.

8.0 Column Performance Case Studies

Table 8-1 lists the case studies run for each of the five tank compositions used in this study (dissolved salt cake in Tanks 1-3, 37 and 41). Case 1 represents nominal operating conditions. Case 2 is operation at lower flow, which sharpens the breakthrough curve and allows more salt solution to be processed during each cycle at the expense of longer operating times. Case 3 is operation at higher flow, which spreads out the breakthrough curve and decreases the amount of salt solution that can be processed during each cycle with a significant savings in operating time. Case 4 is operation with a short column while Case 5 uses a long column. Cases 6 and 7 are operation at nominal column length and feed flow at elevated temperatures of 35 °C and 45 °C, respectively. Operation at elevated temperature reduces overall ion-exchange capacity. Case 8 reduces the capacity of the ion-exchange resin to 80% of the nominal value to simulate resin degradation from chemical and radiation exposure. The reduced capacity is applied throughout the run and not introduced gradually. Case 8 was only run for the RF resin. The 20% reduction is based on the results in Figure 4-11 of the report by Duffey and Walker (2006) which shows approximately a 20% reduction in RF resin capacity after 100 MRad exposure.

A simple matrix showing the pattern of column lengths and feed flows tested is shown in Table 8-2. Note that the TTR specified running the higher temperature cases (6 and 7) at 5 gpm; however, it appeared that 10 gpm was the nominal flow. The percent reduction in throughput is expected to be consistent between conditions, so is was not necessary to run the full matrix at this time.

Table 8-1. VERSE-LC case studies run for each tank composition.

Case	Temperature, C	Feed Flowrate, gpm	Column Length, feet	Capacity, Percent Nominal
1	25	10	15	100%
2	25	5	15	100%
3	25	20	15	100%
4	25	10	10	100%
5	25	10	25	100%
6	35	10	15	100%
7	45	10	15	100%
8	25	10	15	80%

Table 8-2. VERSE-LC case study matrix of column lengths and feed flows

Case Run Matrix		Column Length, Feet		
		10	**15**[1]	**25**
Feed Flow, gpm	**5**		2	
	10[1]	4	1, 6, 7, 8[2]	5
	20		3	

[1]Nominal value [2]Run for RF resin only

9.0 CST Results

9.1 CST Isotherm Parameters

Table 9-1 provides a list of isotherm parameters (*a* and b) used in the VERSE-LC model for the CST column calculations for each of the compositions tested. In the first column the feed concentration of Cs in molarity and Cs^{137} in pCi/ml are listed along with the tank number. The fifth and sixth columns in the table show the total cesium loading on the CST media at equilibrium (Q) and the corresponding curies per liter of packed bed volume (BV). That is, these columns show the cesium loading in a fully loaded column. Since the lead column is typically very close to being fully loaded during column processing, the curie loadings reported in column six of Table 9-1 provide an estimate of the maximum heat load on the column for thermal analysis. Tank 1 and Tank 37 produce the highest curie loadings on the ion-exchange columns. The highest estimated curie loading is 257 Ci/(liter of bed volume) for Tank 37 at 25 °C. As explained below, this is 115% of the nominal value. Curie loadings in the ion-exchange columns with feed from Tanks 2 and 41 are both approximately 10 times lower than the maximum. The cesium loadings listed in columns five and six were calculated using the nominal bed density of 1.0 g resin/ml BV (values of the bed density from 0.9 to 1.13 are estimated by Hamm et al., 2002). Since the nominal bed density corresponds to a bed void fraction of 0.5 which is at the high end of the projected values, cesium loadings at 15% greater resin loading are also listed in the last column of Table 9-1. These values are intended to provide a conservative estimate of the expected cesium loading on CST media for calculating column thermal behavior. The lower cesium loading based on the nominal bed density provides a conservative estimate of loading for the purpose of estimating CST requirements and column cycles. Therefore, the nominal bed density was used for the column simulations and the higher loading is reported only for use in heat transfer calculations.

Maximum curie loadings using the nominal bed density are summarized in Table 9-2. As shown in the table, trends in loading generally correlate with the feed cesium concentrations under these conditions.

Table 9-1. CST isotherm parameters.

Tank # Total [Cs] [^{137} Cs]	Temp., C	*a*	b	Q, moles Cs/L BV	Q, Ci Cs/ L BV	115% Q, Ci Cs/ L BV
1	**25**	0.3944	5.288E-04	1.01E-01	183.34	210.84
1.81×10^{-4} M	**35**	0.3940	5.693E-04	9.51E-02	173.30	199.30
3.30×10^{8} pCi /ml	**45**	0.3941	6.163E-04	8.95E-02	163.12	187.59
2	**25**	0.3945	6.764E-04	9.67E-03	25.83	29.70
1.70×10^{-5} M	**35**	0.3943	7.518E-04	8.72E-03	23.29	26.78
4.54×10^{7} pCi /ml	**45**	0.3942	8.240E-04	7.97E-03	21.28	24.47
3	**25**	0.3944	6.402E-04	3.56E-02	87.99	101.19
6.35×10^{-5} M	**35**	0.3945	7.632E-04	3.03E-02	74.91	86.15
1.57×10^{8} pCi /ml	**45**	0.3943	8.899E-04	2.63E-02	64.93	74.67
37	**25**	0.3944	2.834E-04	1.09E-01	223.67	257.22
1.08×10^{-4} M	**35**	0.3946	3.717E-04	8.88E-02	182.60	209.99
2.22×10^{8} pCi /ml	**45**	0.3945	4.807E-04	7.24E-02	148.77	171.09
41	**25**	0.3944	3.003E-04	9.65E-03	19.99	22.99
7.53×10^{-6} M	**35**	0.3945	3.923E-04	7.43E-03	15.39	17.70
1.56×10^{7} pCi /ml	**45**	0.3944	5.056E-04	5.79E-03	11.99	13.79

Table 9-2. Maximum Curie loadings on CST Media.
(Ci Cs^{137}/Liter Bed Volume)

Tank	Feed Cs [M]	Feed Cs^{137} [pCi/ml]	Temperature °C		
			25	**35**	**45**
1	1.81×10^{-4}	3.30×10^{8}	183.34	173.30	163.12
2	1.70×10^{-5}	4.54×10^{7}	25.83	23.29	21.28
3	6.35×10^{-5}	1.57×10^{8}	87.99	74.91	64.93
37	1.08×10^{-4}	2.22×10^{8}	223.67	182.60	148.77
41	7.53×10^{-6}	1.56×10^{7}	19.99	15.39	11.99

9-2 CST Ion-exchange Column Modeling Results

Tables 9-3 through 9-15 summarize the results from VERSE-LC column modeling calculations for SCIX using CST media. All of the calculations assume a two-column configuration. During the first cycle, both columns contain fresh media. After the first cycle in all subsequent cycles, the partially loaded second or lag column is placed into the lead position and a clean column is placed into the lag position at the start of the cycle. Since a partially loaded column is in the lead position, after the first cycle less waste volume is processed per cycle. Each cycle is run until the integral sum average cesium concentration in the effluent collected from the lag column reaches the saltstone feed limit of 45 nCi/g.

Tables 9-3 through 9-7 list the volumes of waste solution processed during the first three ion-exchange cycles for each of the five tank compositions modeled. The total waste volume processed and the time it would take to run the three cycles are shown in the last two rows of each table. The times represent the amount of time it would take to process the waste volume through the ion-exchange column based on the given flow rate. The results for Tanks 1-3 are all very similar whereas larger volumes of dissolved salt solution from Tanks 37 and 41 can be processed per cycle.

Tables 9-8 through 9-14 list the estimated time it would take to process the waste volumes in each tank through the ion-exchange columns and the number of columns used. The amount of CST media used is also given in metric tons (MT). The ion-exchange processing time is obtained by dividing the waste volume processed by the flow rate through the column and, therefore, only represents the time to run the loading phase of the cycle at full flow. Since, as shown in Tables 9-3 through 9-7, in all cases, the second cycle processed slightly less waste volume than the third cycle, it was assumed that the volume of waste processed during the second cycle would also be processed in subsequent cycles to conservatively estimate the total cycles required and columns used. Tables 9-12 and 9-14 provide results for Tanks 37 and 41 for the estimated volume of solution in each tank that it is planned to process while Tables 9-11 and 9-13 show results based on the total volume in these two tanks. The mass of CST was calculated using the total column volume required and a bulk solid density of 1.0 g/ml. The CST usage is summarized in Table 9-15.

Bucket average breakthrough curves from VERSE-LC modeling for the nominal case (25 °C, 10 gpm, 15 ft column) for each of the five tanks are plotted in Figures 9-1 through 9-5. We note that the breakthrough curves are relatively sharp. For Tanks 1-3, the width of the breakthrough front from 1.0 nCi/g to 45 nCi/g is between 70,000 and 100,000 gallons while for tanks 37 and 41 the width is on the order of 160,000 gallons and 210,000 gallons, respectively. At a flow rate of 10 gpm, the corresponding breakthrough time is 117 hours for Tanks 1-3 and 267 hours for Tanks 37 and 41. To be conservative during actual operations, the run could be terminated at a lower bucket average effluent concentration without sacrificing much volume.

Column profiles showing the concentration of cesium in the liquid phase down the lead and lag columns at the end of the first cycle for the five tank compositions tested at the nominal

operating conditions are shown in Figures 9-6 through 9-10. We find that in all cases, the lead column is very close to being fully loaded at the end of the first cycle. Therefore, the assumption of a fully loaded column used to estimate maximum cesium loadings in Tables 9-1 and 9-2 is reasonable and slightly conservative. Figures 9-11 through 9-15 plot the breakthrough curves (instantaneous C/C_0) from the lead and lag ion-exchange columns during the third cycle for the nominal case for each tank. Note that graphs plotting C/C_0 can be applied to both total cesium or Cs^{137}.

Results from VERSE-LC simulations for Cases 1–5 with a system using a single CST ion-exchange column are presented in Appendix A. The volume of dissolved salt solution that can be processed in each single-column cycle, the number of cycles required to process the total planned waste volume, cesium breakthrough curves and cesium profiles in the ion-exchange columns at the end of a cycle are shown for each tank.

Table 9-3. Tank 1 waste volume in thousands of gallons processed in three CST ion-exchange cycles.

Case	**1**	**2**	**3**	**4**	**5**	**6**	**7**
	15 ft	15 ft	15 ft	10 ft	25 ft	15 ft	15 ft
	10 gpm	5 gpm	20 gpm	10 gpm	10 gpm	10 gpm	10 gpm
	25 °C	25 °C	25 °C	25 °C	25 °C	35 °C	45 °C
Cycle 1	328.0	395.7	242.9	185.7	634.9	310.7	291.5
Cycle 2	210.9	228.7	179.1	129.5	375.3	199.0	185.8
Cycle 3	228.5	238.4	197.3	142.8	394.9	215.1	200.8
Total	767.4	862.8	619.3	458.0	1405.1	724.8	678.1
Time, Days	53.3	119.8	21.5	31.8	97.6	50.3	47.1

Table 9-4. Tank 2 waste volume in thousands of gallons processed in three CST ion-exchange cycles.

Case	**1**	**2**	**3**	**4**	**5**	**6**	**7**
	15 ft	15 ft	15 ft	10 ft	25 ft	15 ft	15 ft
	10 gpm	5 gpm	20 gpm	10 gpm	10 gpm	10 gpm	10 gpm
	25 °C	25 °C	25 °C	25 °C	25 °C	35 °C	45 °C
Cycle 1	319.8	374.1	250.2	186.7	603.3	290.8	267.8
Cycle 2	193.3	211.1	168.2	119.8	344.8	174.9	160.5
Cycle 3	209.0	222.6	186.1	131.9	366.0	188.9	173.4
Total	722.1	807.8	604.5	438.4	1314.0	654.6	601.7
Time, Days	50.1	112.2	21.0	30.4	91.3	45.5	41.8

Table 9-5. Tank 3 waste volume in thousands of gallons processed in three CST ion-exchange cycles.

Case	1	2	3	4	5	6	7
	15 ft	15 ft	15 ft	10 ft	25 ft	15 ft	15 ft
	10 gpm	5 gpm	20 gpm	10 gpm	10 gpm	10 gpm	10 gpm
	25 °C	25 °C	25 °C	25 °C	25 °C	35 °C	45 °C
Cycle 1	317.8	375.4	246.1	184.5	604.0	270.0	234.2
Cycle 2	196.7	215.2	170.5	121.6	351.8	166.5	143.7
Cycle 3	212.8	226.8	188.6	133.7	373.1	180.0	155.5
Total	727.4	817.5	605.1	439.8	1329.0	616.5	533.4
Time, Days	50.5	113.5	21.0	30.5	92.3	42.8	37.0

Table 9-6. Tank 37 waste volume in thousands of gallons processed in three CST ion-exchange cycles.

Case	1	2	3	4	5	6	7
	15 ft	15 ft	15 ft	10 ft	25 ft	15 ft	15 ft
	10 gpm	5 gpm	20 gpm	10 gpm	10 gpm	10 gpm	10 gpm
	25 °C	25 °C	25 °C	25 °C	25 °C	35 °C	45 °C
Cycle 1	615.7	736.0	459.1	350.5	1184.0	487.9	387.9
Cycle 2	390.4	418.2	334.9	241.0	688.9	309.6	246.0
Cycle 3	420.4	434.5	368.6	264.8	721.6	335.3	266.7
Total	1426.6	1588.7	1162.6	856.2	2594.4	1132.9	900.6
Time, Days	99.1	220.7	40.4	59.5	180.2	78.7	62.5

Table 9-7. Tank 41 waste volume in thousands of gallons processed in three CST ion-exchange cycles.

Case	1	2	3	4	5	6	7
	15 ft	15 ft	15 ft	10 ft	25 ft	15 ft	15 ft
	10 gpm	5 gpm	20 gpm	10 gpm	10 gpm	10 gpm	10 gpm
	25 °C	25 °C	25 °C	25 °C	25 °C	35 °C	45 °C
Cycle 1	767.5	883.0	614.5	454.2	1428.8	598.9	468.4
Cycle 2	448.9	486.1	396.0	280.1	796.8	348.5	271.2
Cycle 3	484.8	512.0	437.4	307.3	843.6	375.3	291.7
Total	1701.2	1881.2	1448.0	1041.7	3069.2	1322.7	1031.3
Time, Days	118.1	261.3	50.3	72.3	213.1	91.9	71.6

Table 9-8. Estimated parameters required to process 1.87×10^6 gallons of Tank 1 salt solution with CST.

Case	1	2	3	4	5	6	7
	15 ft	15 ft	15 ft	10 ft	25 ft	15 ft	15 ft
	10 gpm	5 gpm	20 gpm	10 gpm	10 gpm	10 gpm	10 gpm
	25 °C	25 °C	25 °C	25 °C	25 °C	35 °C	45 °C
Days	129.9	259.7	64.9	129.9	129.9	129.9	129.9
Fractional Columns	9.23	8.40	10.98	14.90	5.24	9.75	10.41
Whole Columns	10	9	11	15	6	10	11
CST (MT)	16.34	14.71	17.98	16.34	16.34	16.34	17.98

Table 9-9. Estimated parameters required to process 2.08×10^6 gallons of Tank 2 salt solution with CST.

Case	1	2	3	4	5	6	7
	15 ft	15 ft	15 ft	10 ft	25 ft	15 ft	15 ft
	10 gpm	5 gpm	20 gpm	10 gpm	10 gpm	10 gpm	10 gpm
	25 °C	25 °C	25 °C	25 °C	25 °C	35 °C	45 °C
Days	144.4	288.9	72.2	144.4	144.4	144.4	144.4
Fractional Columns	11.02	10.03	12.77	17.70	6.22	12.15	13.21
Whole Columns	12	11	13	18	7	13	14
CST (MT)	19.61	17.98	21.25	19.61	19.07	21.25	22.88

Table 9-10. Estimated parameters required to process 2.09×10^6 gallons of Tank 3 salt solution with CST.

Case	1	2	3	4	5	6	7
	15 ft	15 ft	15 ft	10 ft	25 ft	15 ft	15 ft
	10 gpm	5 gpm	20 gpm	10 gpm	10 gpm	10 gpm	10 gpm
	25 °C	25 °C	25 °C	25 °C	25 °C	35 °C	45 °C
Days	145.1	290.3	72.6	145.1	145.1	145.1	145.1
Fractional Columns	10.93	9.91	12.71	17.57	6.16	12.85	14.83
Whole Columns	11	10	13	18	7	13	15
CST (MT)	17.98	16.34	21.25	19.61	19.07	21.25	24.52

Table 9-11. Estimated parameters required to process 4.10×10^6 gallons of Tank 37 salt solution with CST.

Case	1	2	3	4	5	6	7
	15 ft	15 ft	15 ft	10 ft	25 ft	15 ft	15 ft
	10 gpm	5 gpm	20 gpm	10 gpm	10 gpm	10 gpm	10 gpm
	25 °C	25 °C	25 °C	25 °C	25 °C	35 °C	45 °C
Days	284.7	569.4	142.4	284.7	284.7	284.7	284.7
Fractional Columns	10.85	10.01	12.77	17.46	6.19	13.58	17.00
Whole Columns	11	11	13	18	7	14	18
CST (MT)	17.98	17.98	21.25	19.61	19.07	22.88	29.42

Table 9-12. Estimated parameters required to process 1.00×10^6 gallons of Tank 37 salt solution with CST.

Case	1	2	3	4	5	6	7
	15 ft	15 ft	15 ft	10 ft	25 ft	15 ft	15 ft
	10 gpm	5 gpm	20 gpm	10 gpm	10 gpm	10 gpm	10 gpm
	25 °C	25 °C	25 °C	25 °C	25 °C	35 °C	45 °C
Days	69.4	138.9	34.7	69.4	69.4	69.4	69.4
Fractional Columns	2.91	2.59	3.51	4.60	1.69	3.57	4.40
Whole Columns	3	3	4	5	2	4	5
CST (MT)	4.90	4.90	6.54	5.45	5.45	6.54	8.17

Table 9-13. Estimated parameters required to process 3.48×10^6 gallons of Tank 41 salt solution with CST.

Case	1	2	3	4	5	6	7
	15 ft	15 ft	15 ft	10 ft	25 ft	15 ft	15 ft
	10 gpm	5 gpm	20 gpm	10 gpm	10 gpm	10 gpm	10 gpm
	25 °C	25 °C	25 °C	25 °C	25 °C	35 °C	45 °C
Days	241.7	483.3	120.8	241.7	241.7	241.7	241.7
Fractional Columns	7.96	7.29	9.13	12.71	4.52	10.19	13.03
Whole Columns	8	8	10	13	5	11	14
CST (MT)	13.08	13.08	16.34	14.16	13.62	17.98	22.88

Table 9-14. Estimated parameters required to process 0.19×10^6 gallons of Tank 41 salt solution with CST.

Case	1	2	3	4	5	6	7
	15 ft	15 ft	15 ft	10 ft	25 ft	15 ft	15 ft
	10 gpm	5 gpm	20 gpm	10 gpm	10 gpm	10 gpm	10 gpm
	25 °C	25 °C	25 °C	25 °C	25 °C	35 °C	45 °C
Days	13.2	26.4	6.6	13.2	13.2	13.2	13.2
Fractional Columns	0.63	0.52	0.82	0.96	0.39	0.75	0.90
Whole Columns	1	1	1	1	1	1	1
CST (MT)	1.63	1.63	1.63	1.09	2.72	1.63	1.63

Table 9-15. Estimated metric tons of CST required to process planned salt solution.

Case	1	2	3	4	5	6	7
	15 ft	15 ft	15 ft	10 ft	25 ft	15 ft	15 ft
	10 gpm	5 gpm	20 gpm	10 gpm	10 gpm	10 gpm	10 gpm
	25 °C	25 °C	25 °C	25 °C	25 °C	35 °C	45 °C
Tank 1	16.3	14.7	18.0	16.3	16.3	16.3	18.0
Tank 2	19.6	18.0	21.2	19.6	19.1	21.2	22.9
Tank 3	18.0	16.3	21.2	19.6	19.1	21.2	24.5
Tank 37	4.9	4.9	6.6	5.5	5.5	6.6	8.2
Tank 41	1.6	1.6	1.6	1.1	2.7	1.6	1.6
Tanks 1 – 3	53.9	49.0	60.5	55.6	54.5	58.8	65.4
All 5 Tanks	60.4	55.5	68.6	62.1	62.7	66.9	75.2

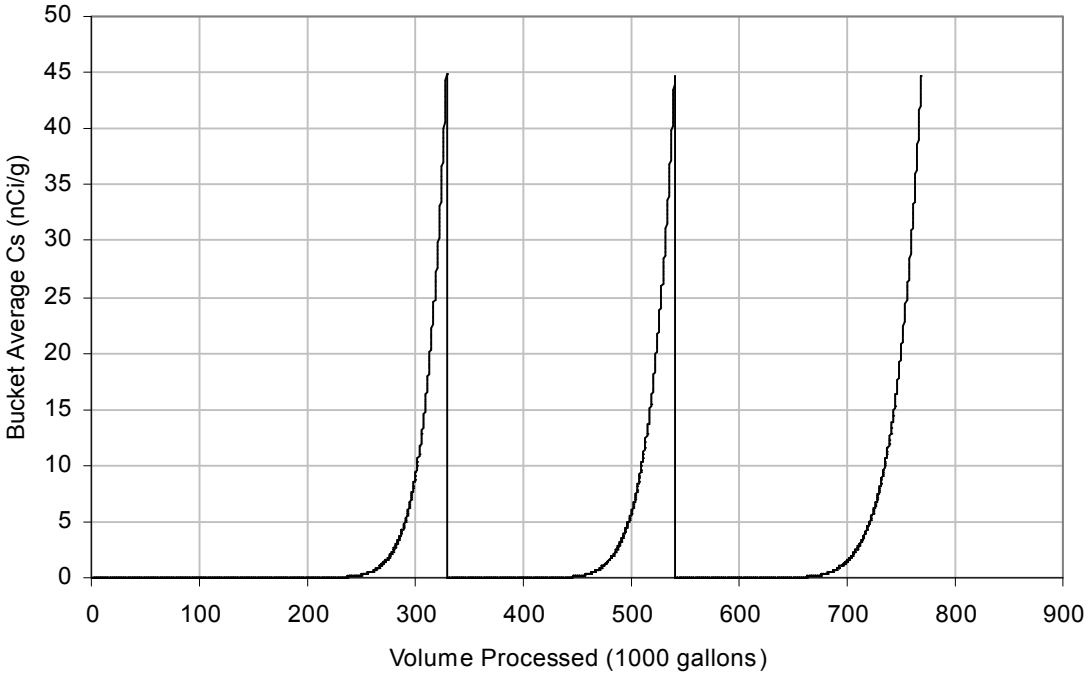

Figure 9-1. Breakthrough curves for Tank 1 nominal case with CST media.

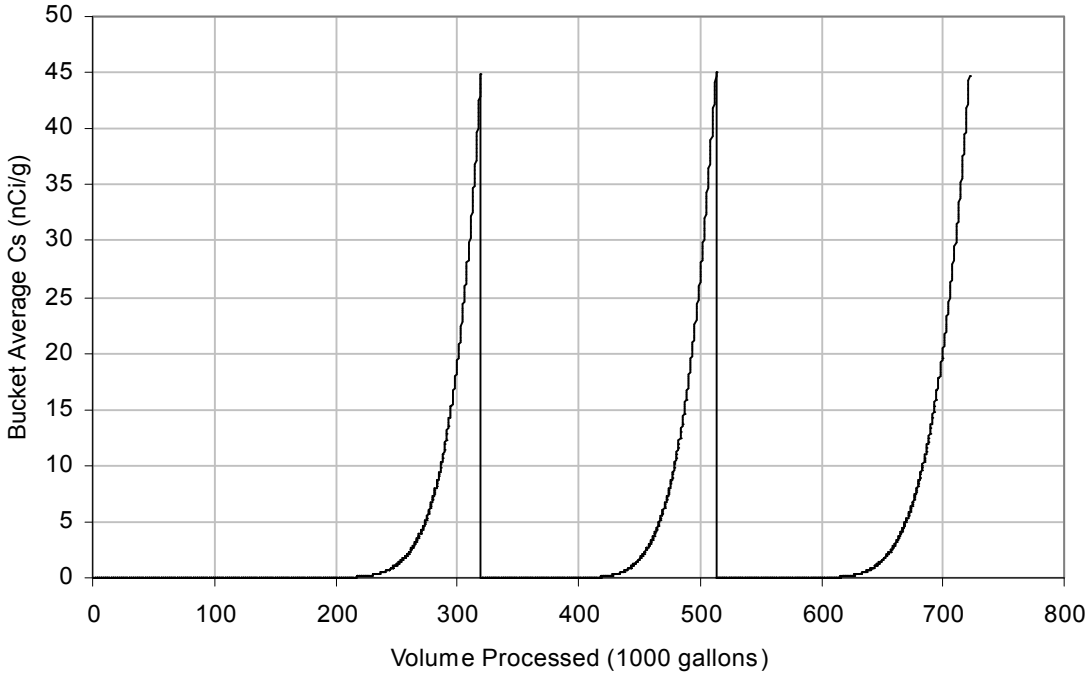

Figure 9-2. Breakthrough curves for Tank 2 nominal case with CST media.

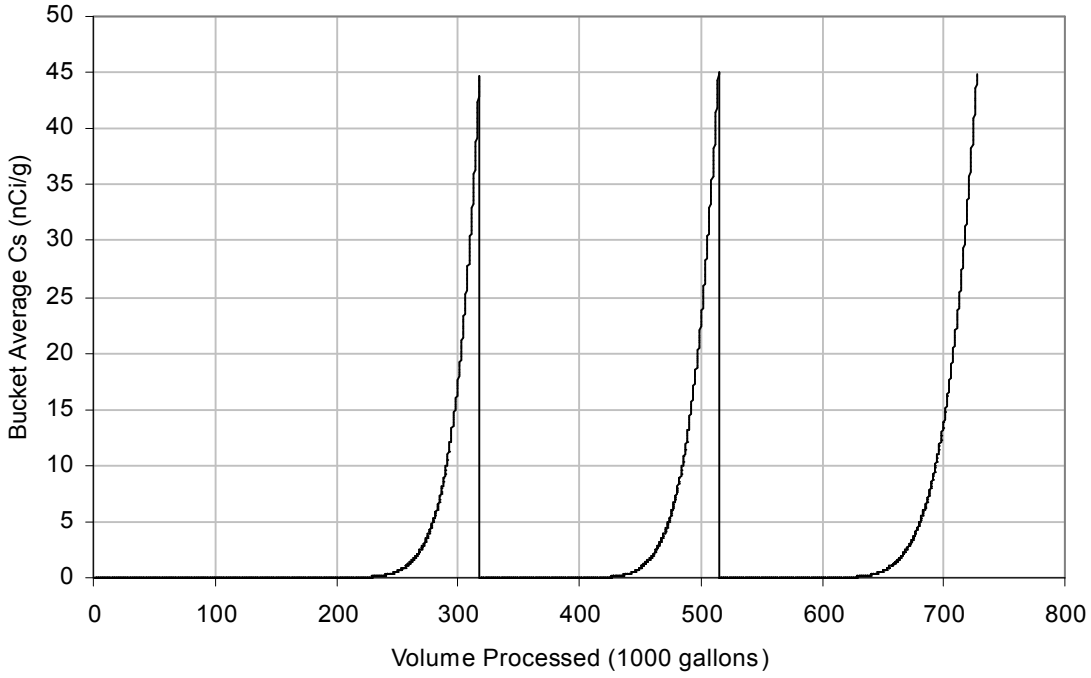

Figure 9-3. Breakthrough curves for Tank 3 nominal case with CST media.

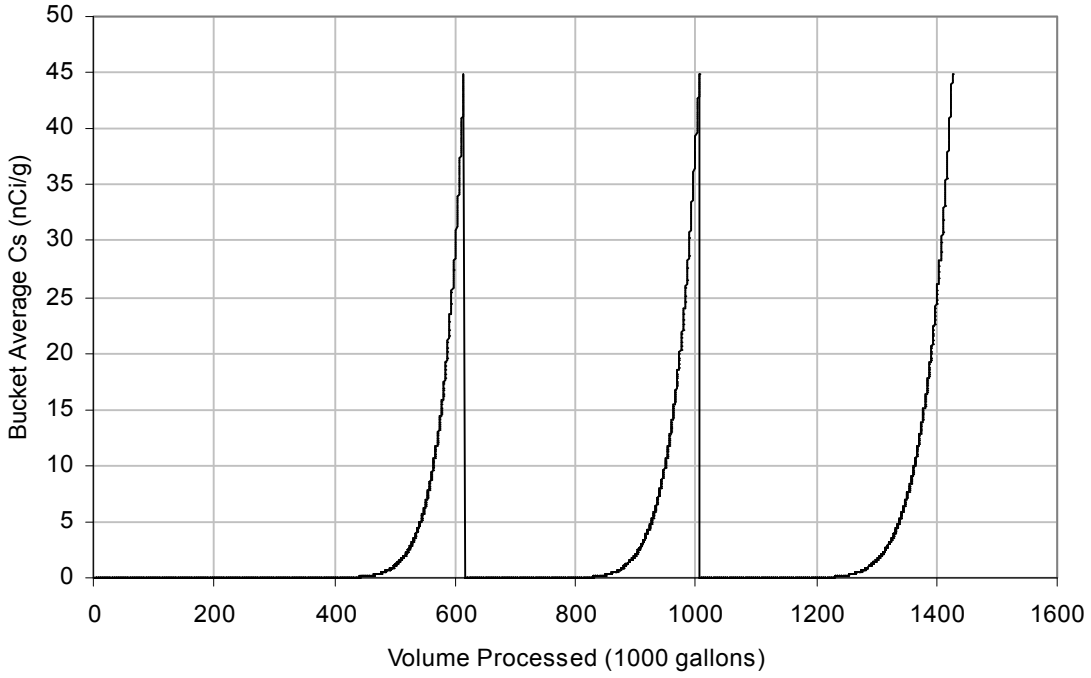

Figure 9-4. Breakthrough curves for Tank 37 nominal case with CST media.

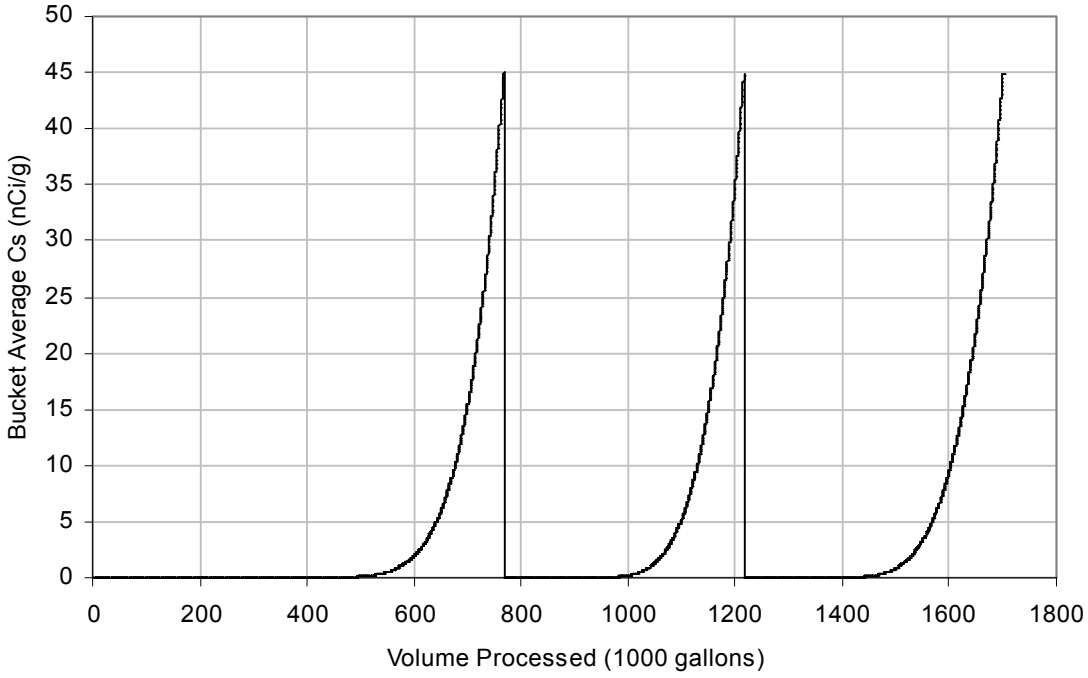

Figure 9-5. Breakthrough curves for Tank 41 nominal case with CST media.

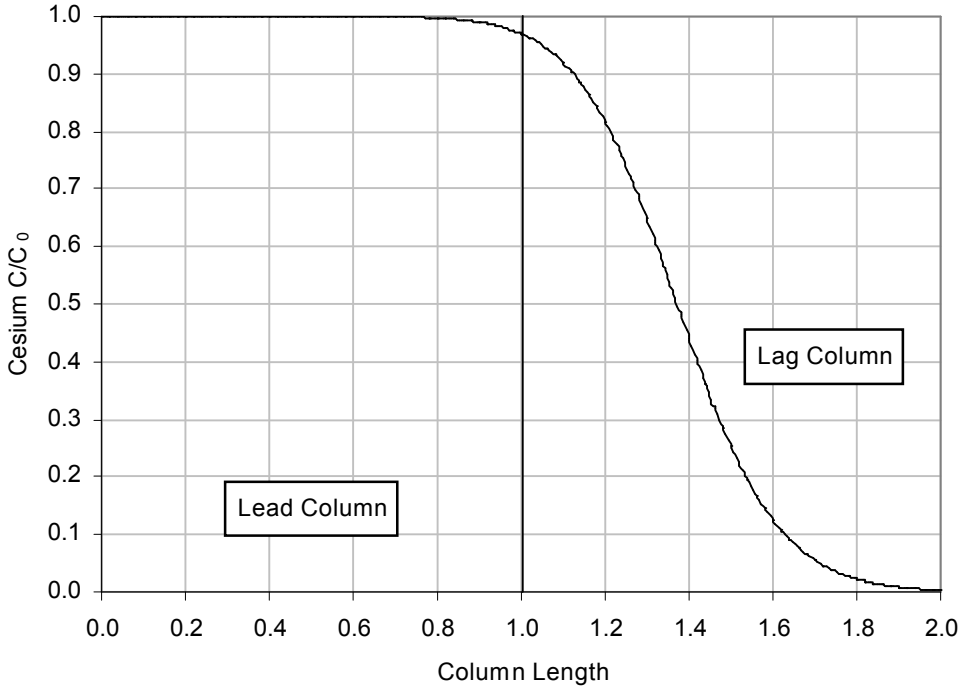

Figure 9-6. Cesium profile in columns at end of first cycle for Tank 1 nominal case with CST media.

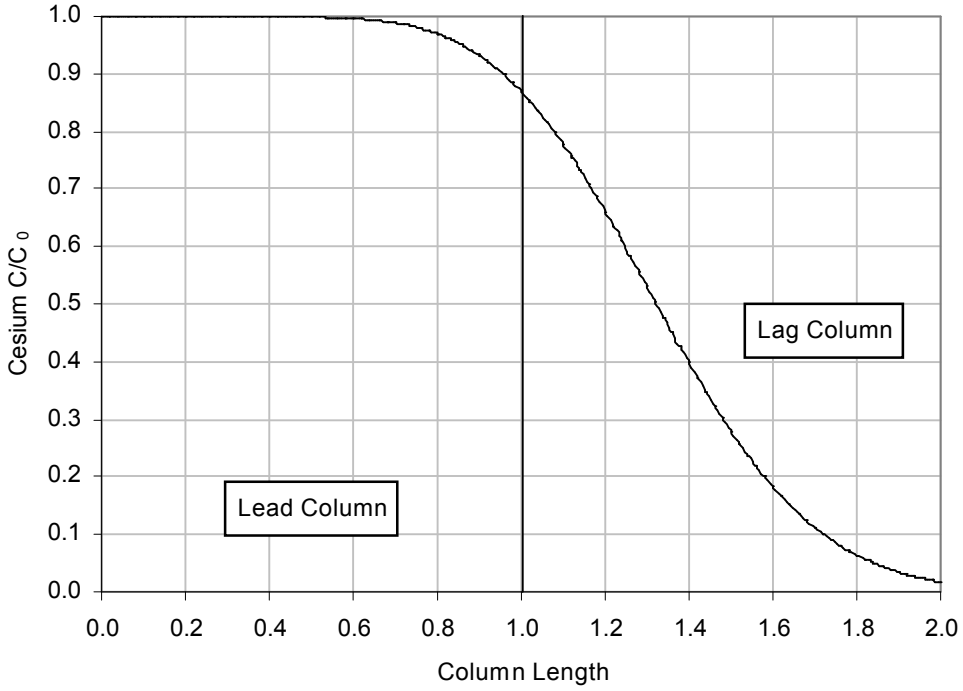

Figure 9-7. Cesium profile in columns at end of first cycle for Tank 2 nominal case with CST media.

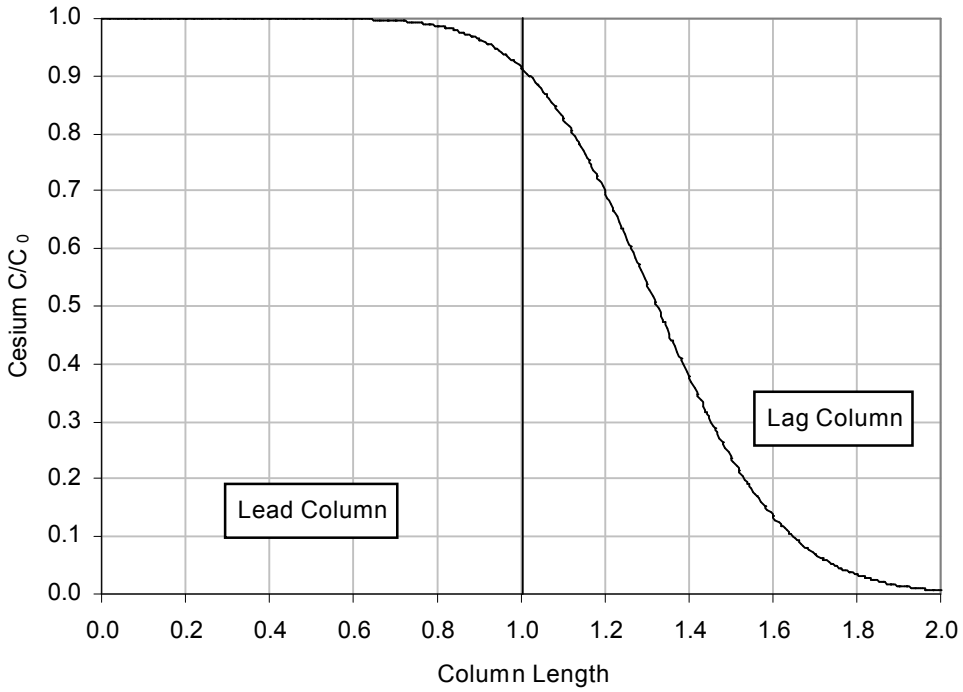

Figure 9-8. Cesium profile in columns at end of first cycle for Tank 3 nominal case with CST media.

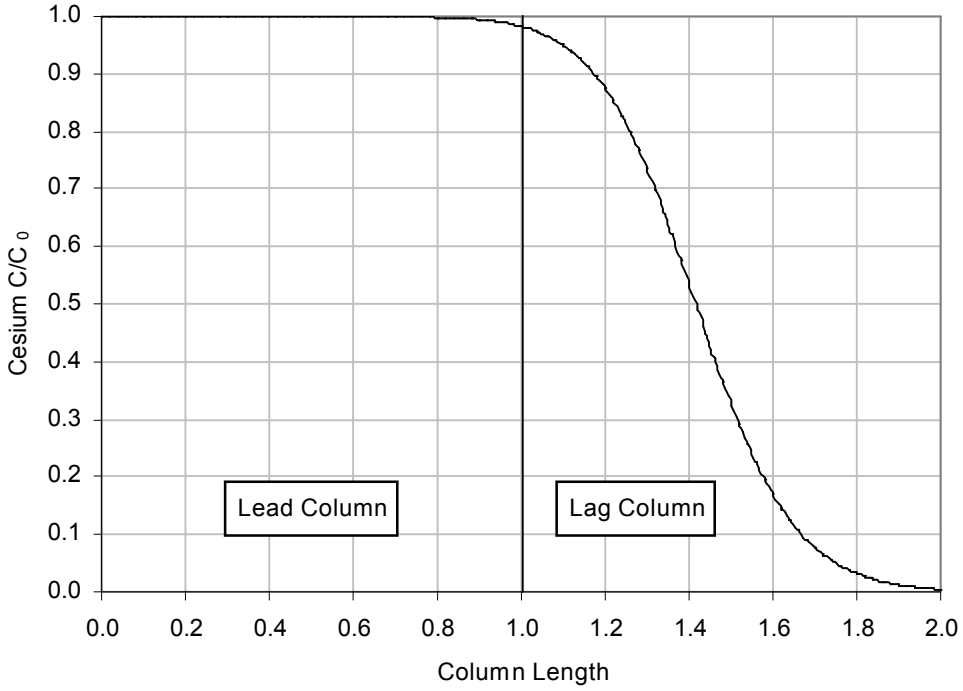

Figure 9-9. Cesium profile in columns at end of first cycle for Tank 37 nominal case with CST media.

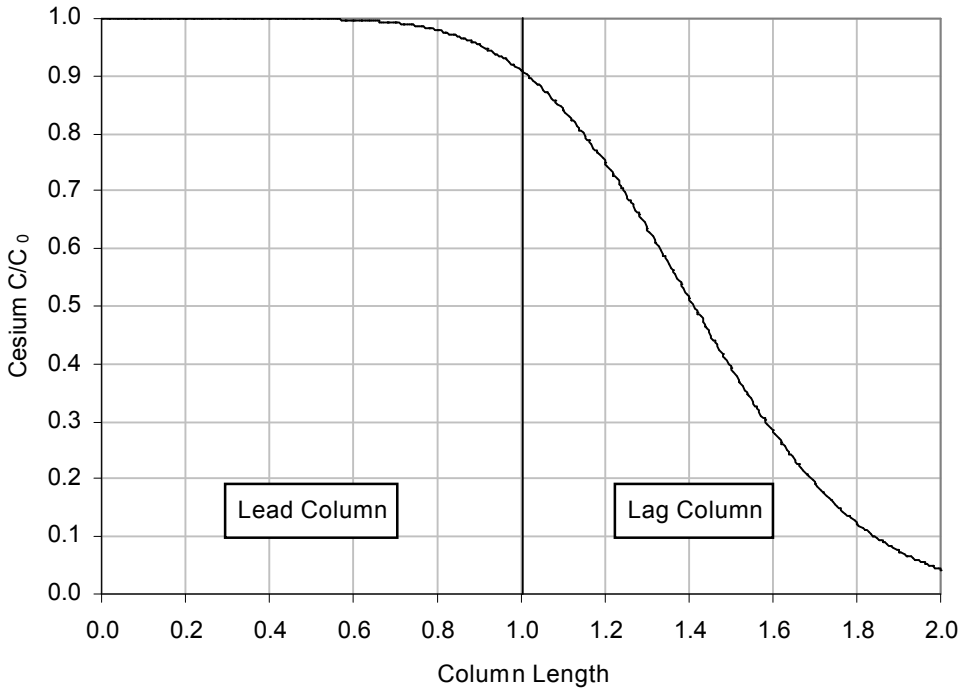

Figure 9-10. Cesium profile in columns at end of first cycle for Tank 41 nominal case with CST media.

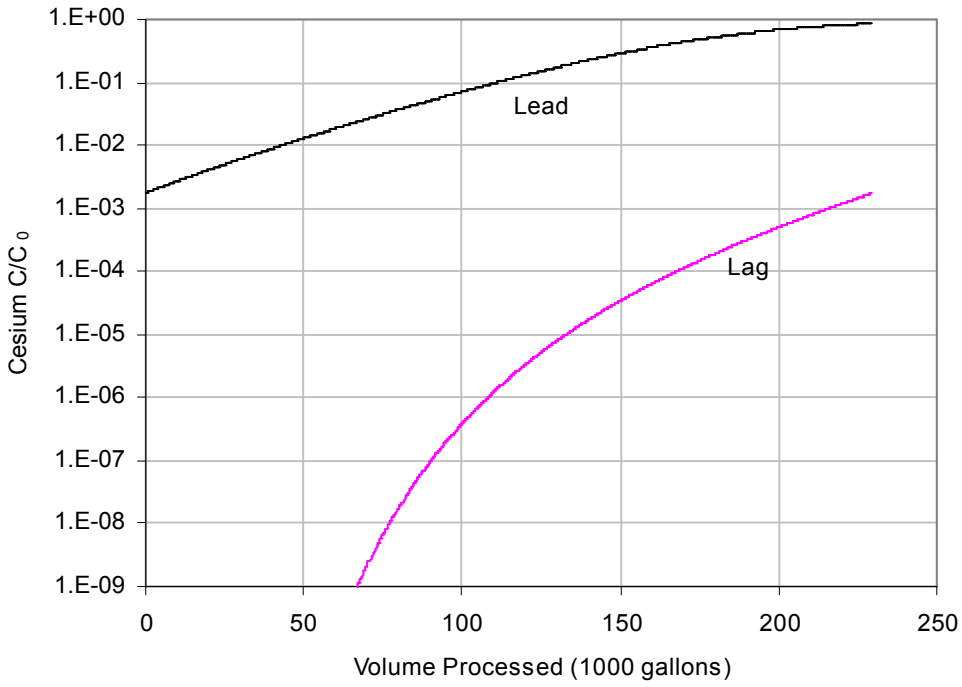

Figure 9-11. Column breakthrough curves during third cycle for Tank 1 nominal case with CST media.

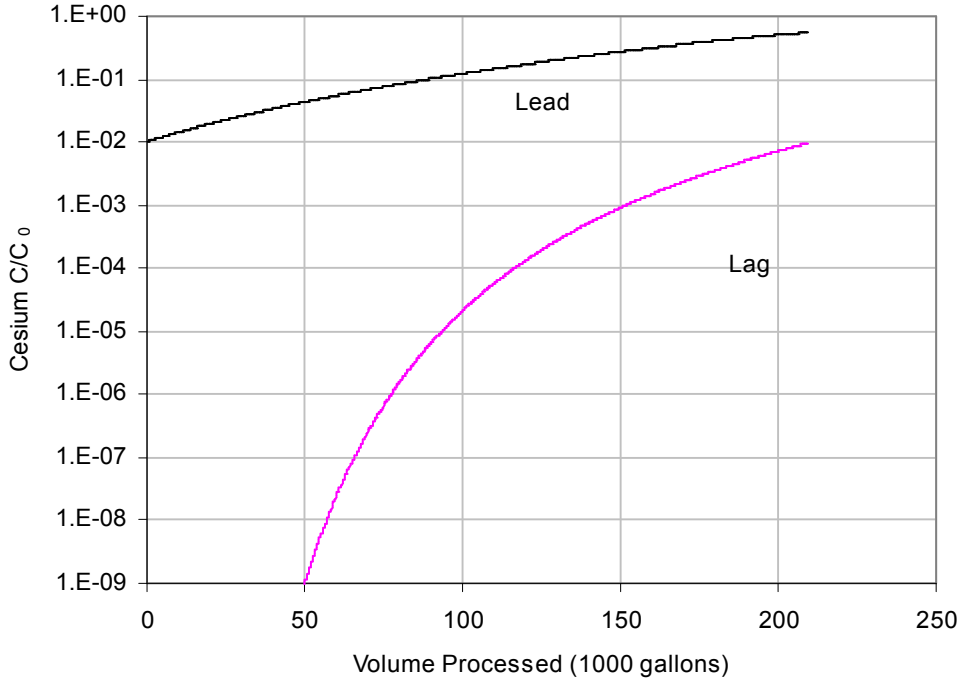

Figure 9-12. Column breakthrough curves during third cycle for Tank 2 nominal case with CST media.

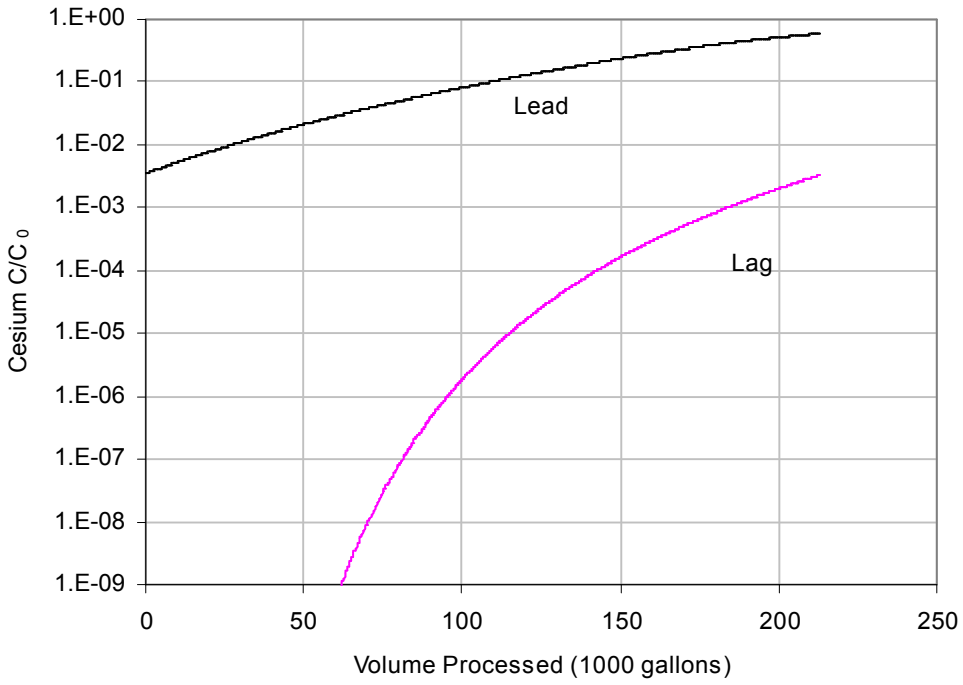

Figure 9-13. Column breakthrough curves during third cycle for Tank 3 nominal case with CST media.

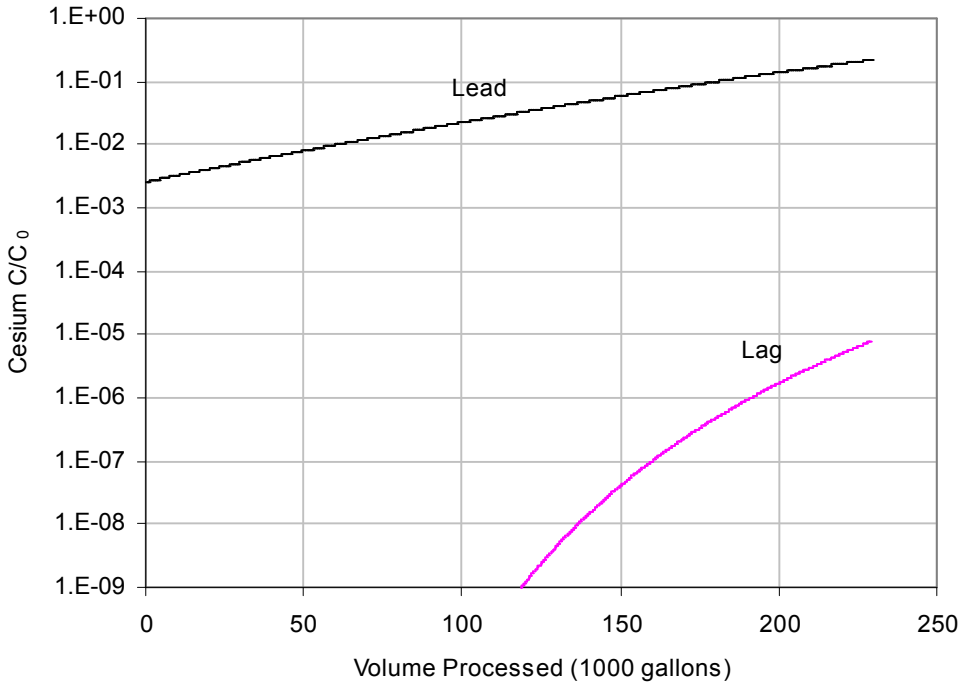

Figure 9-14. Column breakthrough curves during third cycle for Tank 37 nominal case with CST media.

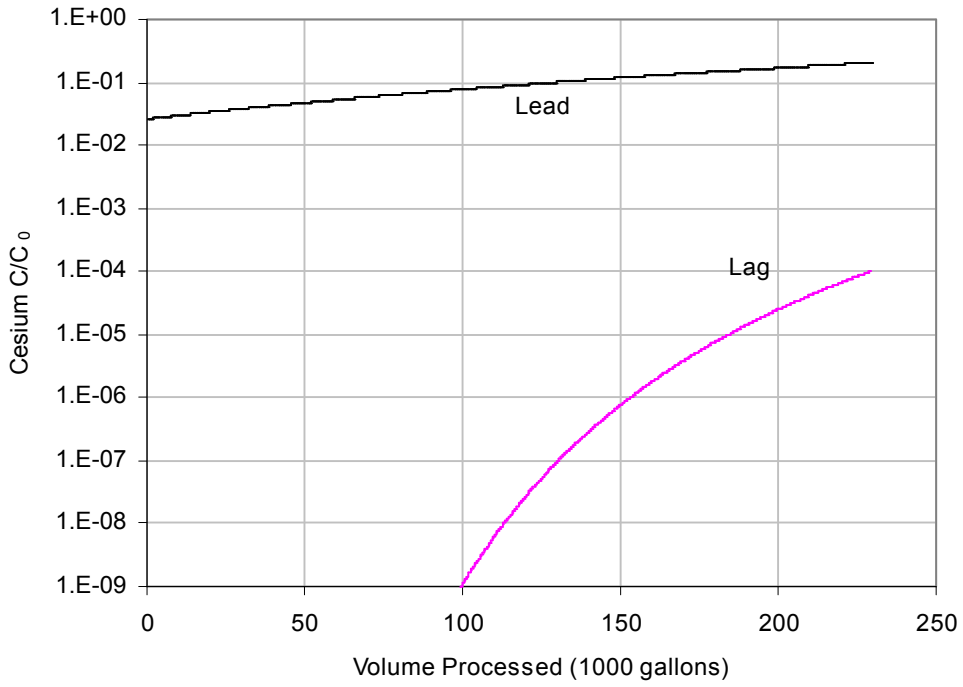

Figure 9-15. Column breakthrough curves during third cycle for Tank 41 nominal case with CST media.

10.0 RF Results with Freundlich/Langmuir Isotherm

10.1 RF Freundlich/Langmuir Isotherm Parameters

The most recent experimental data was fit to a "new" Freundlich/Langmuir isotherm equation which appears to more accurately represent batch contact data with low cesium concentrations (Aleman, et al., 2007). Table 10-1 lists the RF Freundlich/Langmuir isotherm parameters used in the VERSE-LC calculations. The first column in Table 10-1 lists the tanks and the feed cesium concentrations in molar units (total cesium) and pCi/ml (Cs^{137}). The last two columns in the table show the total cesium loading on the RF resin at equilibrium (Q) and the corresponding curies per liter of packed bed volume (BV). That is, these columns show the cesium loading in a fully loaded column. Since the lead column is very close to being fully loaded during column processing, the curie loadings listed in the last column of Table 10-1 provide an estimate of the maximum heat load on the column for thermal analysis. As for CST, Tank 1 and Tank 37 produce the highest curie loadings on the ion-exchange columns. The highest RF curie loading is 133 Ci/liter of bed volume for Tank 37 at 25 °C. Curie loadings in the ion-exchange columns with feed from Tanks 2 and 41 are five to 10 times lower than the maximum.

Maximum curie loadings are summarized in Table 10-2. As shown in the table, trends in loading generally correlate with feed cesium concentrations under these conditions. The RF curie loadings are 30% to 40% less than the corresponding CST values for Tanks 1 and 37 but are comparable to the CST loadings for the other three tanks.

Table 10-1. RF Freundlich/Langmuir isotherm parameters.

Tank # Total [Cs] [^{137} Cs]	Temp., C	*a*	b	M_a	M_b	Q, moles Cs/L BV	Q, Ci Cs/L BV
1	**25**	0.2372	3.717E-04	0.9723	0.9104	7.14E-02	130.15
1.81×10^{-4} M	**35**	0.2423	5.639E-04	0.9744	0.9032	5.58E-02	101.65
3.30×10^{8} pCi /ml	**45**	0.2474	8.262E-04	0.9769	0.8956	4.30E-02	78.36
2	**25**	0.2395	4.879E-04	0.9730	0.9047	1.02E-02	27.27
1.70×10^{-5} M	**35**	0.2455	7.755E-04	0.9760	0.8959	6.55E-03	17.50
4.54×10^{7} pCi /ml	**45**	0.2517	1.183E-03	0.9794	0.8863	4.32E-03	11.54
3	**25**	0.2373	4.805E-04	0.9736	0.9066	3.05E-02	75.47
6.35×10^{-5} M	**35**	0.2435	7.742E-04	0.9765	0.8975	2.05E-02	50.76
1.57×10^{8} pCi /ml	**45**	0.2499	1.196E-03	0.9799	0.8875	1.39E-02	34.41
37	**25**	0.2345	2.737E-04	0.9706	0.9142	6.49E-02	133.49
1.08×10^{-4} M	**35**	0.2393	4.125E-04	0.9724	0.9078	5.01E-02	103.08
2.22×10^{8} pCi /ml	**45**	0.2440	6.016E-04	0.9744	0.9011	3.84E-02	78.84
41	**25**	0.2346	2.911E-04	0.9715	0.9145	7.93E-03	16.43
7.53×10^{-6} M	**35**	0.2395	4.409E-04	0.9732	0.9078	5.34E-03	11.06
1.56×10^{7} pCi /ml	**45**	0.2443	6.455E-04	0.9753	0.9009	3.68E-03	7.61

Table 10-2. Maximum Curie loadings on RF resin using Freundlich/Langmuir isotherm. (Ci Cs^{137}/Liter Bed Volume)

Tank	Feed Cs [M]	Feed Cs^{137} [pCi/ml]	Temperature °C		
			25	**35**	**45**
1	1.81×10^{-4}	3.30×10^{8}	130.15	101.65	78.36
2	1.70×10^{-5}	4.54×10^{7}	27.27	17.50	11.54
3	6.35×10^{-5}	1.57×10^{8}	75.47	50.76	34.41
37	1.08×10^{-4}	2.22×10^{8}	133.49	103.08	78.84
41	7.53×10^{-6}	1.56×10^{7}	16.43	11.06	7.61

10.2 RF Freundlich/Langmuir Ion-exchange Column Modeling Results

Tables 10-3 through 10-14 give a summary of results from VERSE-LC ion-exchange column modeling calculations for SCIX using RF resin and the "new" Freundlich/Langmuir isotherm derived from the latest experimental data. All of the calculations assume a two-column configuration. During the first cycle, both columns contain fresh resin. In all subsequent cycles after the first, the partially loaded second or lag column is placed into the lead position and a clean column is placed into the lag position at the start of the cycle. Since a partially loaded column is in the lead position, after the first cycle less waste volume is processed per cycle before the operating limit is reached. Each cycle is run until the integral sum average cesium concentration in effluent collected from the lag column reaches the saltstone feed limit of 45 nCi/g.

Tables 10-3 through 10-7 list the volumes of salt solution processed during the first five ion-exchange cycles for each of the five tank compositions modeled. The total salt solution volume processed and the time it would take to run the ion exchange columns during the first five cycles are shown in the last two rows of each table. The process time is simply the time it would take the solution volume to run through the column during the loading phase of the ion-exchange cycle, and does not include time for elution, regeneration, maintenance, or outages. The largest volume processed per cycle was observed with Tank 41.

Tables 10-8 through 10-14 list the estimated time it would take to process the volume of the dissolved salt in each tank through the ion-exchange columns and the number of column cycles required. Tables 10-12 and 10-14 provide results for Tanks 37 and 41 for the estimated volume of solution in each tank that it is planned to process while Tables 10-11 and 10-13 show results based on the total volume in these two tanks. The ion-exchange processing time is obtained by dividing the salt solution volume processed by the flow rate through the column. To extrapolate beyond the five cycles calculated, it was assumed that the volume of waste processed during the fifth cycle would be processed in subsequent cycles to estimate the total cycles required. Under nominal operating conditions (Case 1), Tanks 1-3 required 8 to 11 ion-exchange cycles to process the total volume of dissolved salt.

Results of the column modeling for the assumed nominal case (25 °C, 10 gpm, 15 ft column) for each tank are plotted in Figures 10-1 through 10-5. We note that the breakthrough curves are very sharp. Therefore, to be conservative during actual operations, the run could be terminated at a lower bucket average effluent concentration without sacrificing much volume. The width of the bucket average breakthrough curves between 1.0 nCi/g and 45 nCi/g for Tank 1 was approximately 10,000 gallons. At a flow rate of 10 gpm, the breakthrough will take place within about 17 hours. Breakthrough widths for Tanks 3 and 37 were about 20,000 gallons, 40,000 gallons for Tank 2 and 90,000 gallons for Tank 41.

Column profiles showing the concentration of cesium in the liquid phase down the lead and lag columns at the end of the first cycle for the nominal case and each of the five tank compositions tested are plotted in Figures 10-6 through 10-10. We find that in all cases, the lead column is fully loaded at the end of the first cycle. Therefore, the assumption of a fully

loaded column used to estimate maximum cesium loadings in Tables 10-1 and 10-2 is found to be accurate. Figures 10-11 through 10-15 plot the breakthrough curves (instantaneous C/C_0) from the lead and lag ion-exchange columns during the fifth cycle for the nominal case for each tank. Note that graphs plotting C/C_0 can be applied to both total cesium or Cs^{137}.

Table 10-3. Tank 1 waste volume in thousands of gallons processed in five ion-exchange cycles using RF resin and new isotherm.

Case	1	2	3	4	5	6	7	8
	15 ft	15 ft	15 ft	10 ft	25 ft	15 ft	15 ft	15 ft
	10 gpm	5 gpm	20 gpm	10 gpm	10 gpm	10 gpm	10 gpm	10 gpm
	25 °C	25 °C	25 °C	25 °C	25 °C	35 °C	45 °C	25 °C
Cycle 1	328.3	335.5	312.0	213.3	557.0	253.6	193.0	262.7
Cycle 2	169.1	170.0	167.6	112.1	282.9	132.0	101.5	135.3
Cycle 3	170.9	171.0	171.2	114.1	284.6	133.6	103.2	136.8
Cycle 4	171.0	170.8	170.9	114.0	284.8	133.8	103.3	137.0
Cycle 5	170.8	171.1	171.0	114.0	284.8	133.7	103.1	136.7
Total	1010.1	1018.3	992.7	667.5	1694.2	786.6	604.2	808.5
Time, Days	70.1	141.4	34.5	46.4	117.7	54.6	42.0	56.1

Table 10-4. Tank 2 waste volume in thousands of gallons processed in five ion-exchange cycles using RF resin and new isotherm.

Case	1	2	3	4	5	6	7	8
	15 ft	15 ft	15 ft	10 ft	25 ft	15 ft	15 ft	15 ft
	10 gpm	5 gpm	20 gpm	10 gpm	10 gpm	10 gpm	10 gpm	10 gpm
	25 °C	25 °C	25 °C	25 °C	25 °C	35 °C	45 °C	25 °C
Cycle 1	457.2	487.6	409.3	287.1	803.4	289.2	188.8	365.9
Cycle 2	247.4	254.1	235.1	160.5	421.4	157.3	102.7	198.1
Cycle 3	256.6	259.6	248.7	168.3	431.6	163.2	106.9	205.3
Cycle 4	258.1	259.9	252.2	170.2	432.9	164.6	107.9	206.6
Cycle 5	259.0	260.3	254.5	171.4	433.5	165.5	108.5	207.5
Total	1478.3	1521.5	1399.9	957.4	2522.8	939.8	614.8	1183.3
Time, Days	102.7	211.3	48.6	66.5	175.2	65.3	42.7	82.2

Table 10-5. Tank 3 waste volume in thousands of gallons processed in five ion-exchange cycles using RF resin and new isotherm.

Case	1	2	3	4	5	6	7	8
	15 ft	15 ft	15 ft	10 ft	25 ft	15 ft	15 ft	15 ft
	10 gpm	5 gpm	20 gpm	10 gpm	10 gpm	10 gpm	10 gpm	10 gpm
	25 °C	25 °C	25 °C	25 °C	25 °C	35 °C	45 °C	25 °C
Cycle 1	387.5	403.5	354.8	246.8	668.2	254.4	168.6	310.2
Cycle 2	204.5	206.1	200.6	135.1	342.7	136.8	91.8	163.7
Cycle 3	208.3	208.3	207.9	139.0	347.1	140.1	94.7	166.7
Cycle 4	208.4	208.3	208.0	138.8	347.0	140.2	95.1	166.8
Cycle 5	208.3	208.3	208.4	138.9	347.0	140.3	95.3	166.8
Total	1217.0	1234.5	1179.6	798.6	2052.0	811.9	545.5	974.1
Time, Days	84.5	171.5	41.0	55.5	142.5	56.4	37.9	67.6

Table 10-6. Tank 37 waste volume in thousands of gallons processed in five ion-exchange cycles using RF resin and new isotherm.

Case	1	2	3	4	5	6	7	8
	15 ft	15 ft	15 ft	10 ft	25 ft	15 ft	15 ft	15 ft
	10 gpm	5 gpm	20 gpm	10 gpm	10 gpm	10 gpm	10 gpm	10 gpm
	25 °C	25 °C	25 °C	25 °C	25 °C	35 °C	45 °C	25 °C
Cycle 1	497.9	510.2	470.0	322.4	847.0	380.1	286.6	398.5
Cycle 2	257.1	258.5	254.5	170.5	430.2	198.1	151.4	205.6
Cycle 3	260.3	260.2	260.6	173.7	433.7	201.2	154.1	208.4
Cycle 4	260.3	260.3	260.1	173.6	433.6	201.3	154.0	208.5
Cycle 5	260.3	260.2	260.4	173.6	433.7	201.1	154.1	208.3
Total	1535.9	1549.4	1505.5	1013.7	2578.3	1181.8	900.2	1229.3
Time, Days	106.7	215.2	52.3	70.4	179.0	82.1	62.5	85.4

Table 10-7. Tank 41 waste volume in thousands of gallons processed in five ion-exchange cycles using RF resin and new isotherm.

Case	1	2	3	4	5	6	7	8
	15 ft	15 ft	15 ft	10 ft	25 ft	15 ft	15 ft	15 ft
	10 gpm	5 gpm	20 gpm	10 gpm	10 gpm	10 gpm	10 gpm	10 gpm
	25 °C	25 °C	25 °C	25 °C	25 °C	35 °C	45 °C	25 °C
Cycle 1	813.4	861.8	737.2	514.0	1421.5	544.8	373.4	651.0
Cycle 2	432.5	444.2	411.8	280.8	736.6	289.8	198.8	346.1
Cycle 3	448.6	454.5	435.7	294.8	756.0	300.8	206.2	359.1
Cycle 4	451.9	455.8	441.9	297.9	758.4	303.2	208.0	361.7
Cycle 5	453.7	456.5	445.7	299.8	759.9	304.6	209.1	363.1
Total	2600.1	2672.8	2472.2	1687.3	4432.4	1743.2	1195.6	2081.0
Time, Days	180.6	371.2	85.8	117.2	307.8	121.1	83.0	144.5

Table 10-8. Estimated parameters required to process 1.87×10^6 gallons of Tank 1 salt solution using RF resin and new isotherm.

Case	1	2	3	4	5	6	7	8
	15 ft	15 ft	15 ft	10 ft	25 ft	15 ft	15 ft	15 ft
	10 gpm	5 gpm	20 gpm	10 gpm	10 gpm	10 gpm	10 gpm	10 gpm
	25 °C	25 °C	25 °C	25 °C	25 °C	35 °C	45 °C	25 °C
Days	129.9	259.7	64.9	129.9	129.9	129.9	129.9	129.9
Fractional Cycles	10.03	9.98	10.13	15.55	5.62	13.10	17.28	12.77
Whole Cycles	11	10	11	16	6	14	18	13

Table 10-9. Estimated parameters required to process 2.08×10^6 gallons of Tank 2 salt solution using RF resin and new isotherm.

Case	1	2	3	4	5	6	7	8
	15 ft	15 ft	15 ft	10 ft	25 ft	15 ft	15 ft	15 ft
	10 gpm	5 gpm	20 gpm	10 gpm	10 gpm	10 gpm	10 gpm	10 gpm
	25 °C	25 °C	25 °C	25 °C	25 °C	35 °C	45 °C	25 °C
Days	144.4	288.9	72.2	144.4	144.4	144.4	144.4	144.4
Fractional Cycles	7.32	7.15	7.67	11.55	3.98	11.89	18.50	9.32
Whole Cycles	8	8	8	12	4	12	19	10

Table 10-10. Estimated parameters required to process 2.09×10^6 gallons of Tank 3 salt solution using RF resin and new isotherm.

Case	1	2	3	4	5	6	7	8
	15 ft	15 ft	15 ft	10 ft	25 ft	15 ft	15 ft	15 ft
	10 gpm	5 gpm	20 gpm	10 gpm	10 gpm	10 gpm	10 gpm	10 gpm
	25 °C	25 °C	25 °C	25 °C	25 °C	35 °C	45 °C	25 °C
Days	145.1	290.3	72.6	145.1	145.1	145.1	145.1	145.1
Fractional Cycles	9.19	9.11	9.37	14.30	5.11	14.11	21.21	11.69
Whole Cycles	10	10	10	15	6	15	22	12

Table 10-11. Estimated parameters required to process 4.10×10^6 gallons of Tank 37 salt solution using RF resin and new isotherm.

Case	1	2	3	4	5	6	7	8
	15 ft	15 ft	15 ft	10 ft	25 ft	15 ft	15 ft	15 ft
	10 gpm	5 gpm	20 gpm	10 gpm	10 gpm	10 gpm	10 gpm	10 gpm
	25 °C	25 °C	25 °C	25 °C	25 °C	35 °C	45 °C	25 °C
Days	284.7	569.4	142.4	284.7	284.7	284.7	284.7	284.7
Fractional Cycles	14.85	14.80	14.96	22.78	8.51	19.51	25.76	18.78
Whole Cycles	15	15	15	23	9	20	26	19

Table 10-12. Estimated parameters required to process 1.00×10^6 gallons of Tank 37 salt solution using RF resin and new isotherm.

Case	1	2	3	4	5	6	7	8
	15 ft	15 ft	15 ft	10 ft	25 ft	15 ft	15 ft	15 ft
	10 gpm	5 gpm	20 gpm	10 gpm	10 gpm	10 gpm	10 gpm	10 gpm
	25 °C	25 °C	25 °C	25 °C	25 °C	35 °C	45 °C	25 °C
Days	69.4	138.9	34.7	69.4	69.4	69.4	69.4	69.4
Fractional Cycles	2.94	2.89	3.06	4.92	1.36	4.10	5.65	3.90
Whole Cycles	3	3	4	5	2	5	6	4

Table 10-13. Estimated parameters required to process 3.48×10^6 gallons of Tank 41 salt solution using RF resin and new isotherm.

Case	1	2	3	4	5	6	7	8
	15 ft	15 ft	15 ft	10 ft	25 ft	15 ft	15 ft	15 ft
	10 gpm	5 gpm	20 gpm	10 gpm	10 gpm	10 gpm	10 gpm	10 gpm
	25 °C	25 °C	25 °C	25 °C	25 °C	35 °C	45 °C	25 °C
Days	266.7	533.3	133.3	266.7	266.7	266.7	266.7	266.7
Fractional Cycles	7.73	7.56	8.07	12.18	4.22	11.88	17.65	9.84
Whole Cycles	8	8	9	13	5	12	18	10

Table 10-14. Estimated parameters required to process 0.19×10^6 gallons of Tank 41 salt solution using RF resin and new isotherm.

Case	1	2	3	4	5	6	7	8
	15 ft	15 ft	15 ft	10 ft	25 ft	15 ft	15 ft	15 ft
	10 gpm	5 gpm	20 gpm	10 gpm	10 gpm	10 gpm	10 gpm	10 gpm
	25 °C	25 °C	25 °C	25 °C	25 °C	35 °C	45 °C	25 °C
Days	13.2	26.4	6.6	13.2	13.2	13.2	13.2	13.2
Fractional Cycles	0.23	0.22	0.26	0.37	0.13	0.35	0.51	0.29
Whole Cycles	1	1	1	1	1	1	1	1

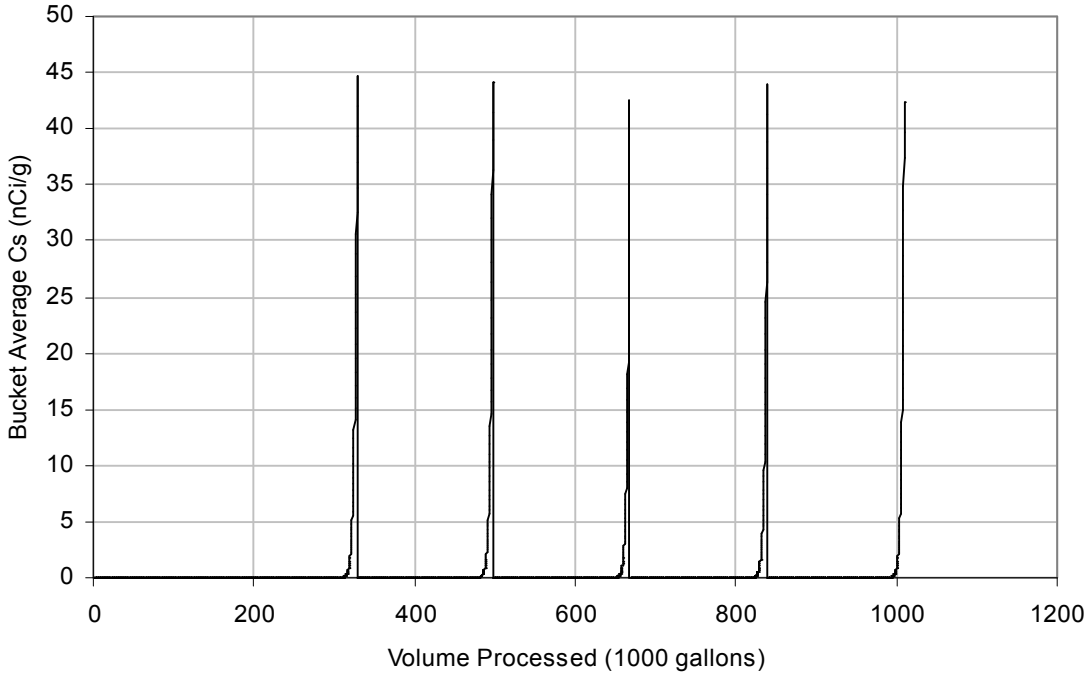

Figure 10-1. Breakthrough curves for Tank 1 nominal case with RF resin and new isotherm.

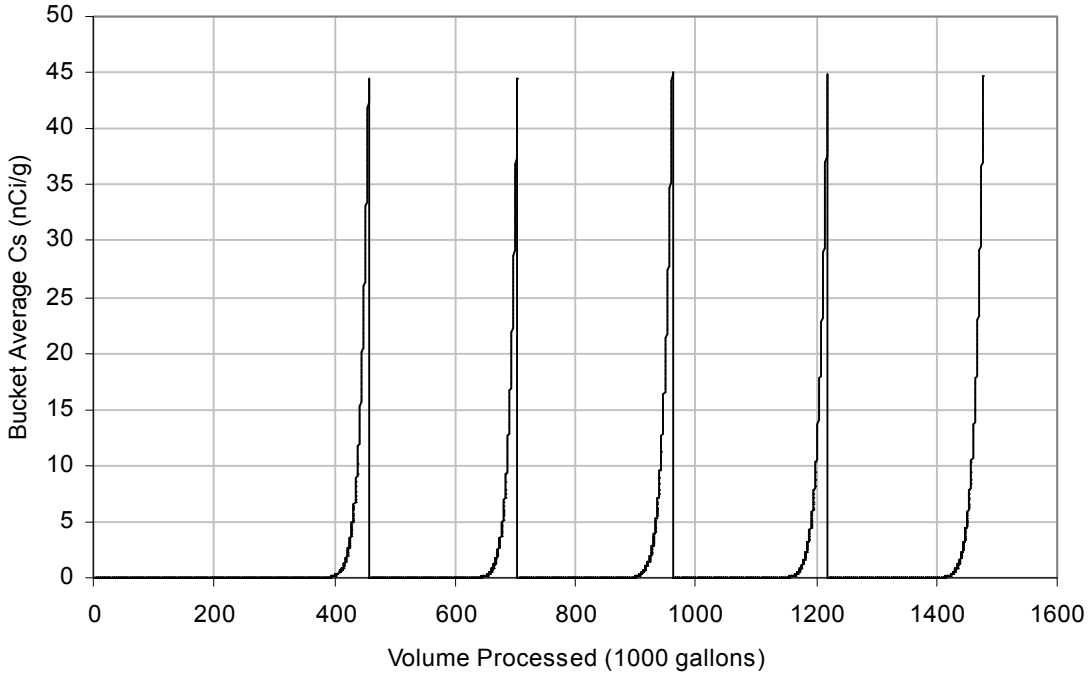

Figure 10-2. Breakthrough curves for Tank 2 nominal case with RF resin and new isotherm.

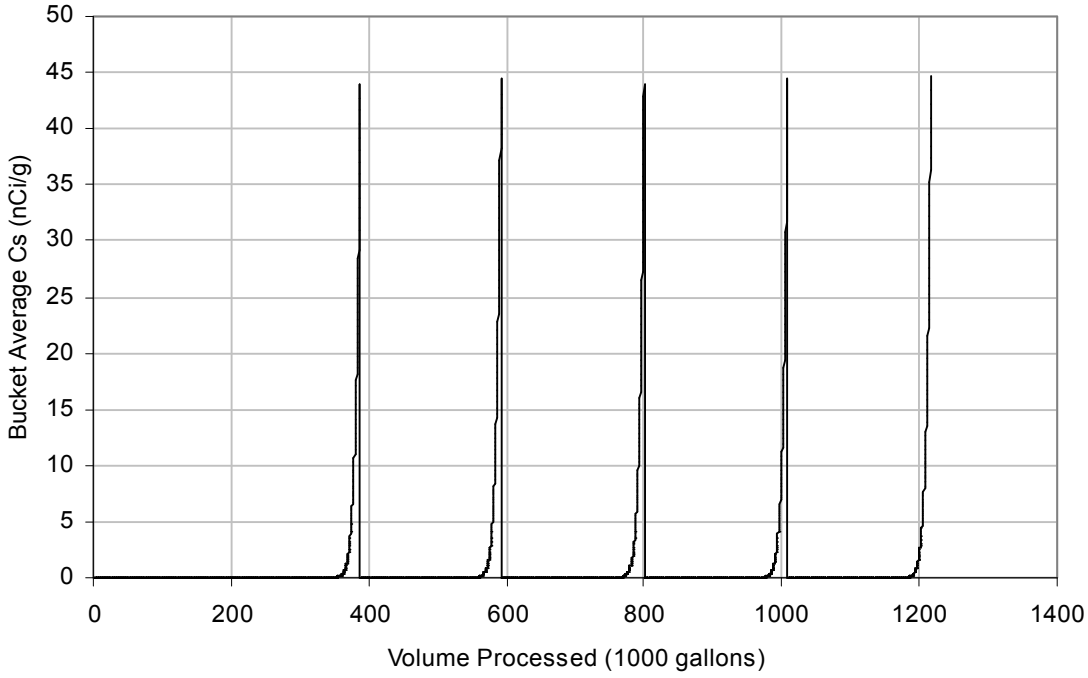

Figure 10-3. Breakthrough curves for Tank 3 nominal case with RF resin and new isotherm.

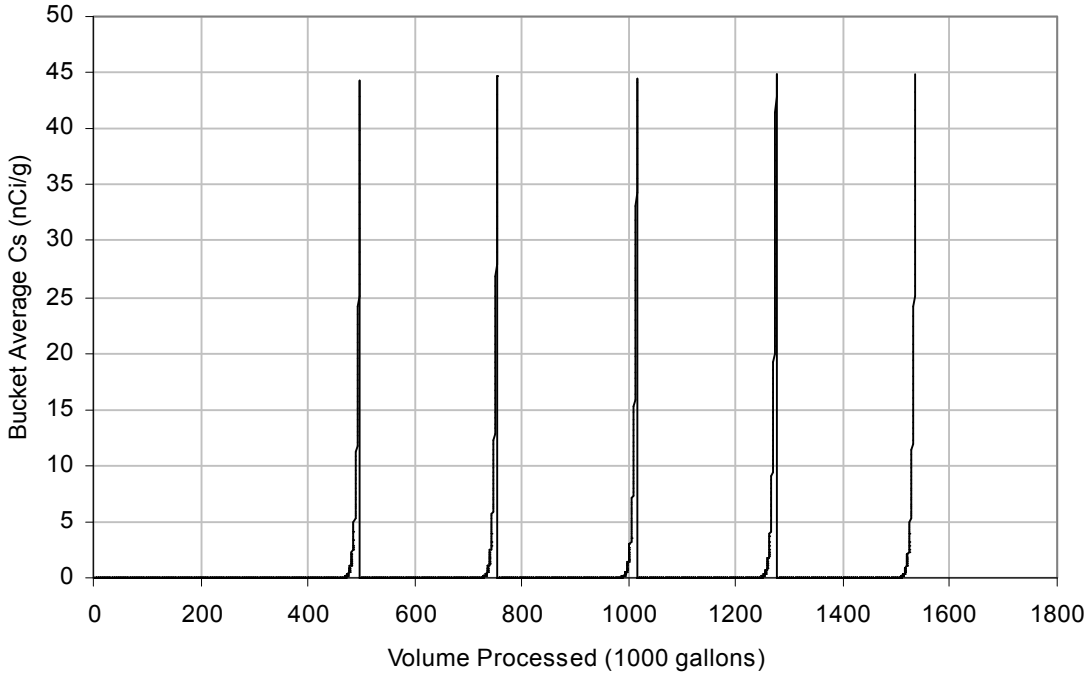

Figure 10-4. Breakthrough curves for Tank 37 nominal case with RF resin and new isotherm.

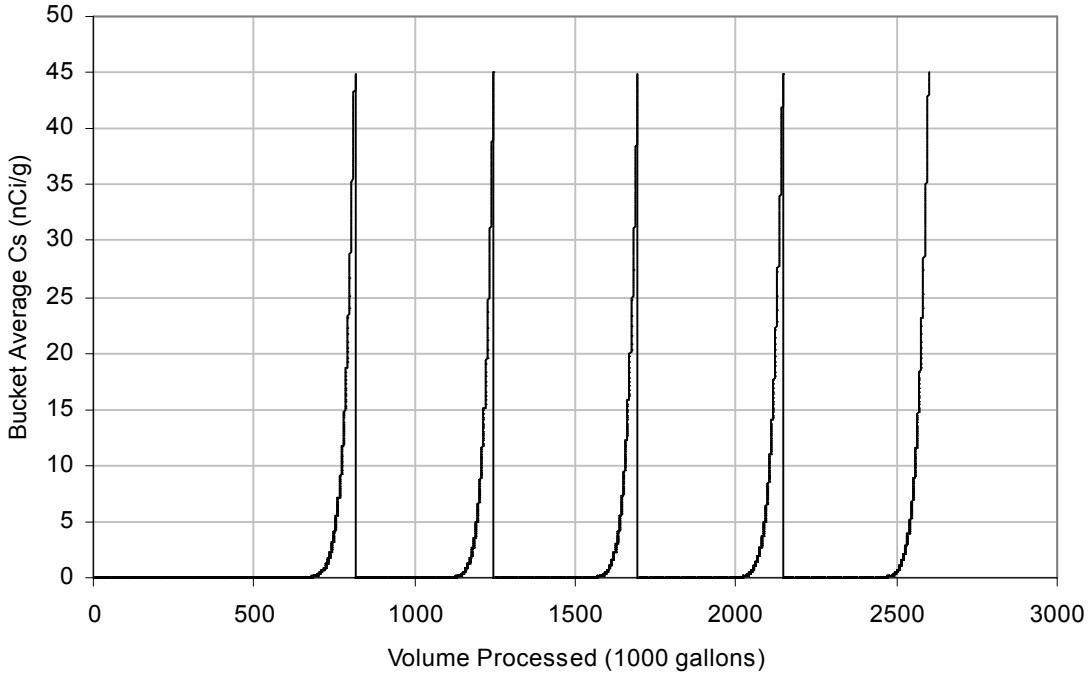

Figure 10-5. Breakthrough curves for Tank 41 nominal case with RF resin and new isotherm.

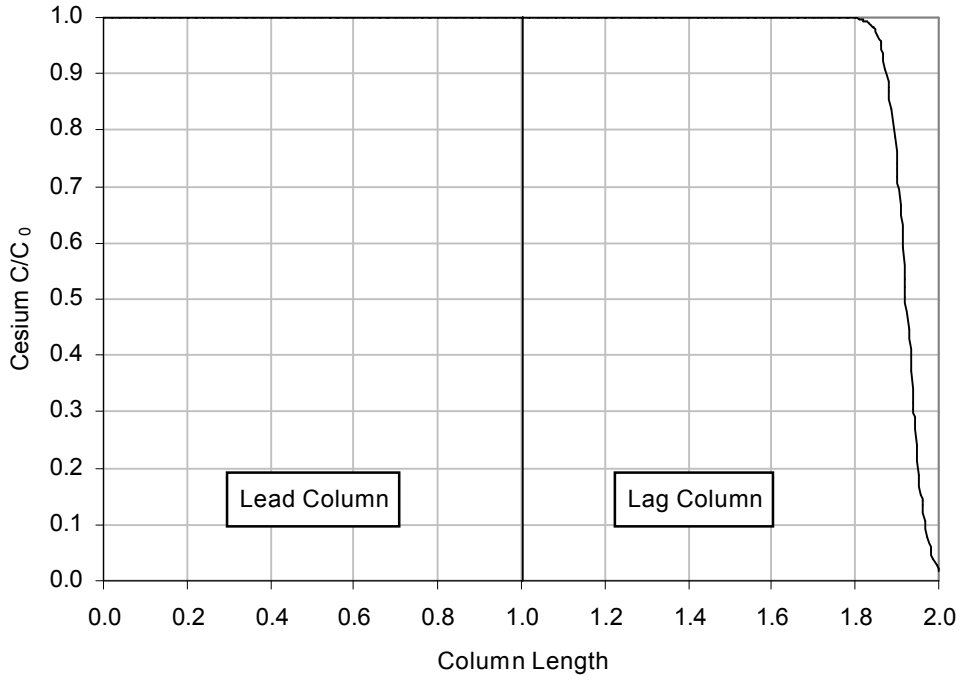

Figure 10-6. Cesium profile in columns at end of first cycle for Tank 1 nominal case with RF resin and new isotherm.

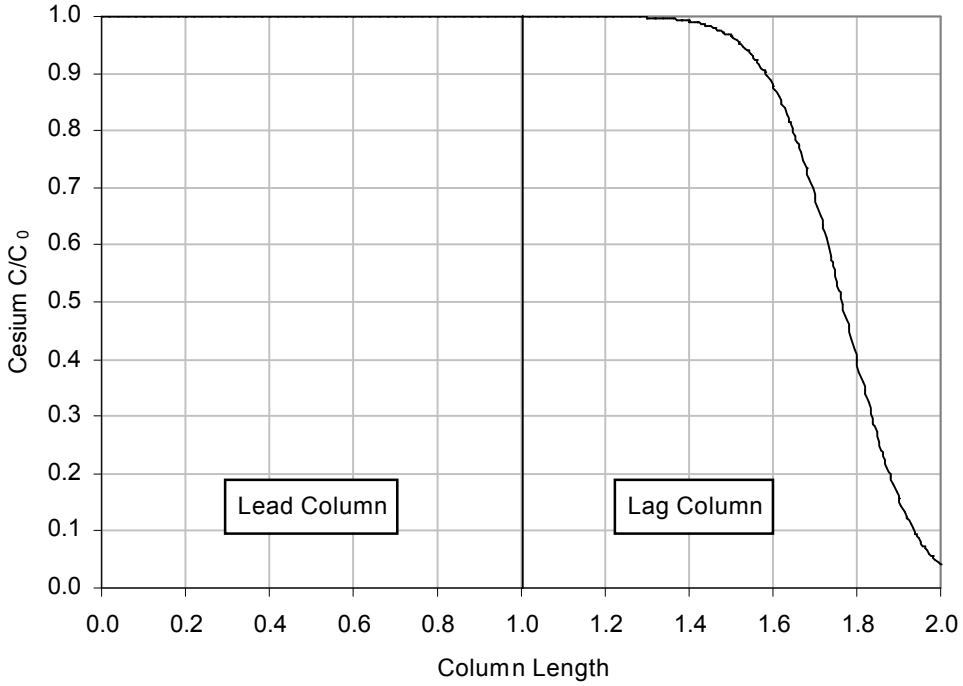

Figure 10-7. Cesium profile in columns at end of first cycle for Tank 2 nominal case with RF resin and new isotherm.

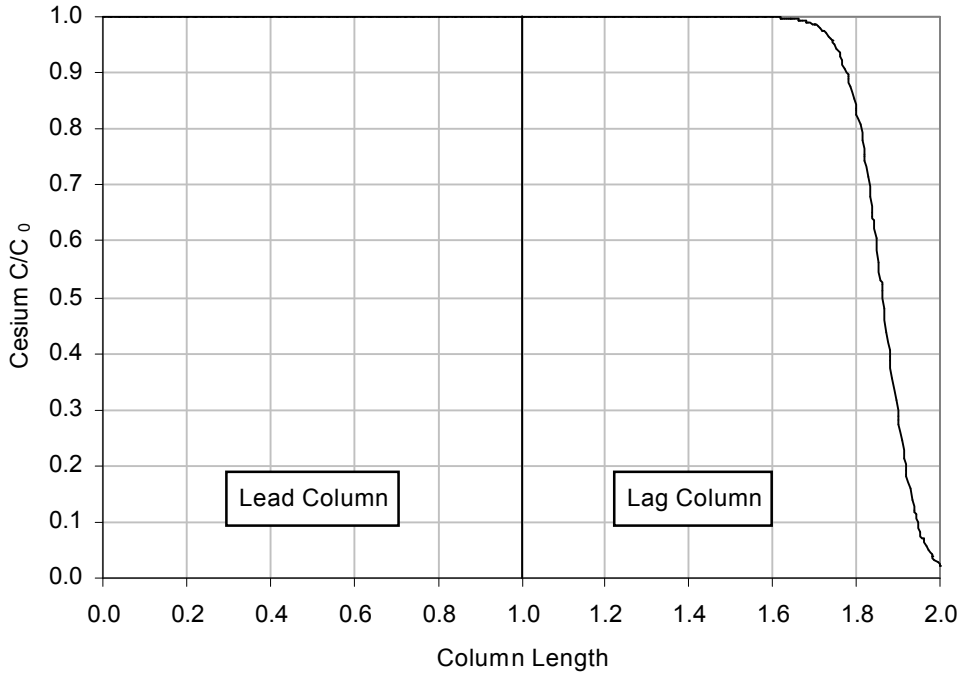

Figure 10-8. Cesium profile in columns at end of first cycle for Tank 3 nominal case with RF resin and new isotherm.

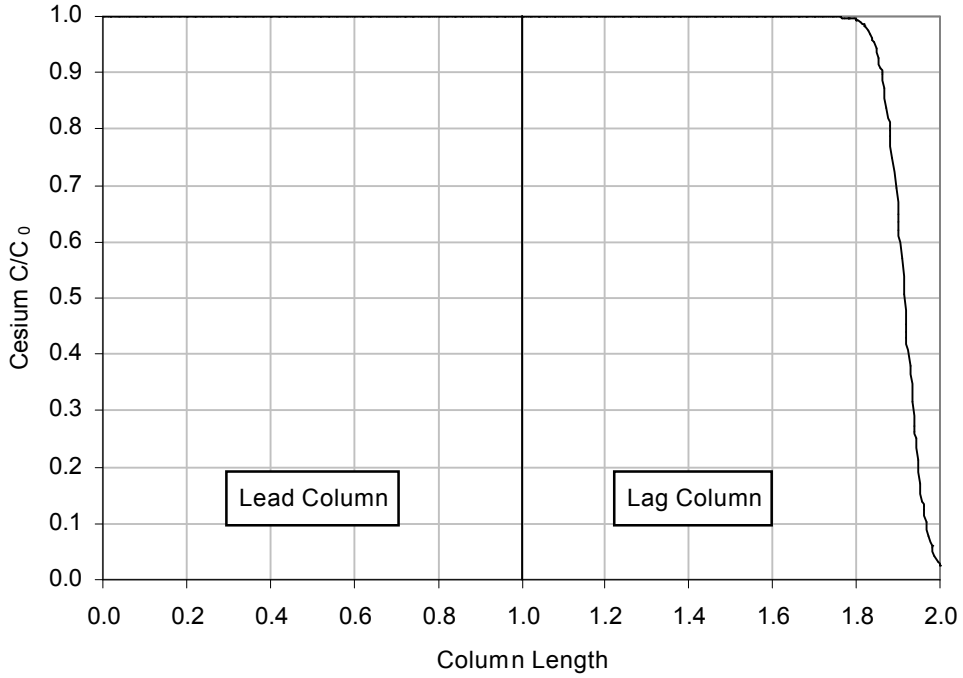

Figure 10-9. Cesium profile in columns at end of first cycle for Tank 37 nominal case with RF resin and new isotherm.

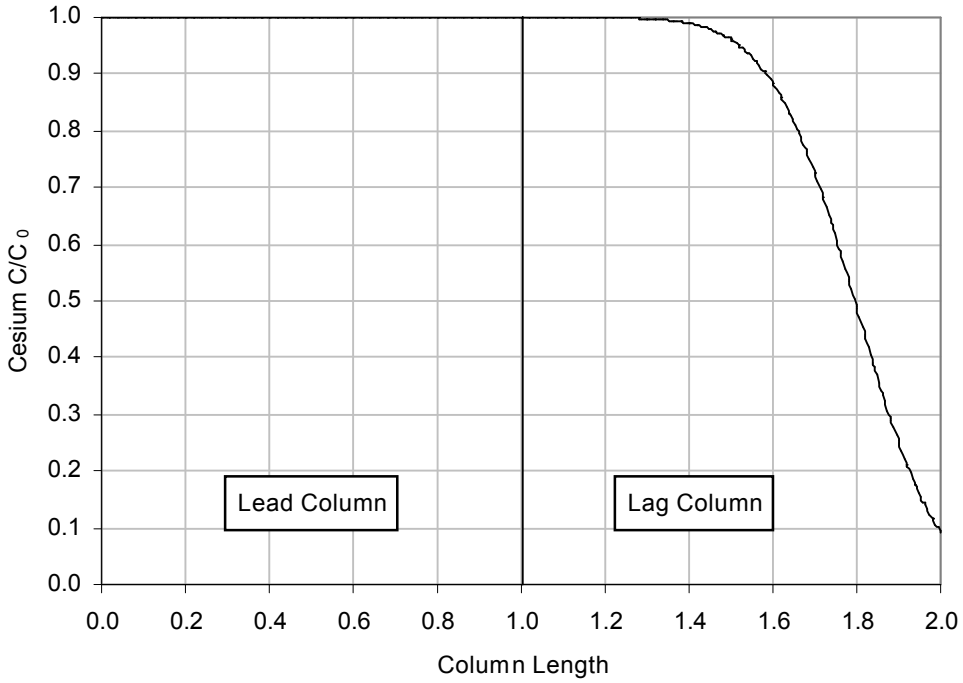

Figure 10-10. Cesium profile in columns at end of first cycle for Tank 41 nominal case with RF resin and new isotherm.

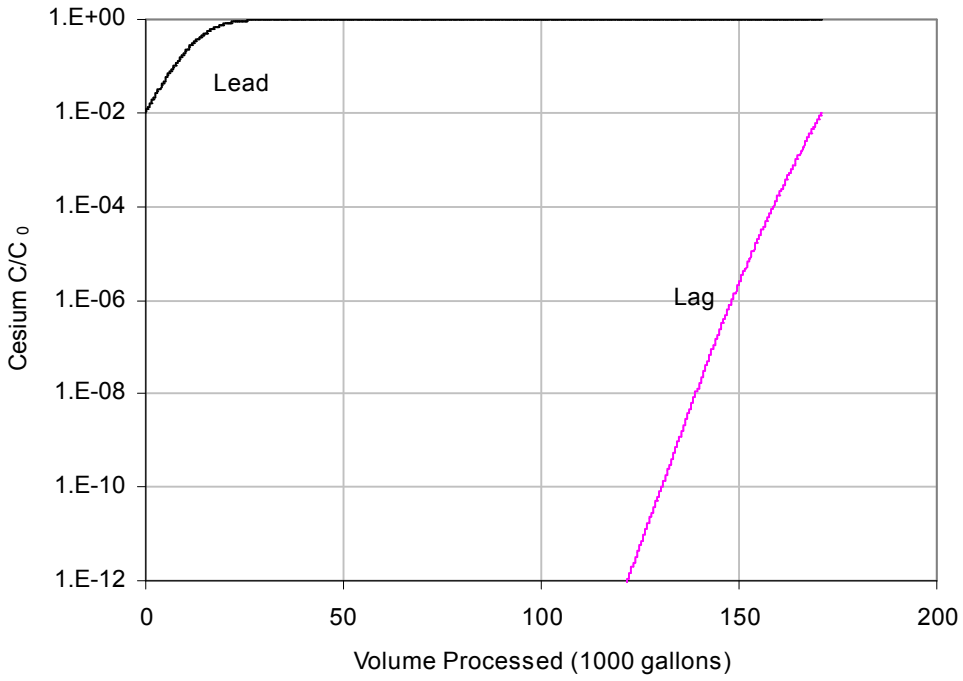

Figure 10-11. Column breakthrough curves during fifth cycle for Tank 1 nominal case with RF resin and new isotherm.

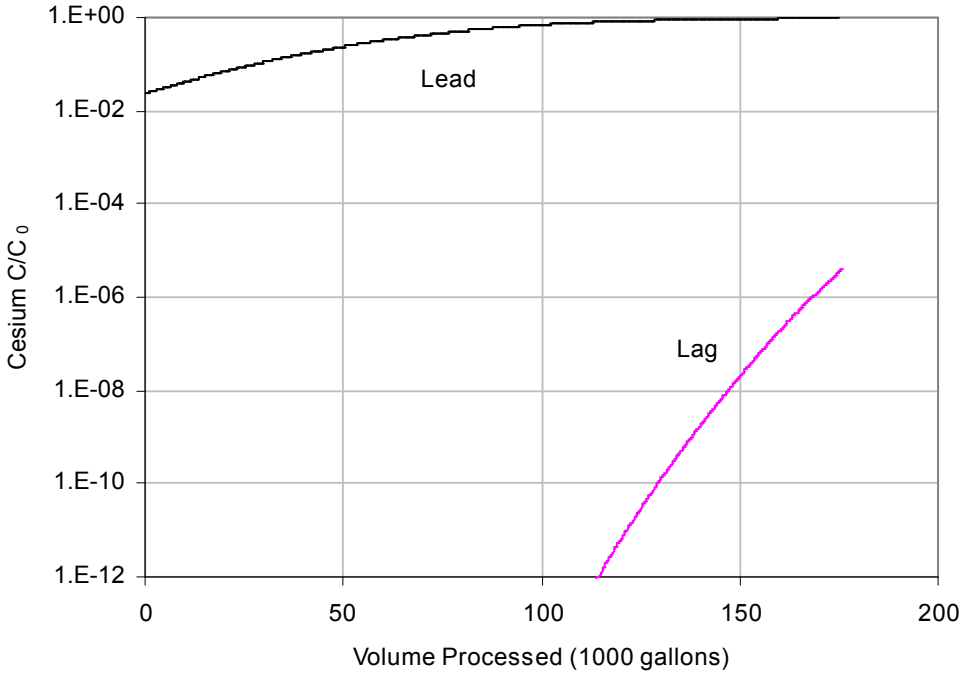

Figure 10-12. Column breakthrough curves during fifth cycle for Tank 2 nominal case with RF resin and new isotherm.

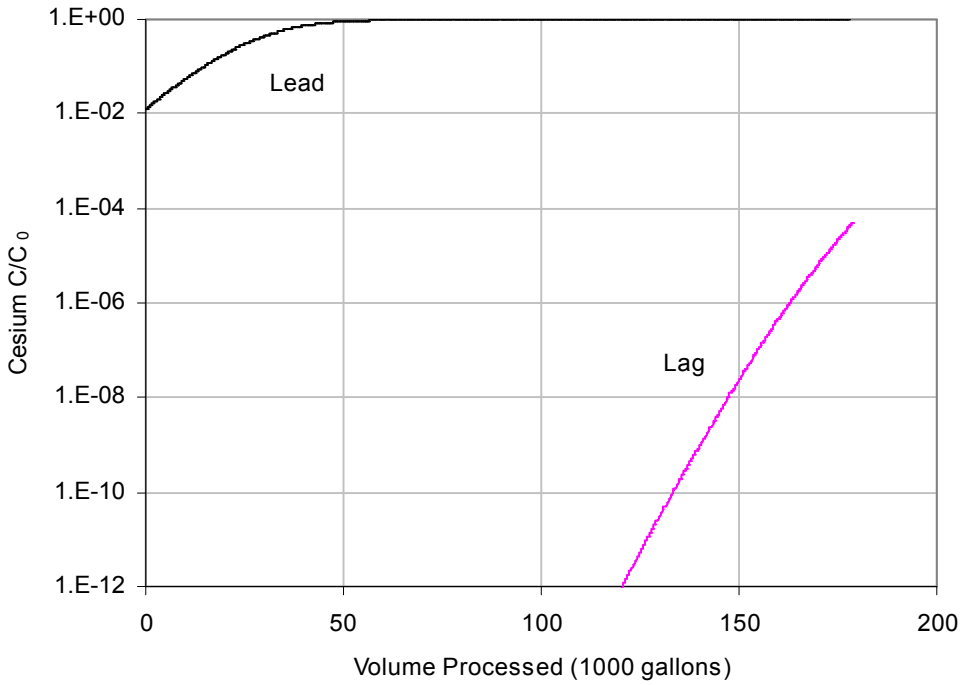

Figure 10-13. Column breakthrough curves during fifth cycle for Tank 3 nominal case with RF resin and new isotherm.

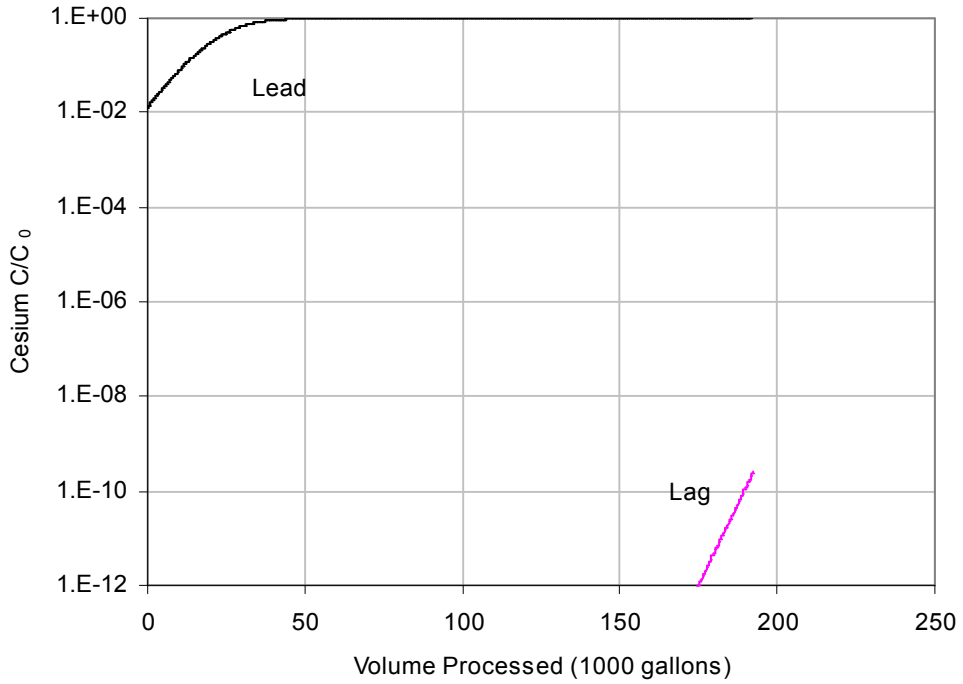

Figure 10-14. Column breakthrough curves during fifth cycle for Tank 37 nominal case with RF resin and new isotherm.

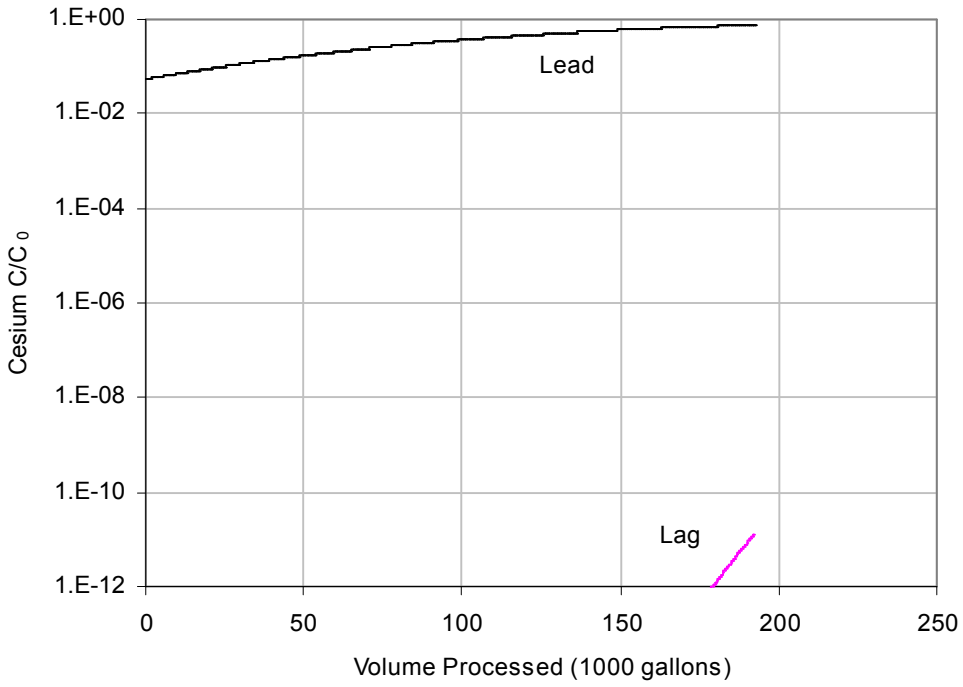

Figure 10-15. Column breakthrough curves during fifth cycle for Tank 41 nominal case with RF resin and new isotherm.

11.0 RF Results with Langmuir Isotherm

11.1 RF Langmuir Isotherm Parameters

Previous experimental data was fit to the "old" Langmuir isotherm equation which appears to more accurately represent batch contact data with high cesium concentrations. Table 11-1 lists the RF Langmuir isotherm parameters used in the SCIX column calculations. The first column in Table 11-1 lists the tanks and the feed cesium concentration in molar units and pCi/ml. The last two columns in the table show the total cesium loading on the RF resin at equilibrium (Q) and the corresponding curies per liter of packed bed volume (BV). That is, these columns show the cesium loading in a fully loaded column. Since the lead column is very close to being fully loaded during column processing, the curie loadings listed in the last column of Table 11-1 provide an estimate of the maximum heat load on the column for thermal analysis. As for CST, Tank 1 and Tank 37 produce the highest curie loadings on the ion-exchange columns. The highest RF curie loading is predicted to be 100 Ci/liter of bed volume for Tank 37 at 25 °C. Curie loadings in the ion-exchange columns with feed from Tanks 2 and 41 are five to 10 times lower than the maximum.

Maximum curie loadings are summarized in Table 11-2. As shown in the table, trends in loading generally correlate with feed cesium concentrations under these conditions. The RF curie loadings are less than the corresponding CST values and RF loadings calculated using the "old" Langmuir isotherm are less than those obtained using the "new" Freundlich/Langmuir isotherm. The appropriate data set should be used to create a conservative estimate of the parameters of interest for a particular application.

Table 11-1. RF Langmuir isotherm parameters.

Tank # Total [Cs] [^{137} Cs]	Temp., C	*a*	b	Q, moles Cs/L BV	Q, Ci Cs/L BV
1	**25**	0.1681	4.291E-04	4.99E-02	90.90
$1.81x10^{-4}$ M	**35**	0.1676	5.509E-04	4.15E-02	75.58
$3.30x10^{8}$ pCi /ml	**45**	0.1671	6.917E-04	3.46E-02	63.17
2	**25**	0.1666	6.359E-04	4.34E-03	11.58
$1.70x10^{-5}$ M	**35**	0.1658	8.390E-04	3.29E-03	8.79
$4.54x10^{7}$ pCi /ml	**45**	0.1650	1.080E-03	2.56E-03	6.83
3	**25**	0.1653	6.454E-04	1.48E-02	36.61
$6.35x10^{-5}$ M	**35**	0.1645	8.577E-04	1.13E-02	28.04
$1.57x10^{8}$ pCi /ml	**45**	0.1638	1.113E-03	8.84E-03	21.86
37	**25**	0.1717	2.737E-04	4.86E-02	99.88
$1.08x10^{-4}$ M	**35**	0.1712	4.170E-04	3.52E-02	72.40
$2.22x10^{8}$ pCi /ml	**45**	0.1707	5.137E-04	2.97E-02	60.96
41	**25**	0.1711	2.911E-04	4.31E-03	8.94
$7.53x10^{-6}$ M	**35**	0.1705	4.480E-04	2.82E-03	5.84
$1.56x10^{7}$ pCi /ml	**45**	0.1700	5.539E-04	2.28E-03	4.72

Table 11-2. Maximum Curie loadings on RF resin using Langmuir isotherm. (Ci Cs^{137}/L Bed Volume)

Tank	Feed Cs [M]	Temperature °C		
		25	**35**	**45**
1	$1.81x10^{-4}$	90.90	75.58	63.17
2	$1.70x10^{-5}$	11.58	8.79	6.83
3	$6.35x10^{-5}$	36.61	28.04	21.86
37	$1.08x10^{-4}$	99.88	72.40	60.96
41	$7.53x10^{-6}$	8.94	5.84	4.72

11.2 RF Langmuir Ion-exchange Column Modeling Results

Tables 11-3 through 11-14 give a summary of results from VERSE-LC ion-exchange column modeling calculations for SCIX using RF resin with the "old" Langmuir isotherm. All of the calculations assume a two-column configuration. During the first cycle, both columns contain fresh resin. After the first cycle in all subsequent cycles, the partially loaded second or lag column is placed into the lead position and a clean column is placed into the lag position at the start of the cycle. Since, after the first cycle, a partially loaded column is in the lead position less salt solution volume is processed per cycle before the operating limit is reached. Each cycle is run until the integral sum average cesium concentration in effluent collected from the lag column reaches the saltstone feed limit of 45 nCi/g.

Tables 11-3 through 11-7 list the volumes of salt solution processed during the first five ion-exchange cycles for each of the five tank compositions modeled. The total waste volume processed and the time it would take to run the ion exchange columns during the first five cycles are shown in the last two rows of each table. As before, the time is calculated by dividing the waste volume treated by the column flow rate. This represents the time required to run the loading phase of the column cycle.

Tables 11-8 through 11-14 list the estimated time it would take to process the waste volume in each tank through the ion-exchange columns and the number of column cycles required. Tables 11-12 and 11-14 provide results for Tanks 37 and 41 for the estimated volume of solution in each tank that it is planned to process while Tables 11-11 and 11-13 show results based on the total volume in these two tanks. The ion-exchange processing time is obtained by again dividing the waste volume processed by the flow rate through the column. To extrapolate beyond the five cycles calculated, it was assumed that the volume of salt solution processed during the fifth cycle would be processed in subsequent cycles when estimating the total number of cycles required.

Results of the column modeling for the assumed nominal case (25 °C, 10 gpm, 15 ft column) for each tank are plotted in Figures 11-1 through 11-5. We note that the breakthrough curves are very sharp. Therefore, to be conservative during actual operations, the run could be terminated at a lower bucket average effluent concentration without sacrificing much volume. The observed breakthrough curves are sharper than those obtained with CST but not quite as sharp as those obtained with RF using the "new" Freundlich/Langmuir isotherm.

Column profiles showing the concentration of cesium in the liquid phase down the lead and lag columns at the end of the first cycle for the nominal operating case and each of the five tank compositions tested are plotted in Figures 11-6 through 11-10. We find that in all cases, the lead column is fully loaded at the end of the first cycle. Therefore, the assumption of a fully loaded column used to estimate maximum cesium loadings in Tables 11-1 and 11-2 is found to be accurate. Figures 11-11 through 11-15 plot the breakthrough curves (instantaneous C/C_0) from the lead and lag ion-exchange columns during the fifth cycle for the nominal case for each tank. Note that graphs plotting C/C_0 can be applied to both total cesium or Cs^{137}.

Results from VERSE-LC simulations for Cases 1–5 with a system using a single RF ion-exchange column and the Langmuir isotherm are presented in Appendix B. The volume of dissolved salt solution that can be processed in each single-column cycle, the number of cycles required to process the total planned waste volume, cesium breakthrough curves and cesium profiles in the ion-exchange columns at the end of a cycle are shown for each tank.

Table 11-3. Tank 1 waste volume in thousands of gallons processed in five ion-exchange cycles with RF resin and old isotherm.

Case	1	2	3	4	5	6	7	8
	15 ft	15 ft	15 ft	10 ft	25 ft	15 ft	15 ft	15 ft
	10 gpm	5 gpm	20 gpm	10 gpm	10 gpm	10 gpm	10 gpm	10 gpm
	25 °C	25 °C	25 °C	25 °C	25 °C	35 °C	45 °C	25 °C
Cycle 1	214.4	227.9	188.3	133.4	375.9	174.4	142.8	171.7
Cycle 2	116.6	117.8	113.0	76.8	196.0	96.5	80.1	93.4
Cycle 3	119.7	119.7	118.7	79.6	199.3	99.4	82.8	95.8
Cycle 4	119.5	119.6	119.3	79.8	199.4	99.5	83.1	95.9
Cycle 5	119.6	119.6	119.5	79.9	199.1	99.5	83.2	95.9
Total	689.9	704.7	658.8	449.6	1169.7	569.3	472.1	552.7
Time, Days	47.9	97.9	22.9	31.2	81.2	39.5	32.8	38.4

Table 11-4. Tank 2 waste volume in thousands of gallons processed in five ion-exchange cycles with RF resin and old isotherm.

Case	1	2	3	4	5	6	7	8
	15 ft	15 ft	15 ft	10 ft	25 ft	15 ft	15 ft	15 ft
	10 gpm	5 gpm	20 gpm	10 gpm	10 gpm	10 gpm	10 gpm	10 gpm
	25 °C	25 °C	25 °C	25 °C	25 °C	35 °C	45 °C	25 °C
Cycle 1	177.9	192.8	157.2	110.8	316.4	135.3	105.4	142.6
Cycle 2	98.1	102.7	91.5	62.9	169.2	74.6	58.0	78.6
Cycle 3	102.5	105.9	97.7	66.7	175.5	77.8	60.4	82.2
Cycle 4	104.2	106.9	99.8	67.9	177.1	79.0	61.4	83.3
Cycle 5	105.1	107.7	101.2	68.8	178.4	79.8	61.9	84.3
Total	587.8	615.9	547.4	377.2	1016.6	446.5	347.0	471.0
Time, Days	40.8	85.5	19.0	26.2	70.6	31.0	24.1	32.7

Table 11-5. Tank 3 waste volume in thousands of gallons processed in five ion-exchange cycles with RF resin and old isotherm.

Case	1	2	3	4	5	6	7	8
	15 ft	15 ft	15 ft	10 ft	25 ft	15 ft	15 ft	15 ft
	10 gpm	5 gpm	20 gpm	10 gpm	10 gpm	10 gpm	10 gpm	10 gpm
	25 °C	25 °C	25 °C	25 °C	25 °C	35 °C	45 °C	25 °C
Cycle 1	165.8	180.3	145.3	102.7	296.0	125.7	97.4	132.8
Cycle 2	92.7	96.8	86.4	59.5	159.8	70.2	54.4	74.2
Cycle 3	96.8	99.7	92.0	62.9	164.9	73.4	56.9	77.5
Cycle 4	98.1	100.3	94.4	64.1	166.3	74.4	57.6	78.6
Cycle 5	99.1	100.9	95.6	64.8	167.3	75.2	58.3	79.4
Total	552.4	577.9	513.7	354.0	954.3	418.9	324.7	442.4
Time, Days	38.4	80.3	17.8	24.6	66.3	29.1	22.6	30.7

Table 11-6. Tank 37 waste volume in thousands of gallons processed in five ion-exchange cycles with RF resin and old isotherm.

Case	1	2	3	4	5	6	7	8
	15 ft	15 ft	15 ft	10 ft	25 ft	15 ft	15 ft	15 ft
	10 gpm	5 gpm	20 gpm	10 gpm	10 gpm	10 gpm	10 gpm	10 gpm
	25 °C	25 °C	25 °C	25 °C	25 °C	35 °C	45 °C	25 °C
Cycle 1	296.3	319.1	257.8	183.3	525.0	243.1	201.5	237.5
Cycle 2	163.9	166.4	155.7	106.7	276.5	135.6	113.0	131.1
Cycle 3	169.0	169.2	165.4	111.8	282.2	140.7	117.7	135.3
Cycle 4	169.2	169.4	167.3	112.5	281.9	141.0	118.6	135.6
Cycle 5	169.4	169.2	168.5	112.8	282.1	141.4	118.9	135.7
Total	967.8	993.3	914.7	627.0	1647.8	801.8	669.6	775.1
Time, Days	67.2	138.0	31.8	43.5	114.4	55.7	46.5	53.8

Table 11-7. Tank 41 waste volume in thousands of gallons processed in five ion-exchange cycles with RF resin and old isotherm.

Case	1	2	3	4	5	6	7	8
	15 ft	15 ft	15 ft	10 ft	25 ft	15 ft	15 ft	15 ft
	10 gpm	5 gpm	20 gpm	10 gpm	10 gpm	10 gpm	10 gpm	10 gpm
	25 °C	25 °C	25 °C	25 °C	25 °C	35 °C	45 °C	25 °C
Cycle 1	415.3	445.3	372.0	260.6	732.4	271.8	220.6	332.5
Cycle 2	224.1	233.1	210.4	144.3	385.4	146.2	118.7	179.3
Cycle 3	233.9	240.1	224.1	152.4	398.1	152.5	123.5	187.3
Cycle 4	236.8	242.3	228.5	154.9	402.0	154.4	125.1	189.5
Cycle 5	238.6	243.4	231.2	156.6	404.1	155.8	126.0	191.1
Total	1348.7	1404.2	1266.2	868.8	2322.0	880.7	713.9	1079.6
Time, Days	93.7	195.0	44.0	60.3	161.3	61.2	49.6	75.0

Table 11-8. Estimated parameters required to process 1.87×10^6 gallons of Tank 1 salt solution using RF resin and old isotherm.

Case	1	2	3	4	5	6	7	8
	15 ft	15 ft	15 ft	10 ft	25 ft	15 ft	15 ft	15 ft
	10 gpm	5 gpm	20 gpm	10 gpm	10 gpm	10 gpm	10 gpm	10 gpm
	25 °C	25 °C	25 °C	25 °C	25 °C	35 °C	45 °C	25 °C
Days	129.9	259.7	64.9	129.9	129.9	129.9	129.9	129.9
Fractional Cycles	14.87	14.74	15.13	22.78	8.52	18.07	21.79	18.74
Whole Cycles	15	15	16	23	9	19	22	19

Table 11-9. Estimated parameters required to process 2.08×10^6 gallons of Tank 2 salt solution using RF resin and old isotherm.

Case	1	2	3	4	5	6	7	8
	15 ft	15 ft	15 ft	10 ft	25 ft	15 ft	15 ft	15 ft
	10 gpm	5 gpm	20 gpm	10 gpm	10 gpm	10 gpm	10 gpm	10 gpm
	25 °C	25 °C	25 °C	25 °C	25 °C	35 °C	45 °C	25 °C
Days	144.4	288.9	72.2	144.4	144.4	144.4	144.4	144.4
Fractional Cycles	19.20	18.59	20.14	29.75	10.96	25.48	33.00	24.08
Whole Cycles	20	19	21	30	11	26	33	25

Table 11-10. Estimated parameters required to process 2.09×10^6 gallons of Tank 3 salt solution using RF resin and old isotherm.

Case	1	2	3	4	5	6	7	8
	15 ft	15 ft	15 ft	10 ft	25 ft	15 ft	15 ft	15 ft
	10 gpm	5 gpm	20 gpm	10 gpm	10 gpm	10 gpm	10 gpm	10 gpm
	25 °C	25 °C	25 °C	25 °C	25 °C	35 °C	45 °C	25 °C
Days	145.1	290.3	72.6	145.1	145.1	145.1	145.1	145.1
Fractional Cycles	20.52	19.99	21.49	31.81	11.79	27.23	35.26	25.76
Whole Cycles	21	20	22	32	12	28	36	26

Table 11-11. Estimated parameters required to process 4.10×10^6 gallons of Tank 37 salt solution using RF resin and old isotherm.

Case	1	2	3	4	5	6	7	8
	15 ft	15 ft	15 ft	10 ft	25 ft	15 ft	15 ft	15 ft
	10 gpm	5 gpm	20 gpm	10 gpm	10 gpm	10 gpm	10 gpm	10 gpm
	25 °C	25 °C	25 °C	25 °C	25 °C	35 °C	45 °C	25 °C
Days	284.7	569.4	142.4	284.7	284.7	284.7	284.7	284.7
Fractional Cycles	23.49	23.36	23.90	35.79	13.69	28.32	33.85	29.51
Whole Cycles	24	24	24	36	14	29	34	30

Table 11-12. Estimated parameters required to process 1.00×10^6 gallons of Tank 37 salt solution using RF resin and old isotherm.

Case	1	2	3	4	5	6	7	8
	15 ft	15 ft	15 ft	10 ft	25 ft	15 ft	15 ft	15 ft
	10 gpm	5 gpm	20 gpm	10 gpm	10 gpm	10 gpm	10 gpm	10 gpm
	25 °C	25 °C	25 °C	25 °C	25 °C	35 °C	45 °C	25 °C
Days	69.4	138.9	34.7	69.4	69.4	69.4	69.4	69.4
Fractional Cycles	5.19	5.04	5.51	8.31	2.70	6.40	7.78	6.66
Whole Cycles	6	6	6	9	3	7	8	7

Table 11-13. Estimated parameters required to process 3.48×10^6 gallons of Tank 41 salt solution using RF resin and old isotherm.

Case	1	2	3	4	5	6	7	8
	15 ft	15 ft	15 ft	10 ft	25 ft	15 ft	15 ft	15 ft
	10 gpm	5 gpm	20 gpm	10 gpm	10 gpm	10 gpm	10 gpm	10 gpm
	25 °C	25 °C	25 °C	25 °C	25 °C	35 °C	45 °C	25 °C
Days	266.7	533.3	133.3	266.7	266.7	266.7	266.7	266.7
Fractional Cycles	15.44	15.01	16.13	23.97	8.76	24.00	29.81	19.44
Whole Cycles	16	16	17	24	9	24	30	20

Table 11-14. Estimated parameters required to process 0.19×10^6 gallons of Tank 41 salt solution using RF resin and old isotherm.

Case	1	2	3	4	5	6	7	8
	15 ft	15 ft	15 ft	10 ft	25 ft	15 ft	15 ft	15 ft
	10 gpm	5 gpm	20 gpm	10 gpm	10 gpm	10 gpm	10 gpm	10 gpm
	25 °C	25 °C	25 °C	25 °C	25 °C	35 °C	45 °C	25 °C
Days	13.2	26.4	6.6	13.2	13.2	13.2	13.2	13.2
Fractional Cycles	0.46	0.43	0.51	0.73	0.26	0.70	0.86	0.57
Whole Cycles	1	1	1	1	1	1	1	1

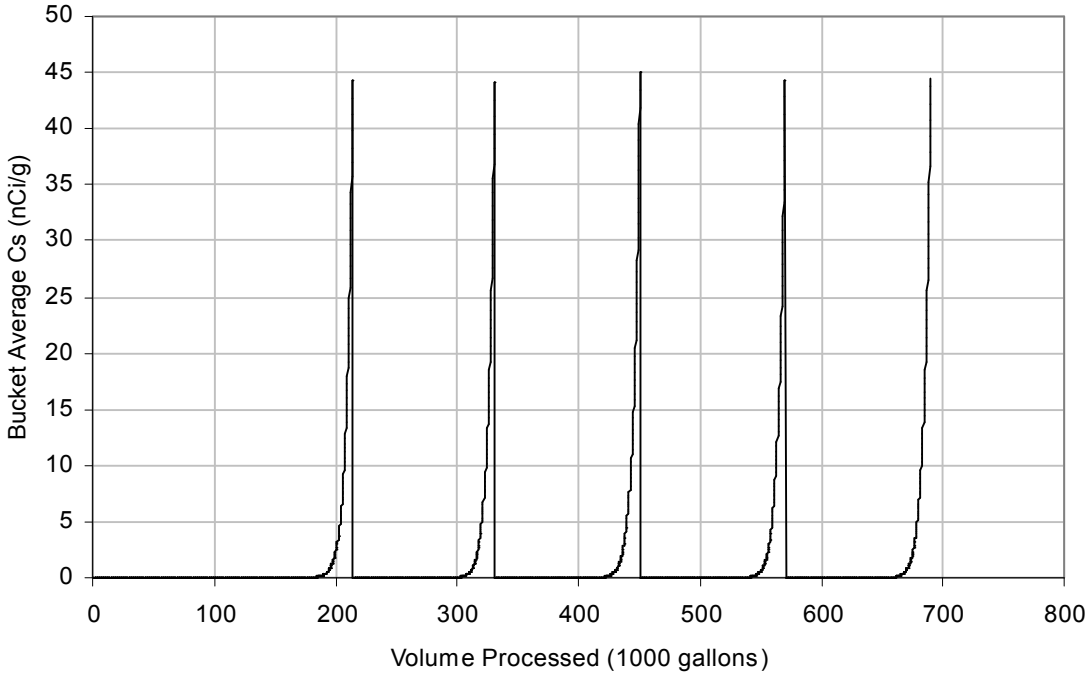

Figure 11-1. Breakthrough curves in first five cycles for Tank 1 nominal case with RF resin and old isotherm.

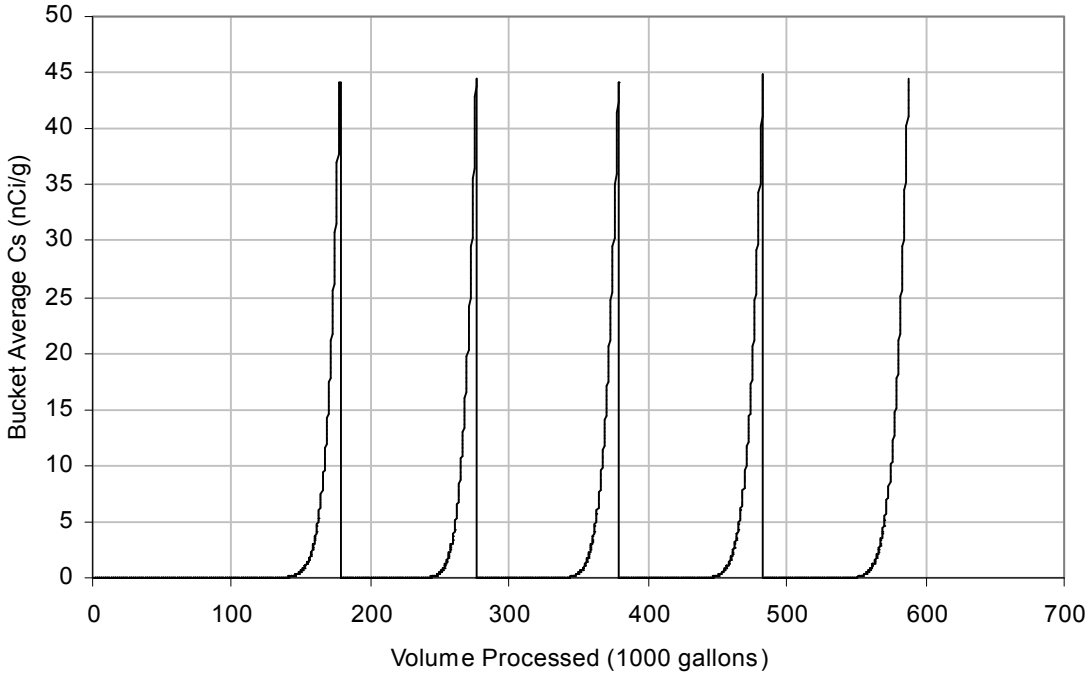

Figure 11-2. Breakthrough curves in first five cycles for Tank 2 nominal case with RF resin and old isotherm.

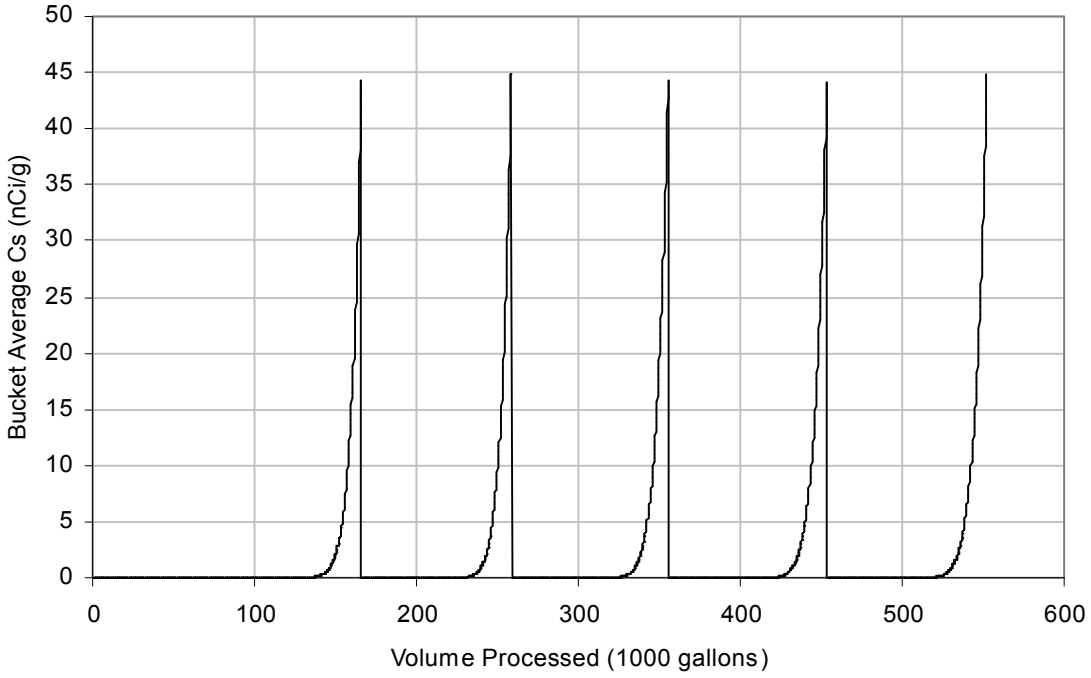

Figure 11-3. Breakthrough curves in first five cycles for Tank 3 nominal case with RF resin and old isotherm.

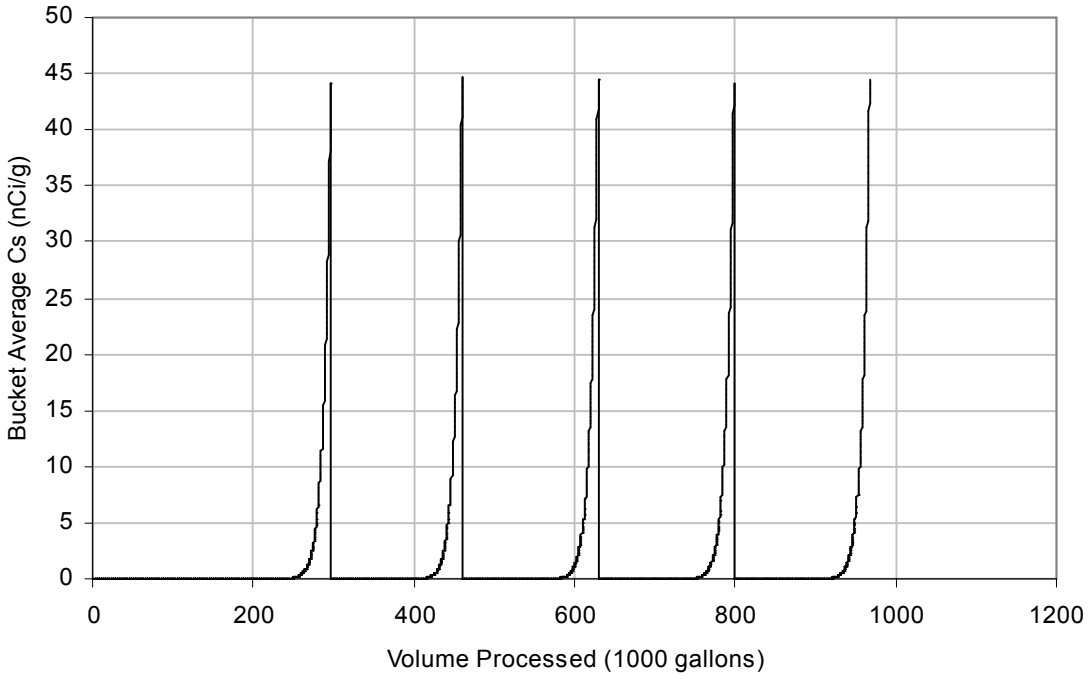

Figure 11-4. Breakthrough curves in first five cycles for Tank 37 nominal case with RF resin and old isotherm.

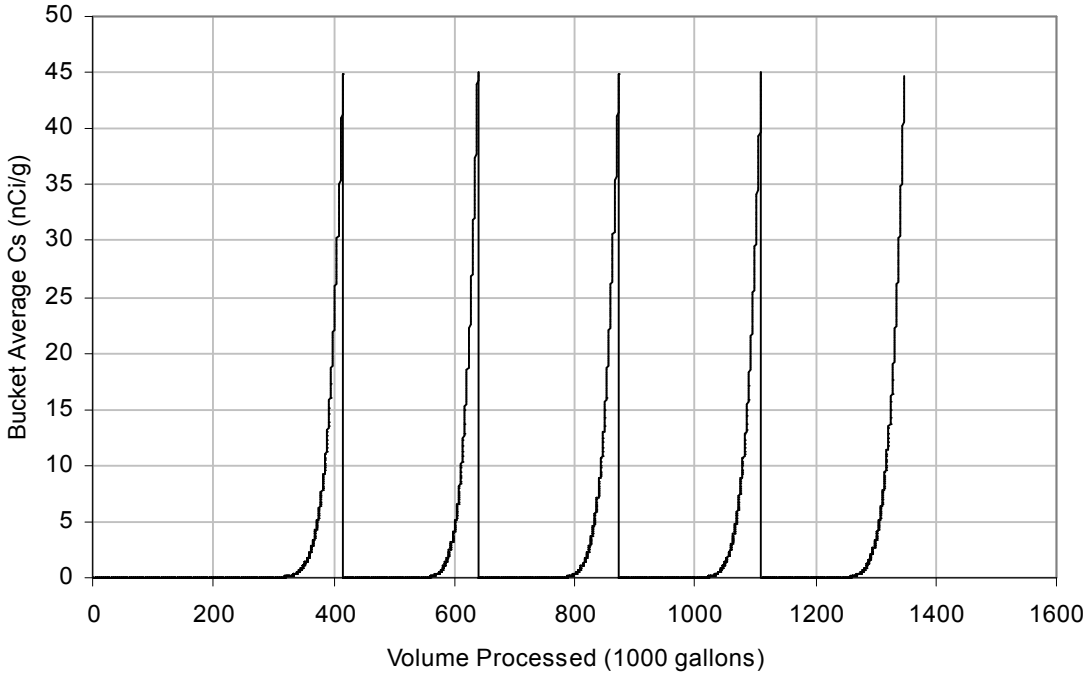

Figure 11-5. Breakthrough curves in first five cycles for Tank 41 nominal case with RF resin and old isotherm.

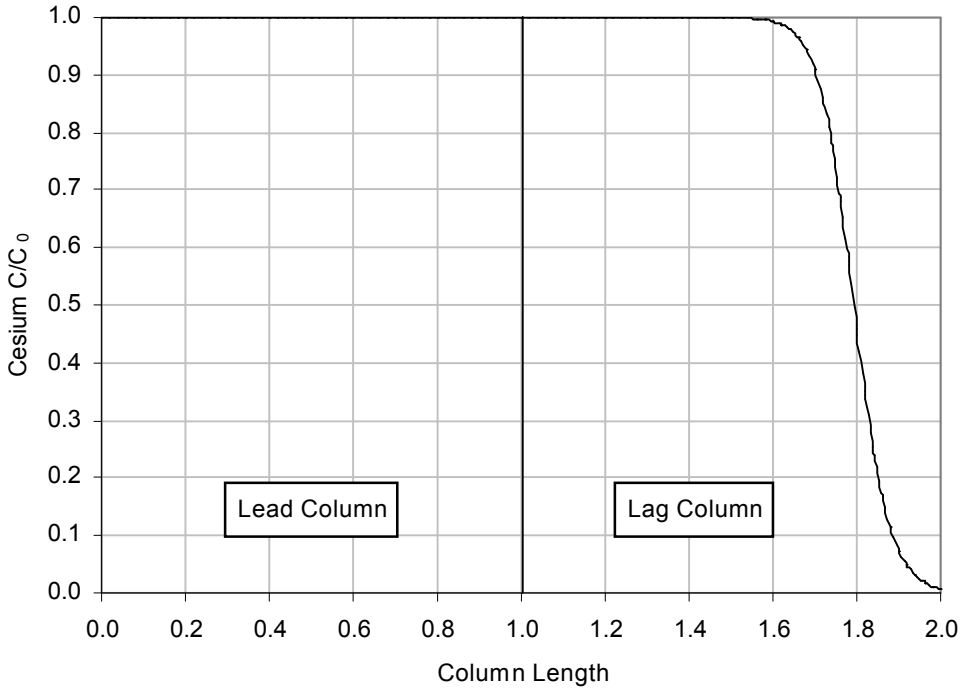

Figure 11-6. Cesium profile in columns at end of first cycle for Tank 1 nominal case with RF resin and old isotherm.

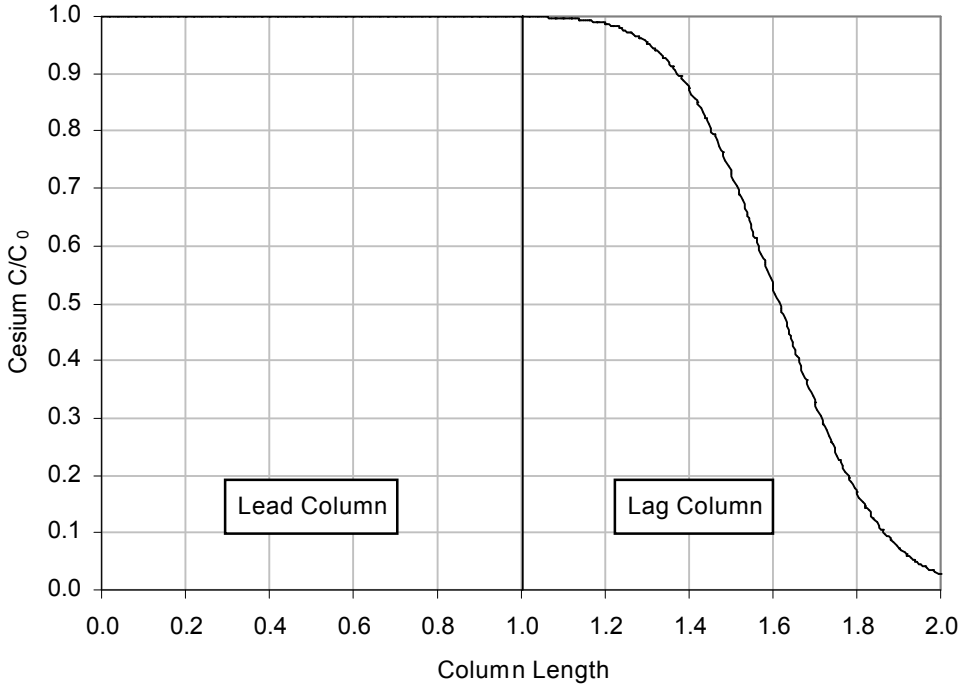

Figure 11-7. Cesium profile in columns at end of first cycle for Tank 2 nominal case with RF resin and old isotherm.

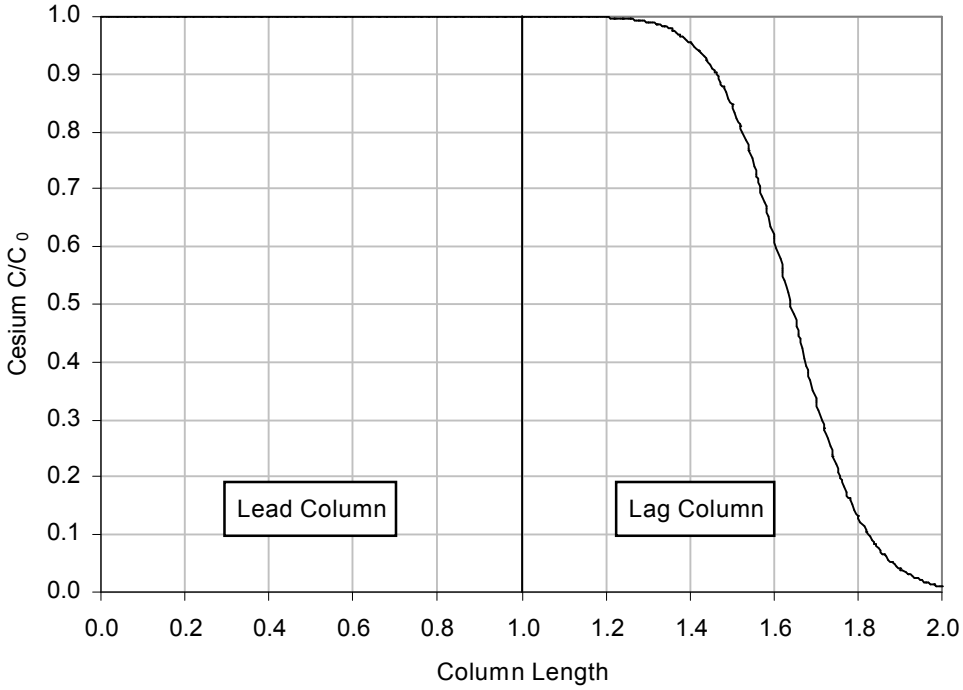

Figure 11-8. Cesium profile in columns at end of first cycle for Tank 3 nominal case with RF resin and old isotherm.

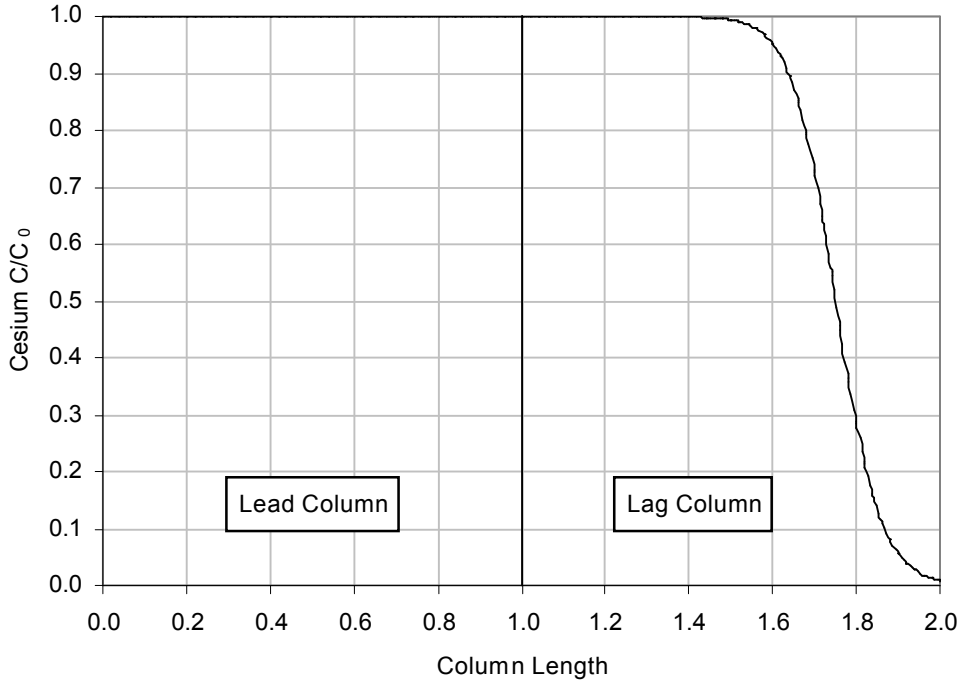

Figure 11-9. Cesium profile in columns at end of first cycle for Tank 37 nominal case with RF resin and old isotherm.

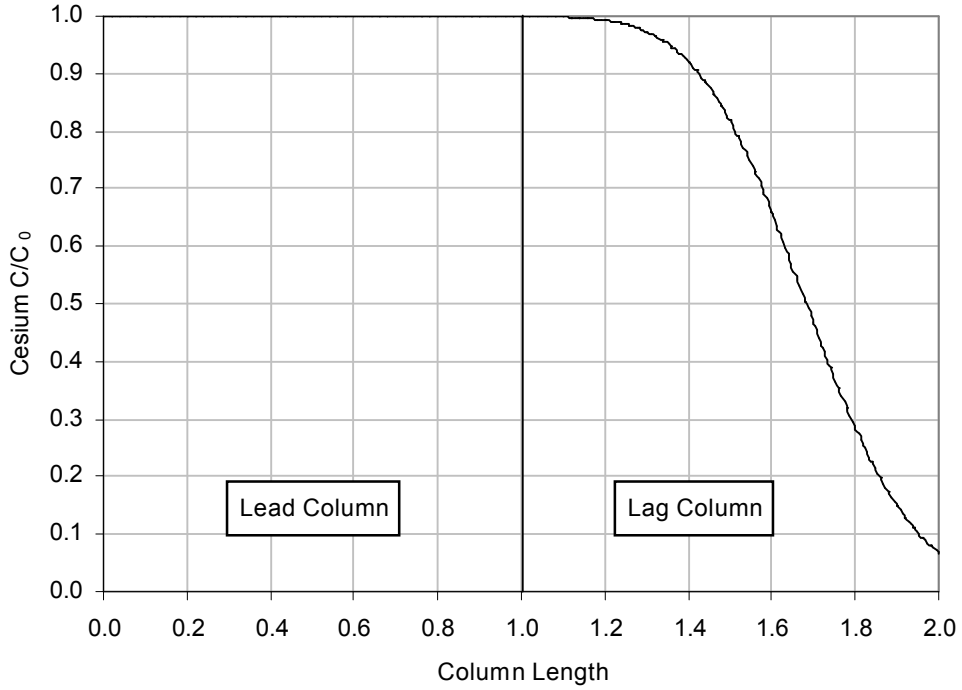

Figure 11-10. Cesium profile in columns at end of first cycle for Tank 41 nominal case with RF resin and old isotherm.

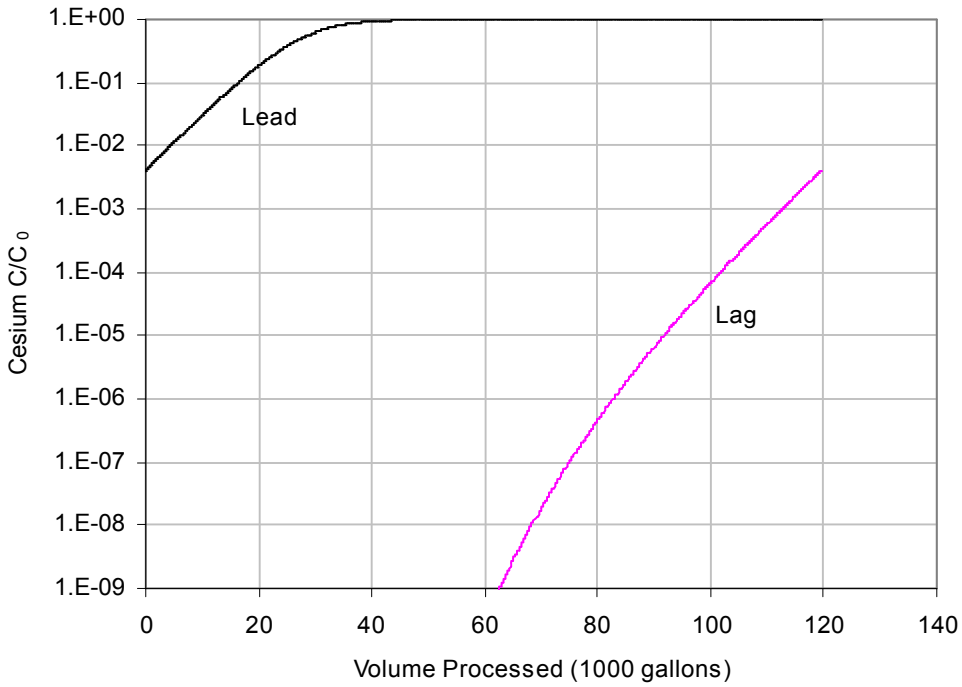

Figure 11-11. Column breakthrough curves during fifth cycle for Tank 1 nominal case with RF resin and old isotherm.

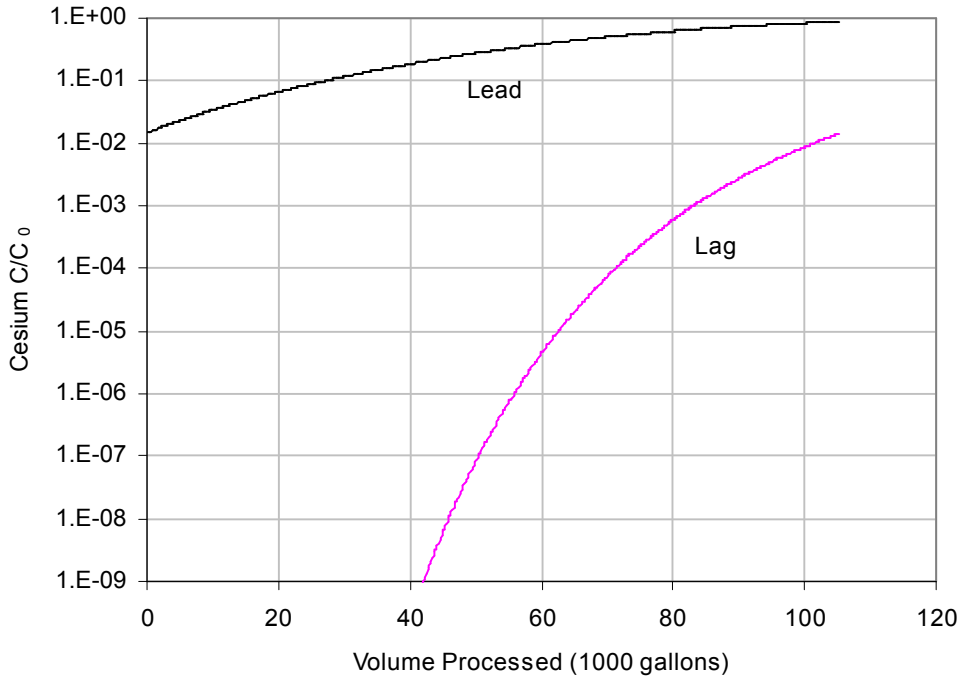

Figure 11-12. Column breakthrough curves during fifth cycle for Tank 2 nominal case with RF resin and old isotherm.

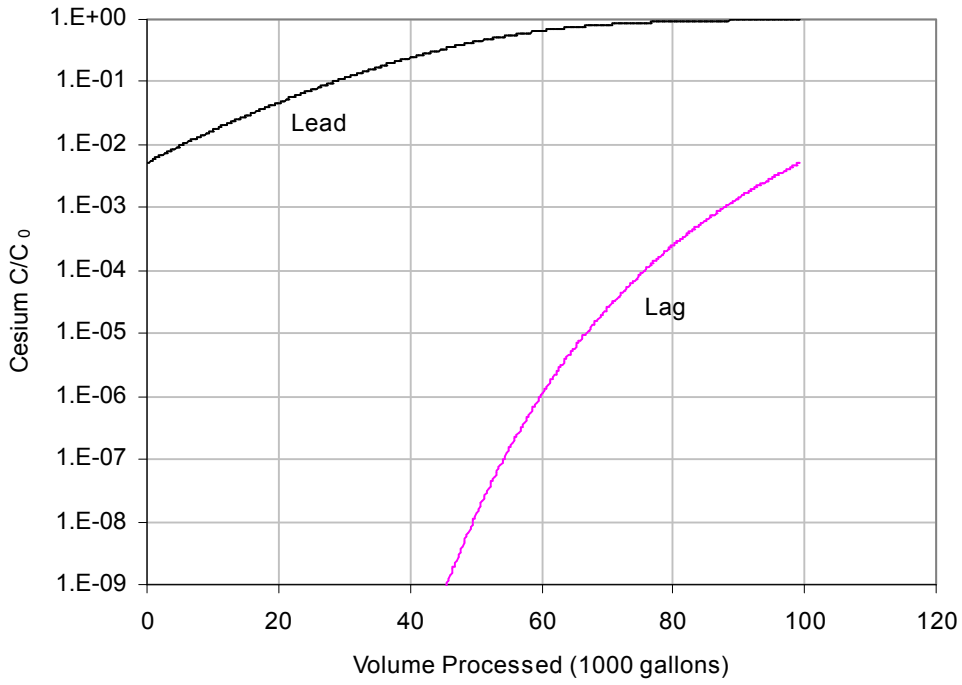

Figure 11-13. Column breakthrough curves during fifth cycle for Tank 3 nominal case with RF resin and old isotherm.

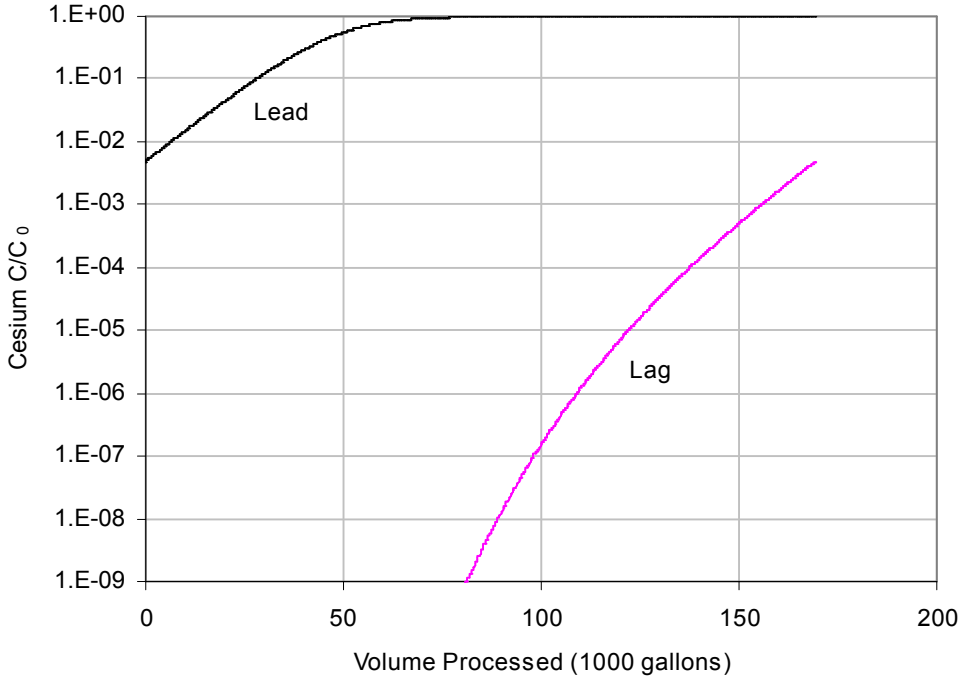

Figure 11-14. Column breakthrough curves during fifth cycle for Tank 37 nominal case with RF resin and old isotherm.

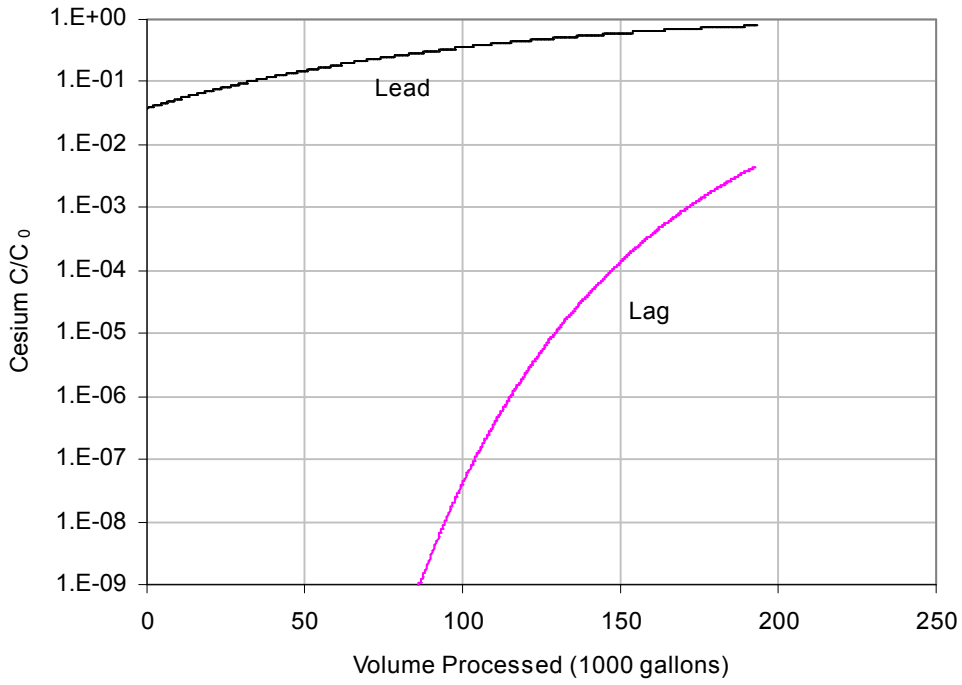

Figure 11-15. Column breakthrough curves during fifth cycle for Tank 41 nominal case with RF resin and old isotherm.

12.0 Conclusions

In all cases, both CST and RF resin were able to process a significant volume of dissolved salt cake during each ion-exchange cycle. During the first cycle, when there are two clean columns in the ion-exchange train, more waste volume can be processed than in subsequent cycles when a partially loaded lag column has been placed in the lead position. After the first cycle, essentially the same volume of waste can be processed in each subsequent cycle. Table 12-1 compares the volume of waste processed during the second cycle for all of the cases evaluated. Comparing the RF results obtained using the original Langmuir isotherm to CST we find that CST consistently has nearly twice the volumetric capacity for cesium adsorption and is able to process approximately twice the solution volume. The revised Freundlich/Langmuir isotherm gives less consistent results. This is because the revision improved adsorption capacity primarily at lower cesium concentrations to obtain better agreement with the most recent experimental data. Therefore, it is not surprising that using the new RF isotherm indicates significantly better performance for Tank 2 and Tank 41 which had the lowest cesium concentrations. For Tank 2 using the revised RF isotherm in some cases predicted column performance exceeding that obtained with CST on a volumetric basis. To determine true RF column performance for this system, testing with actual dissolved saltcake compositions is required.

Other general trends in the results are:

- Lower flow sharpens the breakthrough front and allows more volume to be processed in each ion-exchange cycle. However, decreasing the flow from 10 gpm to 5 gpm roughly increased the volume of solution processed by only about 10% for CST and 1% for RF while at the same time doubling the time required to run the material through the column for both media.

- Higher flow spreads out the breakthrough front and decreases the amount of solution that can be processed in each ion-exchange cycle. However, doubling the flow from 10 gpm to 20 gpm roughly decreased the volume of solution processed by about 17% for CST and about 4% for RF, while also decreasing the time required to run the material through the column by a factor of two. Processing at a higher flow would also decrease the exposure of the RF resin, increasing the volume of waste that each batch could process before it is radiolytically degraded..

- Operating the column at elevated temperatures decreases the adsorption capacity of the resins and decreases the amount of solution that can be treated in each cycle. Operating at 45 °C instead of 25 °C decreased the RF resin capacity by approximately 50% and CST capacity by roughly 30%.

- Depending on operating conditions, estimates of the amount of CST required to process the planned volume of dissolved saltcake in Tanks 1-3, 37 and 41 ranged from about 56 to 75 metric tons.

- For nominal operating conditions, it will take on the order of 10 ion-exchange cycles per tank to process the dissolved salt cake in Tanks 1-3 with CST media or RF resin using the newer RF isotherm. To provide a conservative bracket on the expected operating conditions with SRS waste, modeling was also performed using the older RF isotherm. The original RF isotherm indicates approximately twice as many cycles will be required using RF resin. The latest experimental data was fit to a Freundlich/Langmuir isotherm equation which appears to more accurately represent batch contact data with low cesium concentrations. The earlier Langmuir isotherm seems to fit better at high cesium concentrations. Testing with SRS waste would be required to confirm the expected performance. To bracket conditions for process flow, the appropriate data set should be used to ensure a sufficiently conservative estimate, depending on the application.

- At the nominal flow rate of 10 gpm it will take 1.38 years of operating time to run the planned volume of dissolved salt cake through the ion-exchange columns in the loading phase. Overall operating time must also include time to change out the lead column and, in the case of RF resin, time to elute and regenerate the resin, as well as time for maintenance and outages.

Table 12-1. Waste volume in thousands of gallons processed during second ion-exchange cycle for all test cases run.

Tank	Resin	1	2	3	4	5	6	7	8[1]
		15 ft	15 ft	15 ft	10 ft	25 ft	15 ft	15 ft	15 ft
		10 gpm	5 gpm	20 gpm	10 gpm	10 gpm	10 gpm	10 gpm	10 gpm
		25 °C	25 °C	25 °C	25 °C	25 °C	35 °C	45 °C	25 °C
1	**CST**	212	229	180	130	377	199	187	NA
	RF New	169	170	168	112	283	132	102	135
	RF Old	117	118	113	77	196	96	80	93
2	**CST**	193	211	168	120	345	175	160	NA
	RF New	247	254	235	160	421	157	103	198
	RF Old	98	103	92	63	169	75	58	79
3	**CST**	197	215	170	122	352	166	144	NA
	RF New	204	206	201	135	343	137	92	164
	RF Old	93	97	86	60	160	70	54	74
37	**CST**	390	418	335	241	689	310	246	NA
	RF New	257	258	254	170	430	198	151	206
	RF Old	164	166	156	107	276	136	113	131
41	**CST**	449	486	396	280	797	348	271	NA
	RF New	432	444	412	281	737	290	199	346
	RF Old	224	233	210	144	385	146	119	179

[1]Case 8 used 80% of the nominal RF resin capacity to simulate resin degradation from chemical and radioactive exposure.

13.0 References

Aleman, S. E., L. L. Hamm, and F. G. Smith, 2007. "Ion Exchange Modeling of Cesium Removal from Hanford Waste Using Spherical Resorcinol-Formaldehyde Resin," WSRC-STI-2007-00030, Rev. 0, (Draft C).

Aleman, S. E. and L. L. Hamm, 2007. "Detailed Thermodynamic Equilibrium Model for the Prediction of Ion Exchange Behavior on Monovalent Cation Exchange Resins," WSRC-STI-2007-00054, Rev. 0, (Draft).

Aleman, S. E., 2003. "Small Column Ion Exchange Analysis for Removal of Cesium from SRS Low Curie Salt Solutions Using Crystalline Silicotitanate (CST) Resin," WSRC-TR-2003-00430, Rev. 1, (January, 2004).

Adamson, D. J., M. D. Fowley, J. L. Steimke, T. J. Steeper, M. Williams, C. E. Duffey, F. Fondeur, 2006. "Pilot-Scale Hydraulic Testing of Resorcinol Formaldehyde Ion Exchange Resin," WSRC-TR-2005-00570 (SRNL-RPP-2006-00013), Rev. 0, (March 2006).

Anderko, A and M. M. Lencka, 1977, "Computation of Electrical Conductivity of Multicomponent Aqueous Systems in Wide Concentration and Temperature Ranges," *Ind. Eng. Chem. Res.*, **1997**, 36, 1932-1943.

Berninger, J., R. D. Whitley, X. Zhang, and N.-H.L. Wang, 1991. "A Versatile Model for Simulation of Reaction and Nonequilibrium Dynamics in Multicomponent Fixed-Bed Adsorption Processes," *Comput. Chem. Eng.*, **1991**, *15*(11), 749-768.

Bird, R. B., W. E. Stewart, and E. N. Lightfoot, 1960. Transport Phenomena, John Wiley and Sons, Inc., New York.Cornish, A. R. H., 1965. "Note on Minimum Possible Rate of Heat Transfer from a Sphere when other Spheres are Adjacent to it," Trans. Inst. Chem. Engrs., Vol. 43, pp. 332-333.

Brooks, K. P., 1994. "Cesium Ion Exchange using Actual Waste: Column Size Considerations," TWRSPP-94-091, Battelle PNL, September.

Chung, S. F. and C. Y. Wen, 1968. "Longitudinal Dispersion of Liquid Flowing Through Fixed and Fluidized Beds," AIChE J., Vol. 14, No. 6, pp. 857-866.

Duffey, C. E. and D. D. Walker, 2006. "Radiolytic, Thermal, and Physical Degradation Testing of Spherical Resorcinol-Formaldehyde Resin," WSRC-TR-2005-00075 (SRNL-RPP-2005-00008), Rev. 0, (July 2006).

Fiskum, S. K., S. T. Arm, M. S. Fountain, M. J. Steele, and D. L. Blanchard, Jr., 2006, "Spherical Recorcinol-Formaldehyde Resin Testing for ^{137}Cs Removal from Simulated and Actual Hanford Waste Tank 241-AP-101 Diluted Feed (Envelope A) Using Small Column Ion Exchange," Battelle-Pacific Northwest, WTP-RPT-134, Rev 0, February, 2006.

Foo, S. C. and R. G. Rice, 1975. "On the Predication of Ultimate Separation in Parametric Pumps," AIChE Journal, Vol. 21, No. 6, pp. 1149-1158.

German, R. M., 1989. Particle Packing Characteristics, Metal Powder Industries Federation, Princeton, New Jersey.

Glasstone, S., and D. Lewis, 1960. Elements of Physical Chemistry, D. Van Nostrand Company, Inc., Princeton, N.J.

Hamm, L. L., F. G. Smith, and M. A. Shadday, 2000. "QA Verification Package for VERSE-LC Version 7.80," WSRC-TR-99-00238, Rev. 0 (February).

Hamm, L. L., T. Hang, D. J. McCabe, and W. D. King, 2002. "Preliminary Ion Exchange Modeling for Removal of Cesium from Hanford Waste Using Hydrous Crystalline Silicotitanate Material," WSRC-TR-2001-00400 (SRT-RPP-2001-00134), Rev. 0 (July, 2002).

Hamm, L. L., S. E. Aleman, B. J. Hardy, W. D. King, and C. E. Duffey, 2003. "Ion Exchange Modeling for Removal of Cesium from Hanford Waste Using SuperLig® 644 Resin," WSRC-TR-2003-00555 (SRT-RPP-2003-00242), Rev. 0 (February, 2004).

King, W. D., C. E. Duffey, S. H. Malene, 2003. "Determination of Cesium (Cs^+) Adsorption Kinetics and Equilibrium Isotherms from Hanford Waste Simulants using Resorcinol-Formaldehyde Resins (U)," WSRC-TR-2003-00574 (SRT-RPP-2003-00252), Rev. 0 (March, 2004).

Nash, C. A., M. R. Duignan, and C. E. Duffey, 2006. "Batch, Kinetics, and Column Data from Spherical Resorcinol-Formaldehyde Resin," WSRC-STI-2006-00071 (SRNL-RPP-2006-00024), Rev. 0 (August 14, 2006).

Perry, R. H., C. H. Chilton, and S. D. Kirkpatrick, (eds.) 1973. Chemical Engineer's Handbook, 5th ed., McGraw-Hill, New York.

Reid, R. C., J. M. Prausnitz, and T. K. Sherwood, 1977. The Properties of Gases and Liquids, 3rd ed., McGraw-Hill chemical engineering series, McGraw-Hill Book Company, Inc., New York. pp. 590-592.

Tran, H. Q., 2007. "Tanks 1-3, 37, and 41 Dissolved Salt Solution Projected Compositions," LWO-PIT-2007-00040, Rev. 0 (March 29, 2007).

Whitley, R. D. and N.-H. Wang, 1998. "User's Manual VERSE (VErsatile Reaction Seperation) Simulation for Liquid Phase Adsorption and Chromatography Processes," School of Chemical Engineering, Purdue University, July, 1998.

Wilson, E. J.,Geankoplis, 1966. C. J. "Liquid Mass Transfer at Very Low Reynolds Numbers in Packed Beds", I & EC Fundamentals, Vol 5, No 1 PP, 9-14.

Zheng, Z., R. G. Anthony, and J. E. Miller, 1997. "Modeling Multicomponent Ion Exchange Equilibrium Utilizing Hydrous Crystalline Silicotitanates by a Multiple Interactive Ion Exchange Site Model," Ind. Eng. Chem. Res. 1997, 36, pp. 2427-2434.

Appendix A. CST Single Column Results

Results from model simulations assuming a single ion-exchange column with CST medium are presented in this appendix. Table A-1 lists the volume of dissolved salt solution that can be processed through a single column before reaching the bucket average effluent concentration of 45 nCi/g. Five cases were run testing column lengths of 10, 15 and 25 feet and flow rates of 5, 10 and 20 gpm. All runs were made at 25 °C. Table A-2 shows the fractional number of ion-exchange cycles required to process the volume of dissolved salt cake in each tank. For Tanks 37 and 41 the expected waste volume that will be processed has been used.

Figures A-1 through A-5 show the cesium concentration profiles in the CST columns at the end of a cycle for each case. With a single column, each ion-exchange process cycle is identical. In general, the trend is that lower flows and longer columns give sharper profiles that better utilize the ion-exchange material. Figure A-6 shows breakthrough curves (instantaneous relative cesium concentration at the column exit) for the five compositions.

Results in this appendix can be compared to the two column results for CST ion-exchange medium presented in Section 9.

Table A-1. Waste volumes processed in thousands of gallons with single CST columns.

Flow	**5 gpm**	**10 gpm**	**20 gpm**	**10 gpm**	**10 gpm**
Length	**15 ft**	**15 ft**	**15 ft**	**10 ft**	**25 ft**
Tank 1	163.6	121.1	78.3	63.1	256.1
Tank 2	159.4	124.8	86.6	68.1	252.2
Tank 3	158.3	122.4	83.9	66.1	249.7
Tank 37	306.5	228.6	148.7	119.9	480.3
Tank 41	382.7	306.4	217.8	169.6	608.7

Table A-2. Number of ion-exchange cycles required to process dissolved saltcake volume using a single CST column.

Flow	**5 gpm**	**10 gpm**	**20 gpm**	**10 gpm**	**10 gpm**
Length	**15 ft**	**15 ft**	**15 ft**	**10 ft**	**25 ft**
Tank 1	11.43	15.44	23.88	29.64	7.30
Tank 2	13.05	16.67	24.02	30.54	8.25
Tank 3	13.20	17.08	24.91	31.62	8.37
Tank 37	3.26	4.37	6.72	8.34	2.08
Tank 41	0.50	0.62	0.87	1.12	0.31

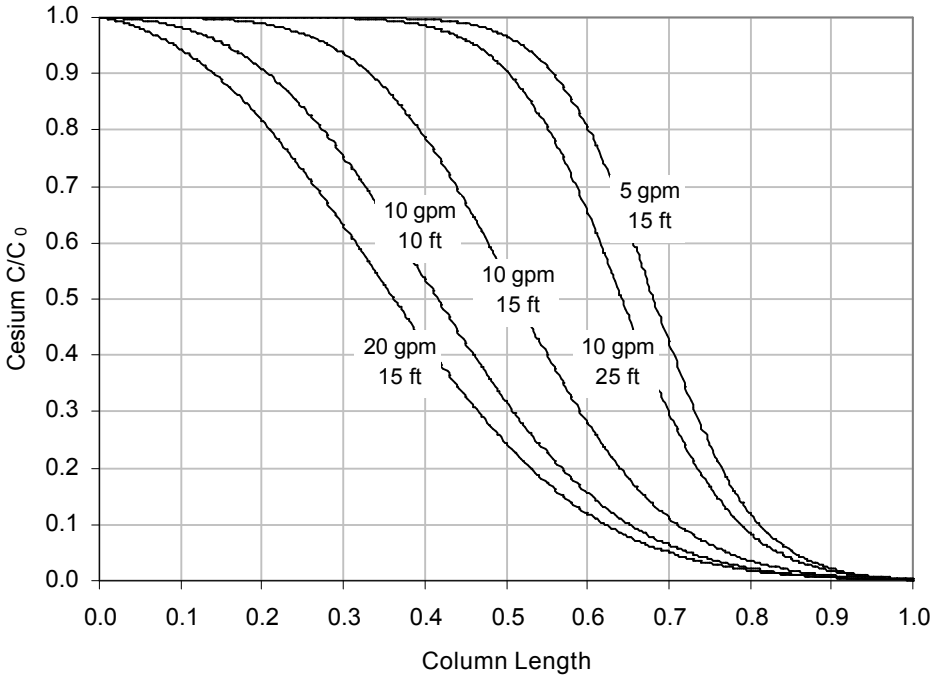

Figure A-1. Cesium concentration profiles in single CST column at end of run for Tank 1.

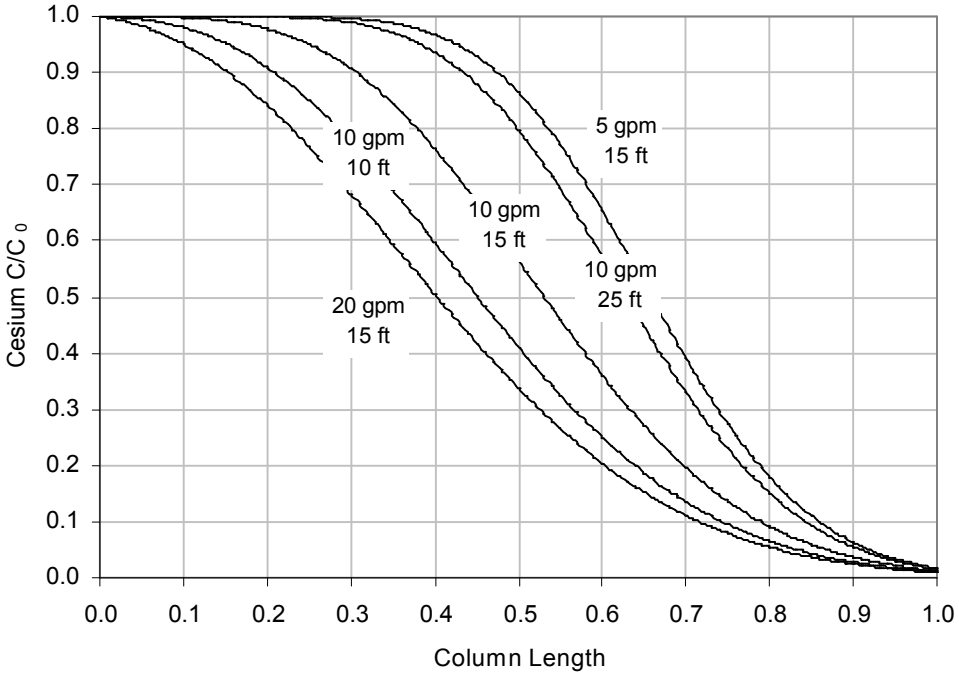

Figure A-2. Cesium concentration profiles in single CST column at end of run for Tank 2.

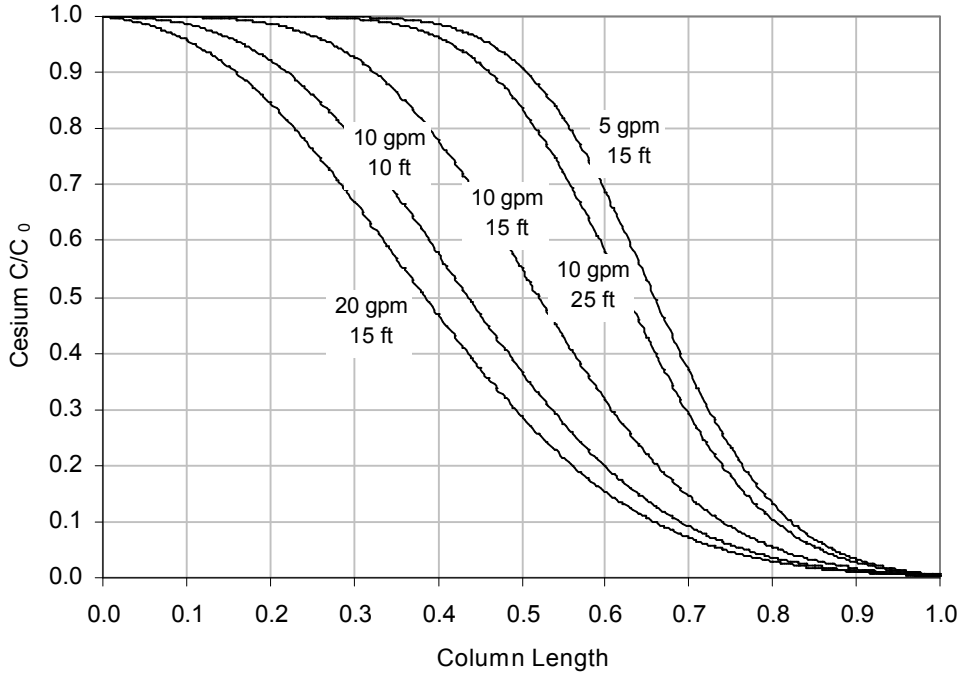

Figure A-3. Cesium concentration profiles in single CST column at end of run for Tank 3.

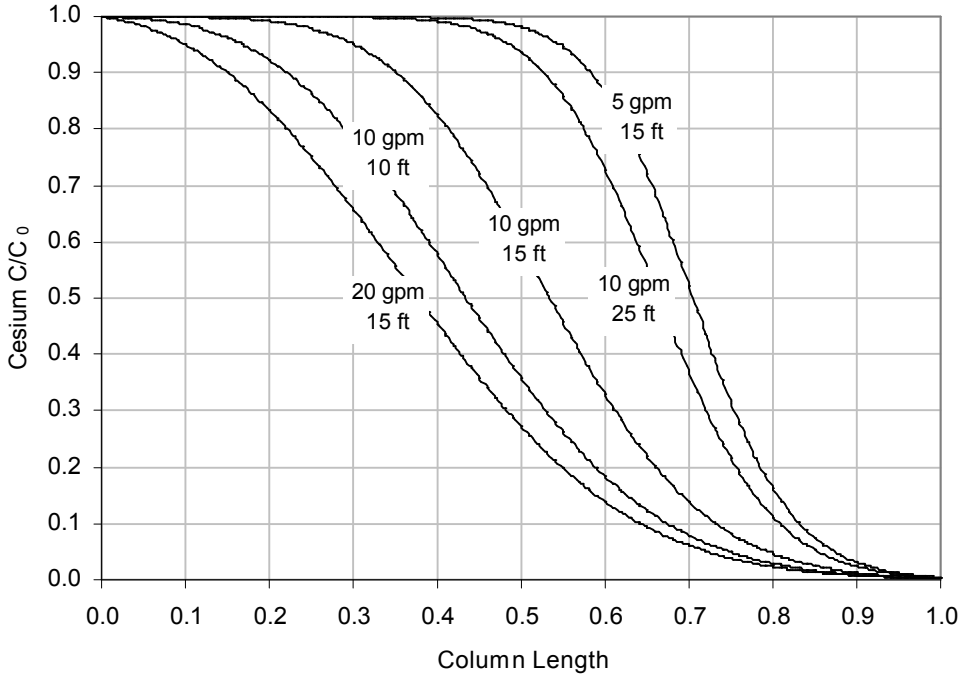

Figure A-4. Cesium concentration profiles in single CST column at end of run for Tank 37.

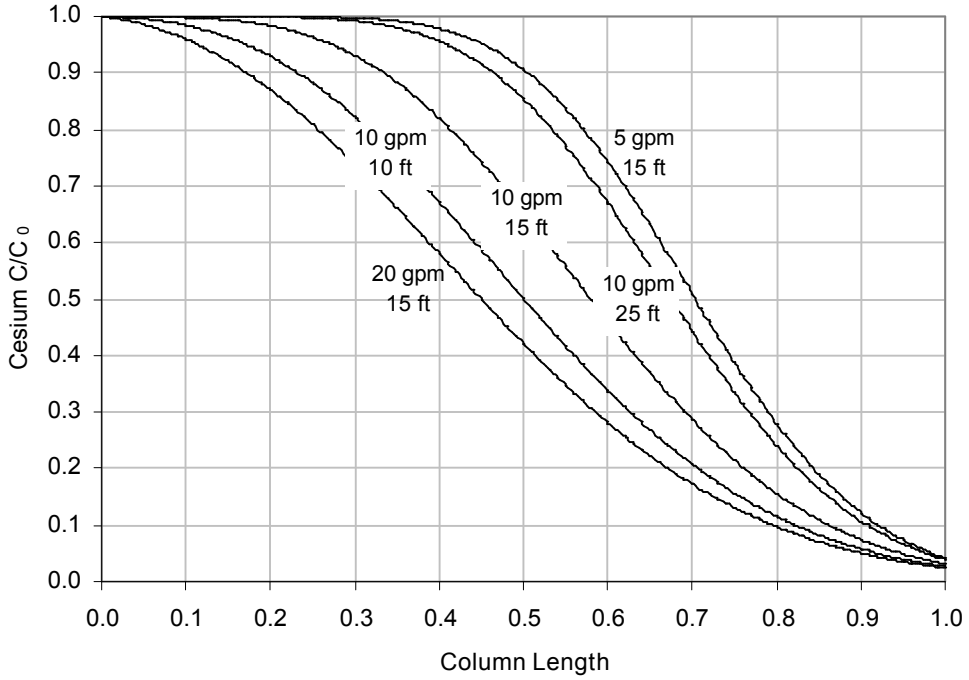

Figure A-5. Cesium concentration profiles in single CST column at end of run for Tank 41.

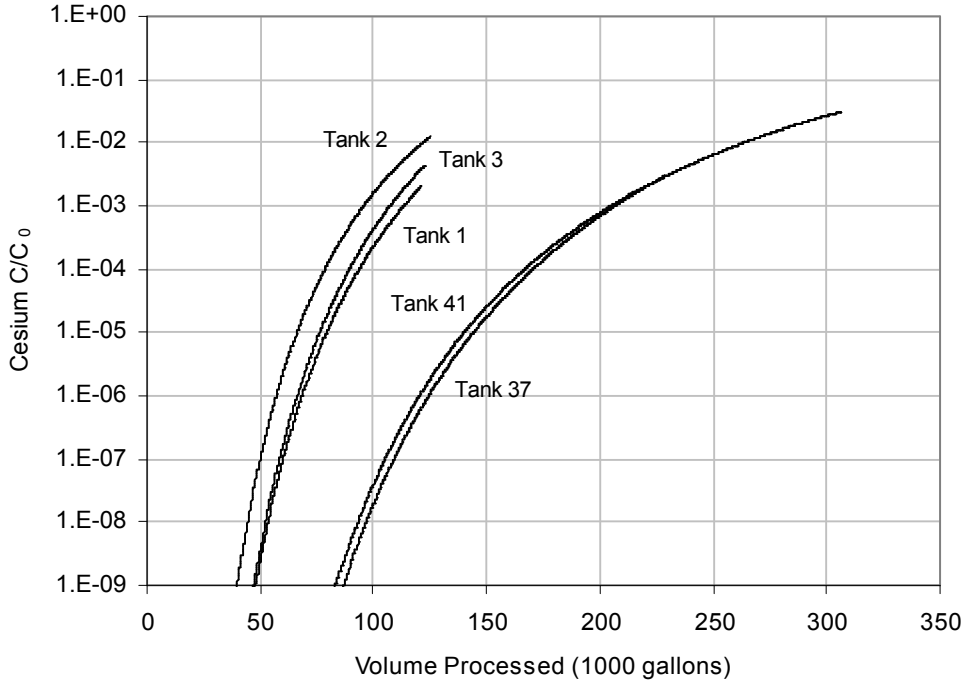

Figure A-6. Cesium breakthrough curves from single CST column runs.

Appendix B. RF Single Column Results

Results from model simulations assuming a single ion-exchange column with RF medium using the "old" or Langimur isotherm are presented in this appendix. Table B-1 lists the volume of dissolved salt solution that can be processed through a single column before reaching the bucket average effluent concentration of 45 nCi/g. Five cases were run testing column lengths of 10, 15 and 25 feet and flow rates of 5, 10 and 20 gpm. All runs were made at 25 °C. Table B-2 shows the fractional number of ion-exchange cycles required to process the volume of dissolved salt cake in each tank. For Tanks 37 and 41 the expected waste volume that will be processed has been used.

Figures B-1 through B-5 show the cesium concentration profiles in the CST columns at the end of a cycle for each case. With a single column, each ion-exchange process cycle is identical. In general, the trend is that lower flows and longer columns give sharper profiles that better utilize the ion-exchange material. Figure B-6 shows breakthrough curves (instantaneous relative cesium concentration at the column exit) for the five compositions.

Results in this appendix can be compared to the two column results obtained for the same ion-exchange medium and isotherm presented in Section 11.

Table B-1. Waste volumes processed in thousands of gallons with single RF columns.

Flow	**5 gpm**	**10 gpm**	**20 gpm**	**10 gpm**	**10 gpm**
Length	**15 ft**	**15 ft**	**15 ft**	**10 ft**	**25 ft**
Tank 1	106.7	93.6	73.9	54.9	173.8
Tank 2	88.5	78.1	64.2	46.8	144.1
Tank 3	82.5	72.2	58.6	42.9	133.9
Tank 37	147.5	127.9	100.9	74.8	239.6
Tank 41	206.8	184.7	155.2	111.8	337.5

Table B-2. Number of ion-exchange cycles required to process dissolved saltcake volume with single RF columns.

Flow	**5 gpm**	**10 gpm**	**20 gpm**	**10 gpm**	**10 gpm**
Length	**15 ft**	**15 ft**	**15 ft**	**10 ft**	**25 ft**
Tank 1	17.53	19.98	25.30	34.06	10.76
Tank 2	23.50	26.63	32.40	44.44	14.43
Tank 3	25.33	28.95	35.67	48.72	15.61
Tank 37	6.78	7.82	9.91	13.37	4.17
Tank 41	0.92	1.03	1.22	1.70	0.56

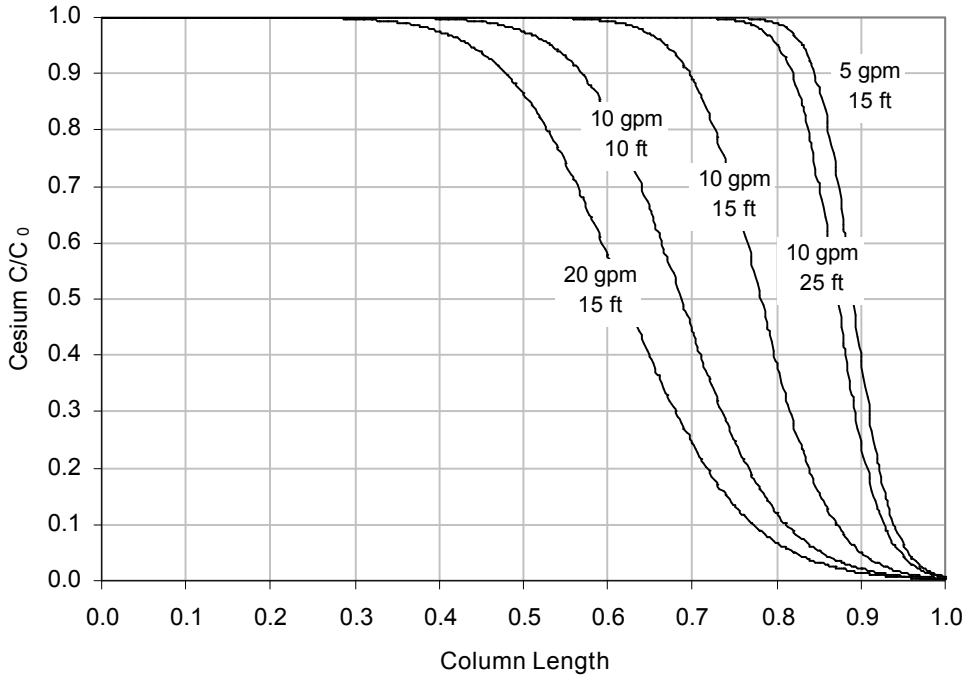

Figure B-1. Cesium concentration profile in single RF column at end of run for Tank 1.

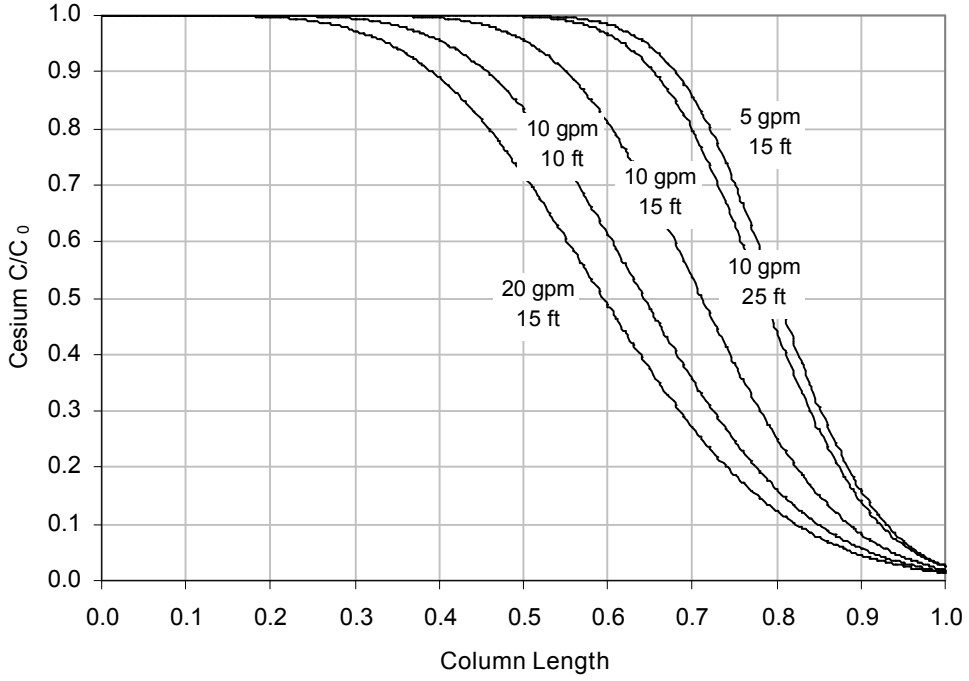

Figure B-2. Cesium concentration profile in single RF column at end of run for Tank 2.

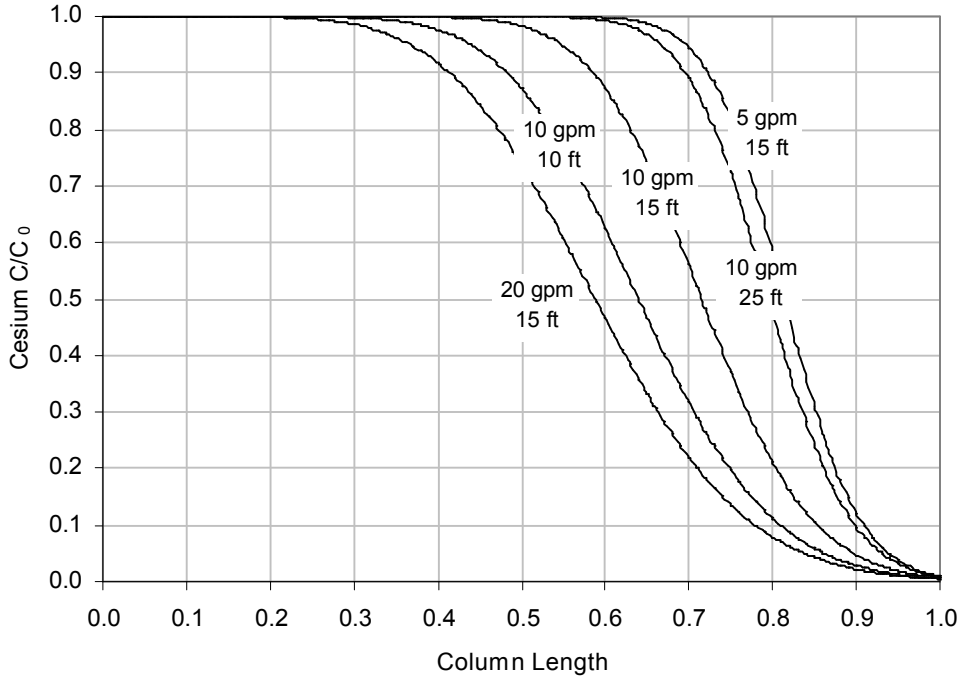

Figure B-3. Cesium concentration profile in single RF column at end of run for Tank 3.

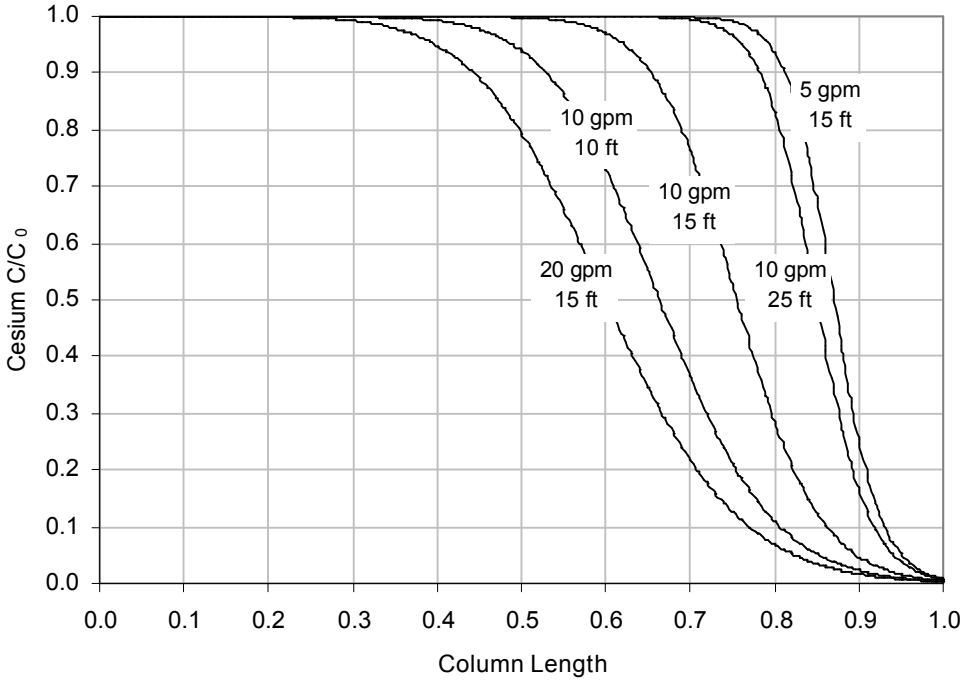

Figure B-4. Cesium concentration profile in single RF column at end of run for Tank 37.

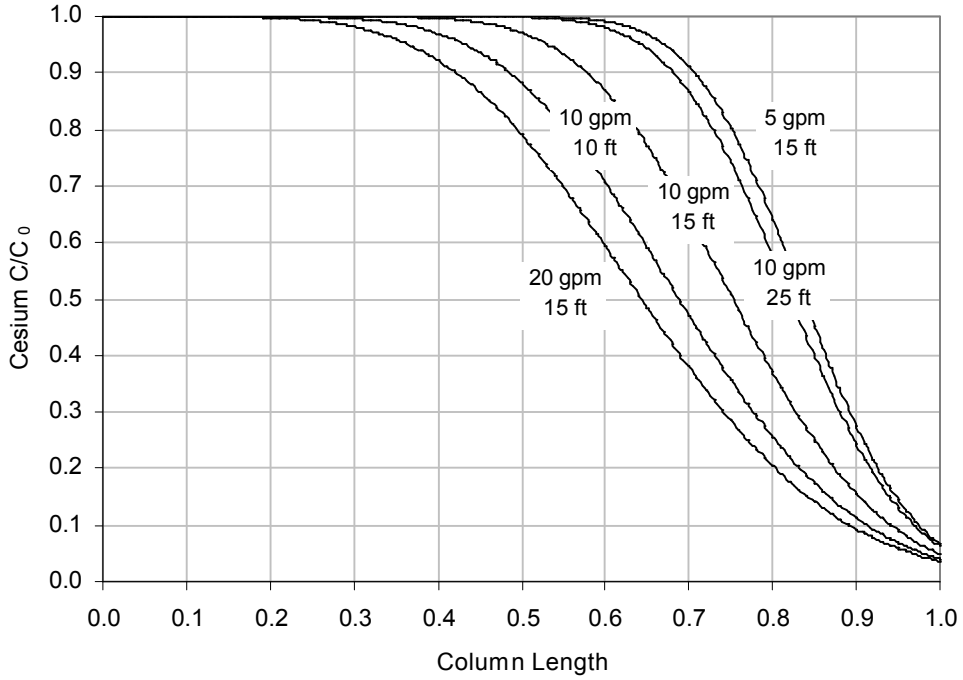

Figure B-5. Cesium concentration profile in single RF column at end of run for Tank 41.

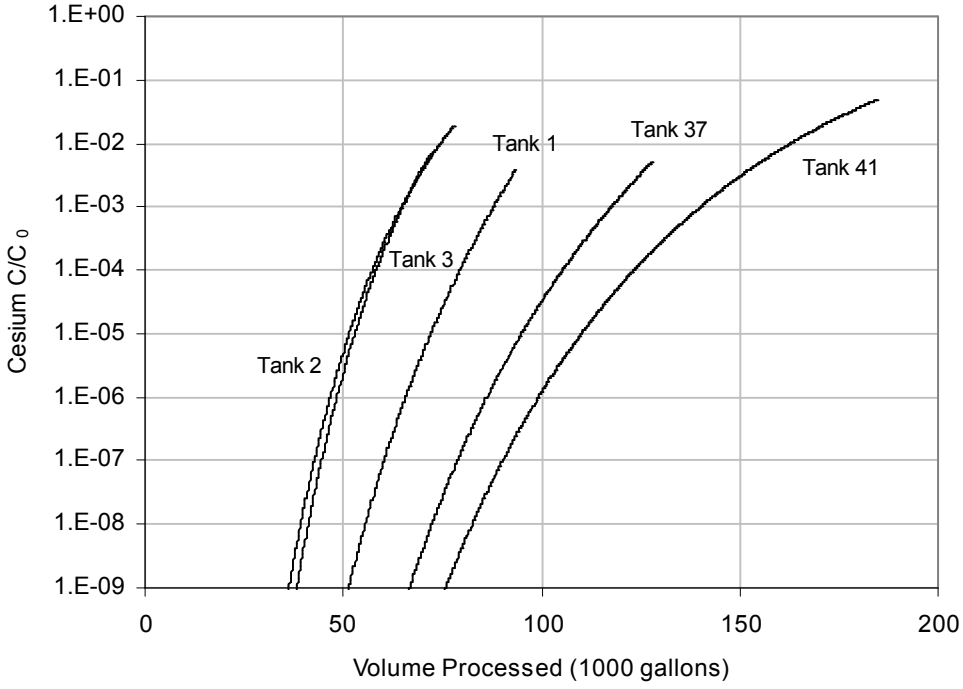

Figure B-6. Cesium breakthrough curves from single RF column runs.